


Liquid Metal Actuators: A Comparative Analysis of Surface Tension Controlled Actuation

Review Article**Author(s):**

Liao, Jiahe; Majidi, Carmel; [Sitti, Metin](#) 

Publication date:

2023

Permanent link:

<https://doi.org/10.3929/ethz-b-000641439>

Rights / license:

[Creative Commons Attribution 4.0 International](#)

Originally published in:

Advanced Materials, <https://doi.org/10.1002/adma.202300560>

Liquid Metal Actuators: A Comparative Analysis of Surface Tension Controlled Actuation

Jiahe Liao, Carmel Majidi, and Metin Sitti*

Liquid metals, with their unique combination of electrical and mechanical properties, offer great opportunities for actuation based on surface tension modulation. Thanks to the scaling laws of surface tension, which can be electrochemically controlled at low voltages, liquid metal actuators stand out from other soft actuators for their remarkable characteristics such as high contractile strain rates and higher work densities at smaller length scales. This review summarizes the principles of liquid metal actuators and discusses their performance as well as theoretical pathways toward higher performances. The objective is to provide a comparative analysis of the ongoing development of liquid metal actuators. The design principles of the liquid metal actuators are analyzed, including low-level elemental principles (kinematics and electrochemistry), mid-level structural principles (reversibility, integrity, and scalability), and high-level functionalities. A wide range of practical use cases of liquid metal actuators from robotic locomotion and object manipulation to logic and computation is reviewed. From an energy perspective, strategies are compared for coupling the liquid metal actuators with an energy source toward fully untethered robots. The review concludes by offering a roadmap of future research directions of liquid metal actuators.

1. Introduction

Advances in soft actuators are transforming every aspect of robotics by taking advantage of a variety of physical principles for generating forces and deformation in highly deformable materials. Similar to natural muscles, development of robotic actuators seeks stimuli-responsive materials that convert electrical, thermal, or chemical energy into mechanical work.^[1–3] Every actuator can be characterized by its operational requirements and actuation performance. Ideally, actuators operate with minimal cost (e.g., low voltage, high efficiency) and maximal performance (e.g., high strain, high speed) but their characteristics are rooted in the underlying physics. One notable example is the electrostatic actuators, which include dielectric elastomer actuators (DEA)^[4,5] and more recently the hydraulically amplified self-healing electrostatic actuators (HASEL).^[6,7] Since these actuators operate at a very high voltage (typically >1 kV, compared to ≈ 0.1 V in natural muscles^[8,9]) that is necessary for

sufficient electrostatic forces of attraction across the material, they are capable of high strain output (>300% in DEA, compared to 20% of natural muscles^[9,10]) and high stress output (>1 MPa in DEA, compared to 0.1 MPa of natural muscles^[4,11]), which makes them powerful but rather vulnerable to dielectric breakdown at high voltages. Design challenges remain for a wide range of robots from mobile robots, microrobots, to human-interactive robots, many of which may not be able to afford such a high voltage without compromising overall volume^[12] or safety.^[13] Another example is soft actuators enabled by thermal phase transition in materials such as liquid crystal elastomers (LCE)^[14] and shape memory alloys (SMA),^[15,16] which are capable of very high stress (200 MPa in SMA^[15]) but have low efficiency (<10% in SMA, compared to 40% in natural muscles^[9,11]) as they require heat to transform. What is the next actuator with comparable performance that does not need as much voltage or heat? As new soft-matter architectures and functionalities continue to evolve, challenges remain for new principles of soft actuators.


The ability to intrinsically deform in response to an external stimulus is not limited to solids such as gels, elastomers, and liquid crystals, which have been widely used in soft actuators. Liquids also share certain characteristics commonly found in other soft matters. Like many soft materials, liquids are highly

J. Liao, M. Sitti
Physical Intelligence Department
Max Planck Institute for Intelligent Systems
Heisenbergstr. 3, 70569 Stuttgart, Germany
E-mail: sitti@is.mpg.de

C. Majidi
Robotics Institute
Mechanical Engineering
Carnegie Mellon University
5000 Forbes Ave, Pittsburgh, PA 15213, USA

M. Sitti
Institute for Biomedical Engineering
ETH Zürich
Zürich 8092, Switzerland

M. Sitti
School of Medicine
College of Engineering
Koç University
Istanbul 34450, Turkey

 The ORCID identification number(s) for the author(s) of this article can be found under <https://doi.org/10.1002/adma.202300560>

© 2023 The Authors. Advanced Materials published by Wiley-VCH GmbH. This is an open access article under the terms of the Creative Commons Attribution License, which permits use, distribution and reproduction in any medium, provided the original work is properly cited.

DOI: 10.1002/adma.202300560

deformable^[17] and tend to approach an equilibrium shape where the total potential energy is locally minimized,^[18,19] which gives rise to their elasticity-like behaviors.^[20–22] Unlike solids, whose shapes are largely determined by volume elements, liquids are predominated by their surfaces, with surface tension being the major force particularly at length scales smaller than the capillary length. For actuation, liquids with higher surface tension are preferred since they are intrinsically capable of higher force output.^[23,24] Liquid metals, which are low-melting point metals in liquid phase at the operating temperature, have the highest surface tension ($\approx 500 \text{ mN m}^{-1}$) among all liquids due to their predominantly strong metallic bonding compared to hydrogen bonding in water.^[25] Mercury (melting point -38.8°C , surface tension 438.4 mN m^{-1} ^[26,27]) is traditionally used in liquid metal studies but is largely replaced by less toxic alternatives^[28] such as Galinstan (eutectic 68.5% Ga, 21.5% In, 10% Sn by weight, melting point -19°C , surface tension 534.6 mN m^{-1} ^[29]) and EGaIn (eutectic 75% Ga, 25% In by weight, melting point 15.5°C , surface tension 624 mN m^{-1} ^[30,31]). Apart from their high deformability and high surface tension, liquid metals are excellent electrical conductors (conductivity $\approx 10^6 \text{ S m}^{-1}$ ^[30]), which make them particularly suitable for electrical-responsive actuation.^[32,33]

From a robotic standpoint, surface tension of liquids as a source of actuation offers a unique combination of high degrees of freedom and force scalability. Since any liquid body with a given volume can take arbitrary shapes, where free motion of every interfacial molecule contributes to the macroscopic fluidic deformation, it follows that actuation of liquids has intrinsically higher degrees of freedom than that of solids.^[34] In this view, liquid-based actuators can be reshaped at higher degrees of freedom than any other solid materials, which gives them a superior deformability among all types of soft actuators. Liquid droplets can also produce motions at lower degrees of freedom with kinematic constraints. Unlike gas-based actuation,^[35,36] however, motion of liquids is influenced by their tendency to minimize the surface energy. Liquid behaviors, particularly at smaller length scales, are dominated by the molecules on the exterior (i.e., surface dependence^[37]) rather than the interior (i.e., volumetric dependence^[1]). This offers a possibility of very high density of actuation output, such as force and work output, at smaller length scales, where a higher ratio of surface molecules contributes to actuation. This length scalability of surface tension, by which forces are proportional to lengths ($F \propto L$) rather than areas ($F \propto L^2$) and volumes ($F \propto L^3$), makes liquid stand out from all other soft materials for performance-dense actuation.

The scaling advantage of actuation of liquids, in particular liquid metals for higher surface tension, offers opportunities in robot actuation at various length scales. For instance, micro-robots can potentially benefit from using liquid metals as a dense source of actuation. To see this, consider scaling down a liquid metal droplet from mm-scale to μm -scale (i.e., decreasing by 3 orders of magnitude), where surface tension forces ($F \propto L$) normalized by volume (L^3) approximately increases by 6 orders of magnitude. For comparison, the force per unit volume would increase by 3 orders of magnitude with electrostatic actuation ($F \propto L^2$ ^[38,39]) and by 0 orders of magnitude with magnetic actuation ($F \propto L^3$ ^[40]). Although this ideal estimation can be influenced by actual implementation such as aspect ratio and transmission, the clear advantage of surface tension shows promise

in microrobots.^[41,42] The same advantage can be applied to actuators at larger scales, such as mm-scales and cm-scales, by splitting the given volume of liquid metals into many smaller droplets to maximize contact area. The total force and deformation can be summed up from every individual unit.^[24] As surface tension is one of the very few types of forces^[39] that would benefit from such a contact splitting strategy, it follows that the scaling characteristics of liquid metals offer great opportunities in a wide range of length scales.

Surface tension modulation is essential to liquid metal actuators, which *contracts* when surface tension increases and *relaxes* when surface tension decreases (Figure 1A) under certain kinematic constraints (Figure 1D). The surface tension is typically controlled by an electrical potential across the interface between the interior and exterior of a liquid metal droplet. Electrocapillarity,^[43] or electrowetting in some context,^[44–46] controls the interface through an electric double layer (EDL) on a charged liquid metal droplet (Figure 1C). This method has been well-studied for many decades and has enabled many applications, typically at a higher voltages $\approx 10^1 - 10^2 \text{ V}$ with electrowetting-on-dielectric requiring $>10^2 \text{ V}$ in the absence of electrolyte. The electrochemical method^[47,48] offers an alternative at lower voltages ($\approx 1 \text{ V}$), where the liquid metal interface is controlled by an oxide layer that can be deposited and removed by redox reactions (Figure 1B). As summarized in Figure 1E,F, certain trends can be observed in the evolution of liquid metal actuators. For instance, the voltage for surface tension modulation has decreased from electrocapillary ($\approx 10^1 - 10^2 \text{ V}$) to electrochemical ($\approx 1 \text{ V}$), thereby enabling a new generation of low-voltage actuators. Another observation is that the volume density of work output has been relatively low with electrocapillarity ($\approx 10^0 - 10^2 \text{ J m}^{-3}$ compared to 8 kJ m^{-3} in natural muscles^[11]) but has since increased in some of the recent literature ($\approx 1 \text{ kJ m}^{-3}$ at mm-scale) with the electrochemical method, where theories predict even higher work densities with smaller droplets. While both methods modulate the surface tension through electrical stimuli, the electrocapillary method relies solely on buildup of electric charges and hence, similar to electrostatic actuators such as DEA, only responds to relatively high voltages. The electrochemical liquid metal actuator, on the other hand, is driven by chemical reactions at an electric potential closer to biological systems ($\approx 1 \text{ V}$ compared to $\approx 0.1 \text{ V}$ in natural muscles^[49]).

This review focuses on liquid metal actuators driven by electrical modulation of surface tension. We adopt the definition of an actuator as a device that produces mechanical work,^[67] which in this case involves changes in forces and displacement of a liquid metal droplet. By this definition, a free droplet that transports itself into a new position^[53] and an anchored capillary bridge that is capable of deforming into a new shape^[23] are both actuators, but an unconstrained and unloaded droplet, even when activated, should not be considered as an actuator if it does not produce any usable work. We emphasize surface tension as the primary driving mechanism. As a counterexample, liquid crystal elastomers with embedded liquid metal droplets^[68–71] operate on liquid crystal phase transitions and therefore do not qualify as liquid metal actuators. Neither are material architectures with non-actuating liquid metal inclusions, such as has been demonstrated with dielectric elastomers,^[72,73] McKibben pneumatic actuators,^[74] and shape memory alloys.^[75–77] We note that

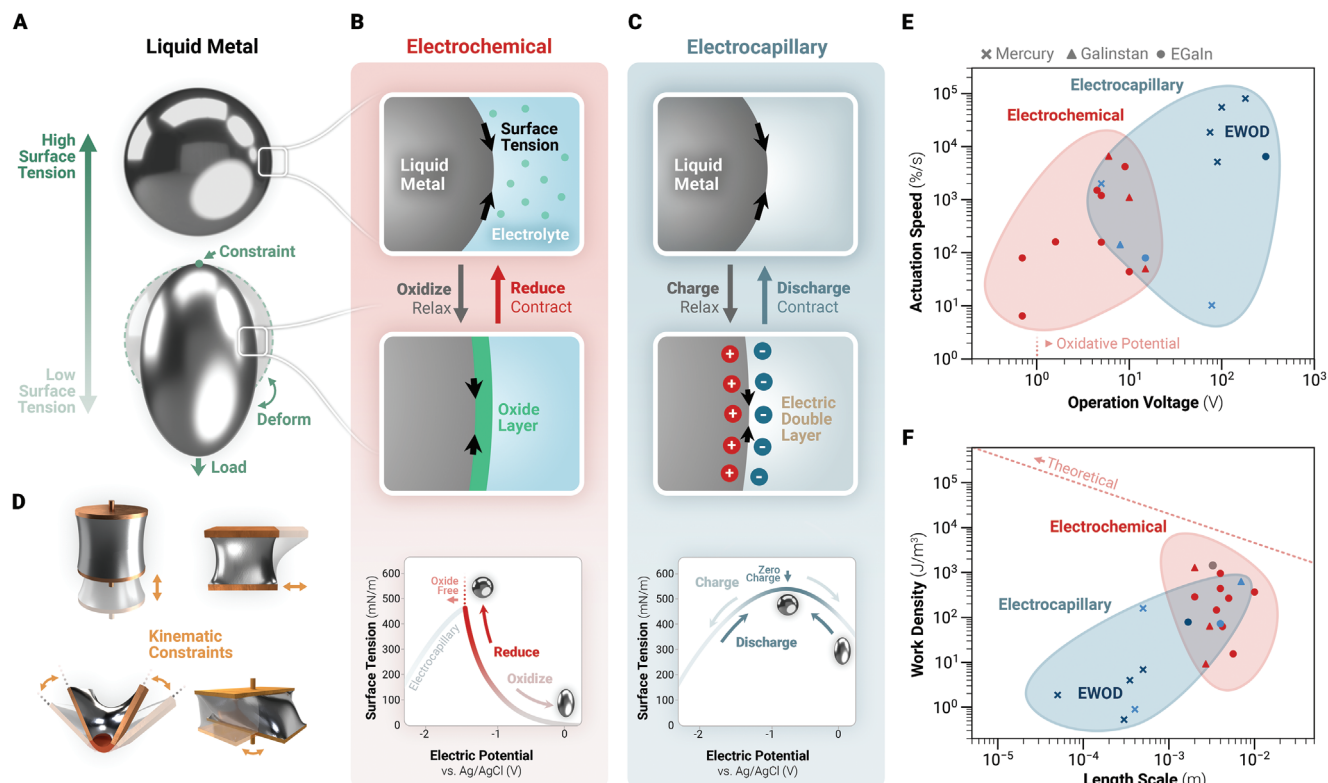


Figure 1. Working principles and key characteristics of liquid metal actuators. A) Actuation of a liquid metal droplet is enabled by modulation of surface tension on a constrained droplet, which generates forces and deformation when the interfacial tension is increased (i.e., droplet contraction) or decreased (i.e., droplet relaxation). B) The electrochemical modulation of surface tension has emerged as a low-voltage method for controlling interfacial properties of gallium-based liquid metals, where electrochemical deposition of gallium oxides results in significant lower surface tension at modest voltages near the oxidative potential (≈ 1 V). Contraction occurs when the gallium surface is reduced by a reversed polarity. C) Electrocapillarity, which is the control of surface tension through charging and discharging the electric double layer on the liquid metal surface, requires higher electric potential to operate compared to the electrochemical method. D) Kinematic constraints are essential to operate a liquid metal droplet for practical actuation, where motion of the droplet is restricted to some desired degrees of freedom. E) Comparison of operation voltage to actuation speed in recent progress on liquid metal actuators. Electrocapillary-actuated liquid metal actuators,^[50–53] which encompass electrowetting-on-dielectric (EWOD) as an electrolyte-free special case,^[54–58] tend to require higher voltages than the electrochemical approach^[23,24,47,59–66] by 1–2 orders of magnitude. F) Comparison of length scale to work density, which has been theoretically predicted (Ref. [23] and; Ref. [24] curve shown is from Ref. [23]) to increase at smaller length scales with the electrochemical approach. By contrast, electrocapillary actuation (including EWOD) has been implemented toward smaller scales ≈ 100 μm with limited work densities. All references used mercury, Galinstan, or EGaln (marked accordingly) as the liquid metal. Values are cited or calculated from the reported data in each reference.

surface tension actuation often needs to be paired with an antagonist to provide a restoring force (Section 3.4). Since liquid metal is viewed in this review as an electrically responsive matter, we will focus on the electrical aspects of surface tension, even though they are also known to be responsive to chemicals (e.g., organic surfactants^[78]) and heat (e.g., surface tension tends to decrease at high temperatures^[79]). Finally, we note that similar actuation principles are not limited to liquid metals but also applicable to non-metallic liquids. Between metallic and non-metallic liquids, we favor the former for their significantly higher surface tension due to stronger metallic bonds between the molecules.^[80,81]

The following sections are intended to examine the state of the art of liquid metal actuators (LMA) and provide the readers with reference information for the ongoing development of LMAs. In particular, they will cover the principle (i.e., how LMA works, Section 2), design and fabrication (i.e., how to build LMA, Sections 3 and 4), theoretical and experimental performance (i.e., how well LMA works, Sections 5 and 6), practical applications (i.e., what

LMA can be used for, Section 7), energy consideration (i.e., how to power LMA, Section 8) and future research directions (Section 9). We will discuss the advantages and limitations of LMA compared to other electrically responsive soft actuators. Lastly, we will outline a roadmap and challenges for the LMA to reach its theoretical high performance that will make it stand out from other types of soft actuators.

2. Liquid Metal Actuators: Principles of Surface Tension Actuation

From an energy standpoint, the work produced by any soft actuator can typically be calculated from the change in the total potential energy between two configurations such as the relaxed and contracted states. By this definition, a soft actuator can be represented by a system of conservative forces \mathbf{F} and displacement \mathbf{x} that is associated to a potential function $\Pi(\mathbf{F}, \mathbf{x})$. To see how the potential explains the work production in soft actuator,

consider a typical example of a linear elastic spring (stiffness k , load F , displacement x) whose total potential energy can be expressed by $\Pi = \frac{1}{2}kx^2 - Fx$. This expression embodies the conversion between elastic energy and work output, which can be controlled by tuning the spring stiffness k , where Π will assume a new local minimum by changing F or x . For linear springs, this implies a closed-form solution to $\frac{d\Pi}{dx} = 0$ as $F = kx$. Likewise, every type of soft actuators can be analyzed in terms of *potentials* between independent input variables such as voltage U in dielectric elastomers,^[82] pressure P in McKibben pneumatic actuators,^[35] and surface tension γ in liquid metal actuators.^[23]

For liquid metal actuators subject to a given load F or deformation x , work is generated when surface tension γ is switched from a high surface tension γ_{\max} to a low surface tension γ_{\min} or vice versa. For this reason, surface tension modulation is the basis of liquid metal actuators. Why is liquid metal an excellent candidate for electrical modulation of surface tension? What is the mechanism of surface tension modulation? How do forces scale with length and what is the implication in actuation? This section addresses these questions by introducing the working principles of surface tension actuation in liquid metals.

2.1. The Role of Surface Tension in Liquid-Based Actuators

2.1.1. Intrinsic Elasticity in Liquids by Surface Tension

One of the major characteristics of liquids is their elastic-like restorative behavior that originates from surface tension. Unlike solid materials, whose elasticity comes from intermolecular forces throughout the volume, liquids are intrinsically elastic due to the attraction between molecules on the surface.^[83] In energy terms, any liquid (surface tension γ , surface area A) tends to approach a stationary position of total potential energy $\Pi = \gamma A - W$ where Π is locally minimized and W is the work done on the surface. This energy-minimizing tendency (or area-minimizing with zero work) gives rise to elastic-like properties in liquids, in particular the intrinsic ability of droplets to stretch and return to their original shape. Elasticity in actuators is also widely seen in nature, where muscles are full of passive elastic components ranging from tendons, extracellular matrices, to elastic titin filaments in the muscle fibers,^[84] all of which contribute to the high nonlinearity and reversibility in muscle contraction.^[85] Likewise, elasticity in liquids plays a central role in the reversibility of actuation, which may benefit more complex motor tasks ranging from underactuated or passive dynamic motions.^[86]

2.1.2. Wettability and Kinematic Constraints

Liquids as actuators are also characterized by their wettability to solids, which is measured by their contact angle ($\theta = 0$ if perfectly wetted, $\theta = 180^\circ$ if non-wetted) and is a central concept to liquid actuation. For moving freely within a container or channel, the liquids should be ideally non-wetted to the walls. On the other extreme, the liquids sometimes need to wet perfectly to solids to form local constraints on the liquid surface. With liquid metals, this is typically achieved by metallic bonding to another metal (e.g., wetting EGaIn to copper).^[23] The most important function

of such a liquid–solid bonding is to provide the liquid with a kinematic link for force and displacement output. A typical example is a liquid bridge (or capillary bridge) formed by wetting a droplet to two rigid bodies in spherical or circular shapes.^[87–89] This configuration, where the liquid bridge serves as the joint between the two rigid bodies with a continuous free surface that pulls the two ends together, is viewed as a type of *kinematic constraint* on the liquid. Without any kinematic constraints, the liquid will always try to assume a spherical shape without the capability of actuation. It is only when constraints are imposed to the liquid surface by intended wetting or non-wetting to solid surfaces that surface tension actuation is possible.

2.1.3. Production of Mechanical Work by Surface Tension Modulation

The production of mechanical work, as previously discussed, is the surface tension-enabled switch from one potential to another. In general, the potential energy associated with a particular configuration consists of two competing terms: surface energy (γA) and work output (Fx). The system equilibrium occurs when the total potential energy $\Pi = \gamma A - Fx$ is minimized subject to a constant volume constraint (assuming incompressible liquid) and other kinematic constraints. Here, we will briefly discuss the principles of two typical actuation schemes in recent literature, both of which are constrained for some 1D motion:

- **Deformation of a liquid bridge restricted to linear motion:** This configuration produces work by linear contraction (x decreasing at a fixed F or vice versa) in response to an increasing γ , which can be explained by the minimization of potential energy $\Pi = \gamma A - Fx$ with constraints on volume and the wetted surface boundaries.^[23,24]
- **Transport of a whole droplet inside a channel:** In this configuration, the droplet is completely unwetted and produces work by moving the whole droplet for a distance x in response to an imbalanced γ across the surface. The potential function here takes the form $\Pi = \int_S \gamma (\nabla \cdot \hat{n}) \hat{n} dV - Fx$, where surface tension γ varies and surface energy is calculated by $P dV$ using the Young–Laplace equation $P = \gamma \nabla \cdot \hat{n}$. Intuitively, when there is higher surface tension on the left hand side of the droplet, it will be *pushed* by the Laplace pressure gradient to the right hand side, producing work with increasing x . This type of actuation is commonly referred to as continuous electrowetting,^[51,62,90] a special case of the Marangoni effect.

While liquid metals appear to be switchable between two or more states in these examples, it should be clarified that surface tension by itself only performs one-way actuation, where the liquid metal droplet always has an “original” shape when the surface tension is maximized. As an actuator, it is only after the droplet is relaxed (decreasing γ) and stretched (increasing F or x) that the droplet can switch back to its original high-tension state. In this sense, surface tension offers a one-way actuation from a low-tension to a high-tension state while the opposite relaxation must be coupled with an antagonistic force to act over the lowered surface tension. This property is also shared by many types of actuators. For instance, many shape memory alloys only transform

into the original austenite phase when activated. They require an antagonist load to deform away from the original shape.^[91] Another example is skeletal muscles, which only produce contractions but not expansion. As a result, they often appear in an antagonistic pair in order to achieve reversible motion.^[92,93]

Liquid metals are particularly well suited for actuation since they have the highest surface tension among all liquids (mercury: 438.4,^[27] Galinstan: 534.6,^[29] EGaIn: 624 mN m⁻¹,^[30] compared to water: 72.74 mN m⁻¹^[94]). In particular, alloys of gallium, such as Galinstan and EGaIn, have emerged as popular liquid metals for their lower toxicity compared to mercury.^[30] Gallium naturally forms a passive layer of gallium oxide (Ga₂O₃) when exposed in air or water. The presence of gallium oxide, which is a hydrophilic solid,^[47] lowers the surface tension by disrupting the interface. As the oxide layer keeps growing, the surface tension drops to near zero with the droplet behavior beginning to be dominated by the solid oxide layer. One typical example is the flattening and spreading of an EGaIn droplet on a plane into a nondeterministic fractal shape.^[95] We note that because the growth of the passivating oxide skin is limited to a thickness ≈ 1 nm,^[47,96,97] this mixture of liquid metal and solid oxide skin, at length scales $\gg 1$ nm, will maintain its liquid characteristics. Gallium oxide dissolves in aqueous solutions of alkaline hydroxide such as NaOH and KOH,^[98] which can also function as the electrolyte for electrochemical oxidation of gallium.^[47] All these relevant properties establish liquid metals, particularly alloys of gallium, as an excellent candidate for surface tension actuation.

2.2. Liquid Metals: Combination of High Deformability and Electrical Responsivity

Among all liquids, which are all capable of surface tension actuation, liquid metals stand out for their unique combination of high surface tension, high deformability, and electrical responsivity. Since liquid metal actuators produce mechanical work when activated by electrical stimuli, it follows that their performance is influenced by how easy they deform and how responsive they are to changes in electric potential. This dependence is illustrated in **Figure 2A**, where a liquid metal droplet in a typical electrochemical setup takes an electrical input ΔU between the electrode and counter electrode. As a soft actuator, the liquid metal droplet undergoes changes in force and deformation, to which the excellent combination of mechanical and electrical properties in liquid metals is central.

To put these properties of liquid metal in context, we compare the electrical conductivity and effective Young's modulus of common types of condensed matter (liquid,^[99–102] tissue,^[17,103–110] elastomer,^[111–114] gel,^[115–120] and metal^[121–123]) and their enabling actuators (**Figure 2B**). Across the wide spectrum of electrical conductivity ($\approx 10^{-14} - 10^6$ S m⁻¹) and Young's modulus (up to 10¹¹ Pa), liquid metals are located at the intersection of highly deformable liquids and highly conductive metals. We note that not every type of actuator will perform better by all metrics with higher conductivity or lower modulus. For instance, at the same input voltage, a more electrically conductive shape memory alloy may be less efficient due to higher current and hence higher power loss. We also note that Young's modulus is typically defined for elastic solids but, for our comparison here, adopt the

argument^[17,124] that liquids have zero Young's modulus as they would deform without any tensile or compressive stress. By this definition, liquid metals (Young's modulus = 0, electrical conductivity $\approx 10^6$) mark a special regime in which very soft actuators that respond easily to electricity can be created.

How do we define electrical responsivity for a soft actuator? One ideal is for an electrically responsive actuator to take a minimal voltage input and produce a maximum strain output. In practice, both the voltage requirement and strain dependence vary by the mechanism of actuation, the actual usage of electricity, and work production in the material. We also note that there are applications where pursuing low voltages is less important than high power efficiencies, but this review focuses on the actuator's responsivity to *voltage*. **Figure 2C** summarizes the input-output relationships of selected types of soft actuators. In this comparison, the electrostatic actuators such as DEA and HASEL generate the highest strains at the cost of the highest voltages. Actuators based on phase transition, such as SMA and LCE, on the other hand, do not require the same extreme voltages and instead can be sufficiently Joule-heated at lower voltages.^[125,126] Electrochemically driven actuators, such as LMA tend to use lower voltages as their actuation is triggered by chemical reactions that take place at a certain potential difference. Compared to natural muscles, which generate contractions from chemical energy but are triggered by an action potential ($\approx 10^{-1}$ V) that is significantly lower than the electrical activation of the existing actuators (electrothermal: $\approx 10^0 - 10^1$ V, electrostatic: $\approx 10^4 - 10^5$ V, **Figure 2C**), liquid metals, despite operating on different principles, provides another low-voltage alternative to the actuators that require giant voltages. Liquid metals, with a substantial strain output ($\approx 40\%$,^[24] design-dependent) enabled by low voltages less than electrostatic actuators by 4–5 orders of magnitudes, are closer to the ideal actuator proposed above.

When comparing electrical actuators, it is necessary to consider how the electrical energy is used. In electrostatic actuators, very high voltages are required to pull the charges densely toward the electrodes across the medium such as elastomer or liquid, which is fundamentally limited by the dielectric properties of the medium.^[4–6] In actuators based on phase transition, heat is a result of electric power, which is supplied by the combination of current and voltage.^[68,91] For liquid metal actuation, electrical energy is used to initiate an otherwise non-spontaneous chemical reaction, which is limited by the oxidative potentials (typically ≈ 1 V). In general, the voltages at which the conversion of electrical energy into mechanical work occurs is one of the key characteristics of an electrically responsive actuator,^[1] where liquid metals offer a desirable option at low voltages.

2.3. Methods of Surface Tension Modification in Liquid Metals

Surface tension γ is traditionally linked to *electrocapillarity*, or the charging and discharging of the electric double layer,^[43,127–129] which is characterized by the Lippmann equation $d\gamma/dU = -q$, where γ is maximized when fully discharged. This method requires higher voltages ($U \approx 10^1 - 10^2$ V) since γ decreases quadratically with U ,^[47] compared to decreasing exponentially with the recent electrochemical method (**Table 1**). While the exact definitions vary in the literature, we view all surface

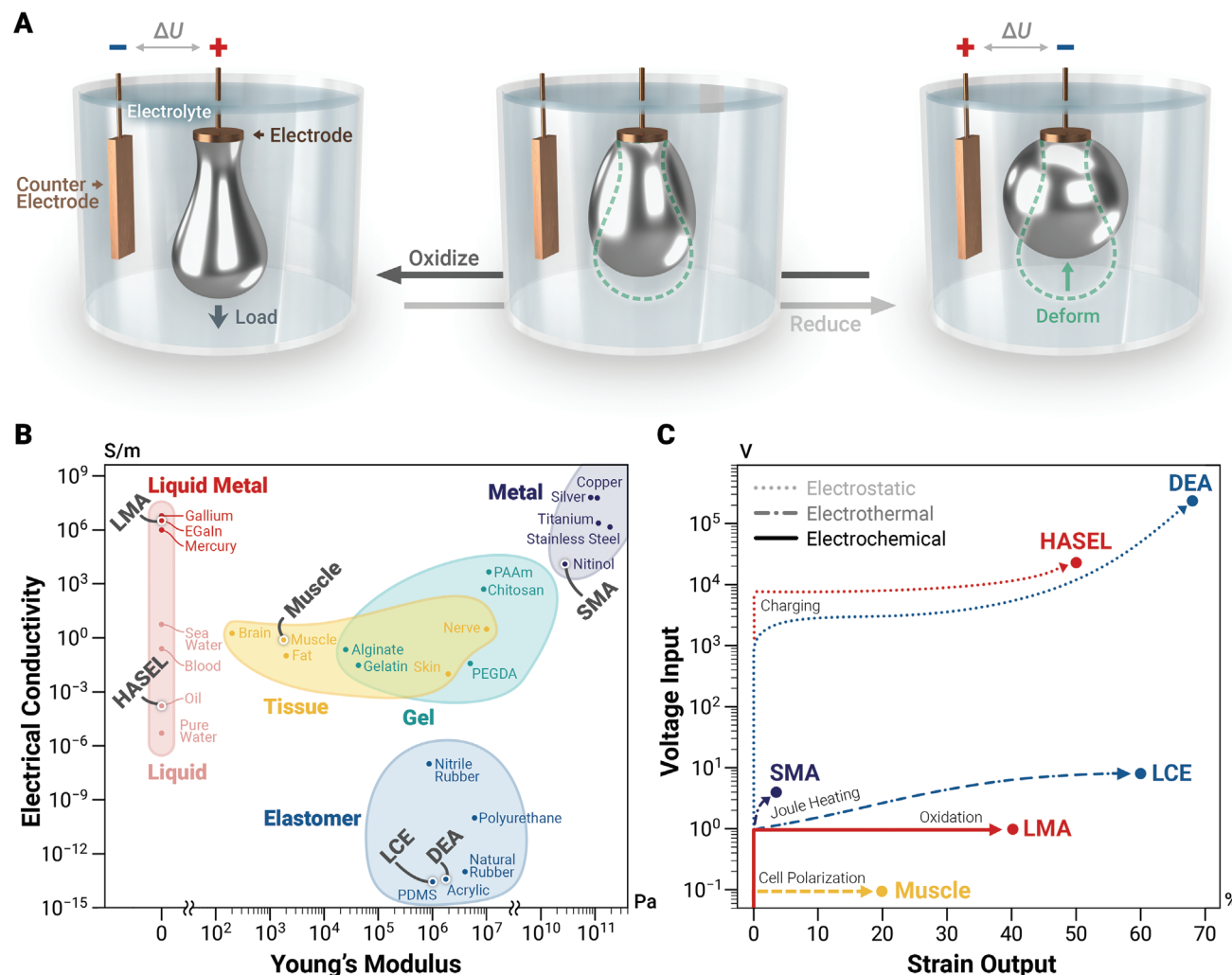


Figure 2. Electrical responsivity of liquid metal actuators. A) Liquid metals, which are characterized by their high deformability as liquids, respond to electrical stimuli in a typical electrochemical setting for redox reactions. When an electrical potential is applied across the interface between the liquid metal droplet and the surrounding electrolyte, the droplet deforms in response to the modulated surface tension. B) Comparison of electrical conductivity to Young's modulus with common types of materials and actuators. Unlike all the other solid materials, liquids are not typically characterized by Young's modulus as they do not have tensile stiffness. We assume zero modulus for liquids for a qualitative comparison. Among the selected types of actuators (gray rotated labels) represented by their base soft materials, the liquid metal actuators (LMA) display a very high electrical conductivity with a presumably zero Young's modulus compared to natural muscles, shape memory actuators (SMA), dielectric elastomer actuators (DEA), liquid crystal elastomers (LCE), and hydraulically amplified self-healing electrostatic (HASEL) actuators. Note that electrical responsivity is to be compared among actuator types and does not necessarily guarantee higher performance with higher conductivity or lower modulus. C) Representative input-output relationship between voltage and strain in selected types of actuators. Liquid metal actuators are capable of decent strain output at voltages less than electrostatic actuators by 4–5 orders of magnitudes.

modification methods by charging liquid metal surfaces as belonging to electrocapillarity. These include electrowetting,^[44,130] continuous electrowetting,^[51,53,62,90] and electrowetting on dielectric (EWOD).^[46,54–58]

2.3.1. Surface Tension Modulation From a Molecular Perspective

Actuation of liquid metals relies on surface tension modulation. In this regard, the mechanism of actuation should be considered as interfacial rather than volumetric. For liquid metals, this implies that in order to disrupt their high surface tension,

which arises from the strong metallic bonds between neighboring molecules at the interface, modulation should generally occur across the interface. Mathematically, interfacial tension γ controls the relation between the shape (mean curvature $\frac{1}{2}\nabla \cdot \hat{n}$) and forces (Laplace pressure P) of a liquid interface by $\vec{P} = -\gamma \nabla \cdot \hat{n}$ (Young–Laplace equation). This explains the ability of liquid metals to change their shapes and forces in response to modulation of γ .

How can the interface be electrically disrupted such that γ is modulated? For liquid metals, the modulation generally takes place by electrically adding or removing a surfactant-like layer surrounding the liquid metal surface. Surface tension is

Table 1. Methods of surface tension modulation in liquid metals.

Modulation method	Mechanism of modulation	Governing equations	Characteristics
Electrochemical	Oxidation versus reduction of LM surface ^[47] <ul style="list-style-type: none"> Reaction occurs at ≈ 1 V 	$\gamma(U) \approx \gamma_0 \exp(-U/U_0)$ Electrical Potential versus Surface Tension (Empirical) ^[61]	<ul style="list-style-type: none"> Surface tension γ modulated by oxide skin. Maximum γ occurs when LM is fully reduced and minimally charged. Exponential relationship between U and γ. Requires aqueous electrolyte. Involves electrolysis of water (with H_2 byproduct).
Electrocapillary	Charging versus discharging of LM surface ^[43] <ul style="list-style-type: none"> Charged at any U but typically $\approx 10^1 - 10^2$ V for useful actuation^[50,52,54,56] 	$d\gamma/dU = -q$ Charged Surface (Lippmann equation) $\gamma(U) = \gamma_0 - \frac{1}{2} C_d (U - U_0)^2$ Electrical Potential versus Surface Tension	<ul style="list-style-type: none"> Surface tension γ modulated by electrical double layer. Maximum γ occurs when LM is fully discharged^[131]. Parabolic relationship between U and γ. Aqueous electrolyte is typically needed but can be eliminated with higher voltages (e.g., EWOD).^[48]

lowered with the presence of the surfactant-like layer and is maximized when it is completely removed. The behaviors of such a surfactant-like layer (i.e., how much electric potential is required and how much surface tension is lowered) depend on the exact mechanism.

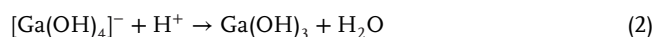
2.3.2. Electrochemical Modulation of Surface Tension

The electrochemical modulation (Figure 1B) of surface tension of liquid metals (particularly Ga-based low-melting-point alloys) takes place at significantly lower voltages (≈ 1 V) that are only limited by the oxidative potential of gallium. Surface tension is lowered exponentially when oxidized, where the gallium oxide layer disrupts the gallium interface, and maximized when the liquid metal is fully reduced^[47] (Table 1). This implies a voltage-dependent surface tension $\gamma(U)$ that peaks at an oxide-free $\gamma_0(U_0)$. During oxidation, surface tension decreases drastically toward zero, where the gallium–gallium oxide mixture gradually loses its liquid behaviors.^[95,132] We note that the deviation of the oxidized $\gamma(U)$ from the quadratic electrocapillary curve $\gamma(U) - U_0 \approx (U - U_0)^2$ ^[47,133] has been empirically described as exponential with electric potential (i.e., $\gamma(U) \approx \gamma_0 \exp(-U/U_0)$ ^[61]), though the exact mechanism between U and the resulting surface tension γ remains an open question.

Typical reactions that cause the formation of gallium oxide skin (Ga_2O_3) in response to voltages can be explained as follows. When surrounded by an alkaline solution in water (e.g., potassium hydroxide, KOH), surface gallium is spontaneously dissolved into gallate ions ($[Ga(OH)_4]^-$).^[98] With KOH as the electrolyte, this dissolution can be described as:



When the voltage on the gallium surface (anode) in reference to the counter-electrode (cathode) is raised above the minimum potential for water electrolysis (standard potential: $1.23 V^{[134]}$), water is electrolyzed with hydrogen ions H^+ forming on the gallium and hydrogen gas H_2 forming on the counter-electrode. This may result in the formation of gallium hydroxide ($Ga(OH)_3$) and gallium oxide (Ga_2O_3) as a result:



We note that although the liquid metal of interest in this review is an alloy of gallium and indium, the overall composition and behavior of the oxide skin has been attributed predominantly to gallium oxide,^[30,135] which forms a passivating layer.^[30] Furthermore, these reactions offer an explanation of the oxide formation, which may vary with specific gallium-based oxide species.^[135,136] For the purpose of this review, we emphasize that the electrochemical modulation method here, in terms of electrical activation, is likely one that depends on water electrolysis. This dependence is essential to the operation of actuators for several reasons. First, formation of hydrogen gas on the cathode is unavoidable.^[48] Second, aqueous electrolyte is necessary, as the reactions leading to the formation of gallium oxide Ga_2O_3 involve spontaneous dissolution of gallium as gallate ions $[Ga(OH)_4]^-$ into the aqueous alkaline solution, which is not currently known to occur in non-aqueous and organic solvents.

The electrochemical method is particularly useful for actuation for several reasons. First, the large range of surface tension (from $>500 \text{ mN m}^{-1}$ to ≈ 0) switchable at low voltages gives liquid metal the potential to achieve high performances without having

to use the significantly higher voltages as in charge-driven actuators such as electrocapillary liquid metal actuators, and dielectric elastomers. Second, it has been observed that liquid metals, when electrochemically reduced, contract at exceptionally high strain rates ($>1000\% \text{ s}^{-1}$ ^[24]) compared to other high-speed actuators that operate with high voltages. Lastly, the low voltage requirement makes liquid metal a desirable source of actuation in mobile robots, particularly at smaller length scales.^[1] Despite high strain rates, however, we note that the currently measured specific power (estimated: $\approx 0.2 \text{ W kg}^{-1}$ from Ref. [24], Section 5.1.2) and efficiency ($<0.1\%$,^[24] Section 5.1.2) are low with the electrochemical method. How these characteristics are influenced by principles (e.g., what is the minimum energy required to change the oxidation state?) or designs (e.g., how can the power loss be minimized by optimizing the electrodes and electrolyte setup?) remains unclear and further studies are necessary for possible improvements.

2.3.3. Other Mechanisms for Surface Tension Modulation

While the electrocapillary and electrochemical methods are widely used for liquid metal actuation, there exist other modulation methods, each with their own remarkable characteristics, that bring new functionalities to liquid metal actuators. One example is the liquid metal “mollusk”^[137] and “amoeba”^[138,139] that are propelled by feeding the liquid metal droplet with aluminum, which corrodes the gallium and disrupts the EDL, thereby generating thrust. This electricity-free, EDL-disrupting actuation of liquid metal powered by aluminum can be viewed as an instance of chemical modulation of surface tension and, furthermore, an example of self-powered liquid metal actuation.

2.3.4. Discrete versus Continuous Modulation of Surface Tension

In recent literature, liquid metal actuation is mostly implemented as a binary, two-state transducer for achieving maximal strain and stress, that is, a relaxed state with low surface tension and contracted state with high surface tension. However, voltage-dependence of surface tension^[47] makes it possible to control and maintain surface tension at any arbitrary value in between. From an actuator perspective this also implies the possibility of accurate position control.^[140] One challenge in precise control of the liquid metal actuator at a desired surface tension is the high nonlinearity in the voltage-surface tension relationship,^[59] where the electrochemical reactions, growth of oxide skins and their effects on surface tension are such complex functions that depend on several factors such as voltage, current, mobility of ions, and electrical activation, whose controllers may be hard to generalize. This underlies the current trend in liquid metal actuators, which are predominantly limited to binary switching between contraction and relaxation.

In two-state actuation, it is also possible to implement contraction with zero voltages, at which surface oxide will partly dissolve in the alkaline electrolyte without any potential difference. Theoretically, this will sacrifice the performance since contraction is not driven by a reductive potential and the surface tension will not reach its maximum. However, this allows for an actuator that

does not need any energy input ($U = 0$) to maintain at a near-reduced, partly-contracted stable state.

2.3.5. Effects of Voltage and Electrolyte Concentration

Since actuation strain is a result of changing surface tension, strain rate is influenced by the rate of change in surface tension. With the electrochemical method, a higher rate of change in surface tension is equivalent to a higher rate of deposition or removal of surface oxide,^[133] which is linked to higher voltages^[141,142] and higher electrolyte concentration.^[24,143] It has been observed that liquid metal contracts >10 times faster than it relaxes at the same activation voltage $|\Delta U|$.^[24] It is unknown whether this hysteresis is influenced by the difference between the rates of oxidation and reduction or between the acceleration due to increasing surface tension or the antagonistic force. Apart from voltages and electrolyte concentration, the rate of oxidation can be increased by decreasing the distance between liquid metal and the counter electrodes, which can increase the electrolytic conductance.^[59]

2.3.6. Balance and Imbalance in Surface Tension

Modulation of surface tension can vary across the surface, thereby creating an imbalance in the Laplace pressure and moving the whole droplet along a surface tension gradient.^[144,145] Unlike liquid metal droplets with balanced surface tension, the continuous surface modification of the surface results in asymmetric strain across the surface. This concept has been used in continuous electrowetting,^[51,53,62] electrochemical droplet manipulation,^[61] and chemical propulsion of liquid metal droplets.^[137] In most of these cases, the surface imbalance is controlled by a uniform electric field outside the droplet, which attracts the droplet toward the cathode. From an actuator standpoint, these gradient-driven behaviors are similar to electrorheological (ER) fluids, which flow in a very strong electric field (strength $\approx 3 \text{ kV mm}^{-1}$ ^[146]). We emphasize that the field strength here describes the electric field applied across a distance that is typically larger than the moving body itself. By contrast, the electrochemical droplet manipulation^[61] uses a significantly smaller electric field ($\approx 132 \text{ mV mm}^{-1}$, >2000 times smaller than the ER fluids), which demonstrates the promises in liquid metal actuation by electrical modulation of surface tension.

2.4. Scaling Advantages of Liquid Metal Actuators

As the advances in soft actuators span a wide range of length scales, the scaling laws of their behaviors become central to their characteristics and performance.^[1] The analysis of the scaling laws provides a convenient way to approximate and compare the performance between different actuators for a particular application such as microrobots. To understand how the behaviors of liquid metal actuators scale with length, we will consider a hypothetical liquid metal volume (sphere or cylinder with characteristic radius R) and analyze its force, energy, and dominance of surface tension ranging from cm-scale to μm -scale. We note that the analysis here is limited to static metrics for their established models, while the scaling laws of other dynamic metrics (e.g. strain rate, power density) are unknown in the literature.

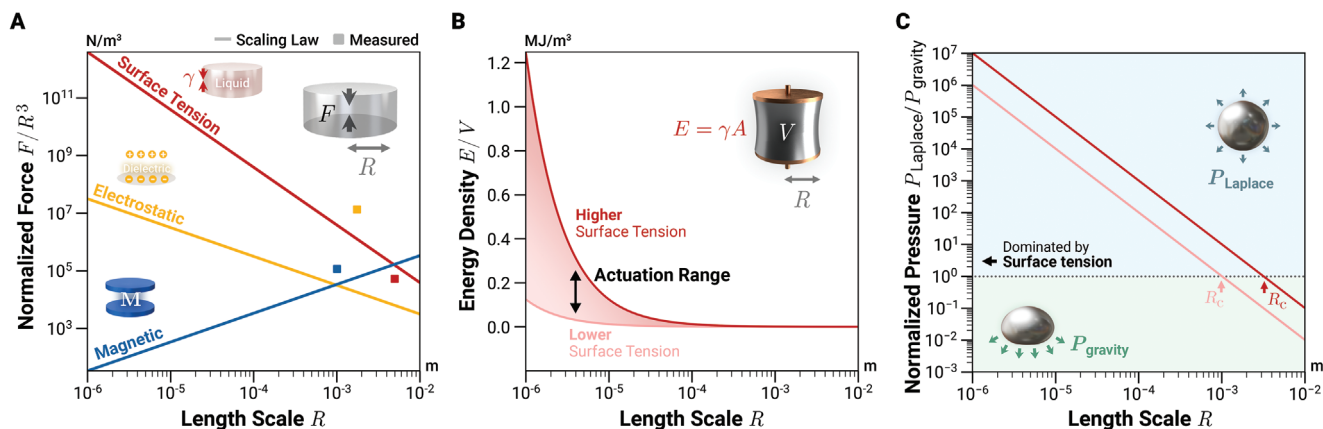


Figure 3. Scaling advantages of liquid metal actuators. A) Theoretical comparison of attractive force F across a cylinder (radius R) assuming surface tension, electrostatic, or magnetic as the governing force. Measured values (square marks) calculated from Refs. [4, 24, 147]. The scaling laws show a dominance of surface tension at $R \ll 1$ mm. Surface tension: Modeled with EGaln (surface tension: 624 mN m^{-1} [30]). Electrostatic: Modeled with a voltage of 1 kV across a thin film of VHB 4950 (dielectric constant 2.28). Magnetic: Modeled with magnetization of 1.1 MA m^{-1} . B) Theoretical surface energy per unit volume for a liquid metal cylinder (fixed gap: 1 mm). Surface tension is varied between a maximum of 624 mN m^{-1} and a minimum of 62.4 mN m^{-1} . The scaling laws show that at smaller R , the liquid metal has significantly higher energy density $E = \gamma A$ per unit volume (not to be confused with work output per unit volume, Section 5.3) and, as a result, has higher actuation range between the two extremes of surface tension. C) Theoretical excess pressure across a liquid metal droplet. Dark red curve (With higher surface tension 624 mN m^{-1}): At $R < R_c$ where R_c is the capillary length (3.2 mm for EGaln assuming the higher surface tension[23]), Laplace pressure dominates hydrostatic pressure due to gravity, which is a suitable length scale for all liquid metal actuators intended for zero influence by gravity. Light red (lower surface tension 62.4 mN m^{-1}) curves show a slightly smaller capillary length and less dramatic dominance by surface tension, which should also be considered in the actuator length scale selection.

- **Force:** The attractive force across a cylinder with a fixed gap (Figure 3A) is calculated and normalized by R^3 . Compared to electrostatic and magnetic forces as a source of attraction, surface tension has a clear advantage at smaller length scales.
- **Energy:** The surface energy of a liquid metal cylinder with a fixed gap (Figure 3B) is calculated and normalized by volume, which shows that surface energy is denser at smaller length scales, thereby increasing the range of actuation between the low surface tension and high surface tension.
- **Pressure:** Defined as the Laplace pressure (surface tension) normalized by hydrostatic pressure (gravity), a spherical liquid metal droplet is analyzed at different length scales. The influence by gravity becomes dominated by surface tension at smaller scales. For liquid metal actuators, the favorable length scale should be less than the capillary length (EGaln: 3.2 mm [23]).

While downscaling shows promise for many actuators by their scaling laws, there are other factors beyond scaling laws that affect the actuator behaviors. For instance, electrostatic actuators are more vulnerable to dielectric breakdown when the high voltages are applied across a smaller gap,^[148] which makes it impractical at very small scales. For liquid metal actuators, which have superior scaling properties in theory, several engineering challenges still need to be addressed. At microscales, the liquid metal actuator will be assembled from liquid metal droplets and other supporting components such as electrodes and electrolytes. One potential challenge is in the microfabrication of these supporting components, which may have greater implications in overall actuator performance than the creation and deposition of microdroplets. Delivering electrical current across the droplet and electrolytes at such a small scale presents another challenge. Lastly, we know no analysis of a theoretical lower bound for droplet

length scale, which can only be informed by the literature on microdroplet actuation (Figure 1F).

3. Design Principles: From Surface Tension to Actuation

The simplest design of a liquid metal actuator is a standalone droplet of liquid metal, which will not produce any useful work until placed in an electrolyte where surface tension of the droplet is modulated by a voltage applied across the electrodes (Figure 2A). Even such a working setup is hardly a real actuator, as the real challenges lie in addressing the following engineering requirements: How would the droplet move an object? How would it restore to the original shape? Would it ever stretch over the limit? Can we have multiple droplets working in synergy for higher performance? This section answers these questions by analyzing the major design principles for constructing practical liquid metal actuators based on the physics of surface tension modulation.

In order to analyze the design principles for liquid metal actuators in a systematic manner, this section is organized into the following distinct levels, where higher levels are built upon the foundations of the lower levels:

- **Elemental principles (low-level):** Droplet kinematics and degrees of freedom (Section 3.1). Electrochemical setup and activation (Sections 3.2 and 3.3).
- **Structural principles (mid-level):** Reversibility (agonist vs antagonist, Section 3.4). Structural integrity (coalescence vs separation, Section 3.5). Structural scalability (single-droplet vs multi-droplet, Section 3.6).
- **Functional principles (high-level):** Overall actuation functionalities (self-contractility,^[149,150] self-mobility,^[151]

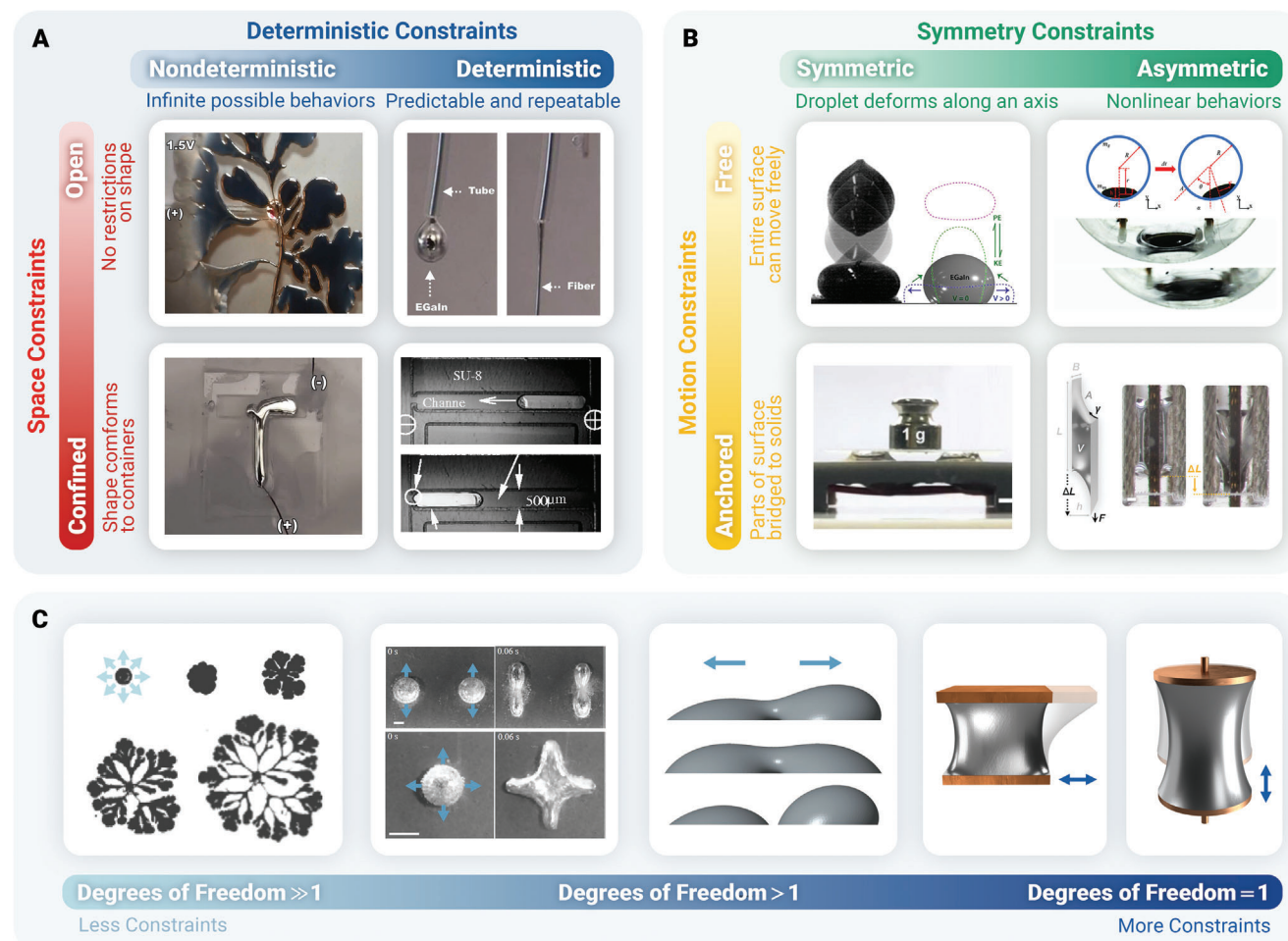


Figure 4. Kinematic constraints and degrees of freedom of liquid metal actuators. A) Left: By default, liquid metal droplets display nondeterministic behaviors in open space (e.g., fractal fingering of oxidized EGaIn droplet^[47]) or partially confined space (e.g., irregular spreading along the channel^[47]). Right: Further constraints can be imposed to the liquid metal droplet such that the outcome is predictable and repeatable (e.g., continuous stream^[47] and digital droplet traveling in a microchannel^[51]). Reproduced with permission.^[47] Copyright 2014, National Academy of Sciences. Reproduced with permission.^[51] Copyright 2000, IEEE. B) Left: When liquid metal droplets are restricted to symmetrical motion, their actuation is intended to be directed along a single axis and hence more likely to have a closed-form solution (e.g., vertical droplet bouncing^[66] and vertical compression^[60]). Right: More sophisticated motion is possible when motion is not necessarily symmetric (e.g. liquid metal wheel^[160] and muscle-inspired contraction^[24]). Reproduced with permission.^[66] Copyright 2022, American Chemical Society. Reproduced with permission.^[24] Copyright 2022, Wiley-VCH. Reproduced with permission.^[60] Copyright 2021, Wiley-VCH. Reproduced with permission.^[160] Copyright 2018, Wiley-VCH. C) The degrees of freedom (DOF) in a liquid metal actuator is dependent on the number and types of constraints imposed. From left to right: Unconstrained spreading of an oxidized droplet (DOF $\gg 1$),^[95] magnetically controlled 2D separation and merging of droplets,^[161] electrically controlled 1D separation and merging of droplets,^[61] 1D shear^[24] and normal^[23] motion liquid metal bridges. Reproduced with permission.^[95] Copyright 2017, American Physical Society. Reproduced with permission.^[161] Copyright 2020, American Chemical Society. Reproduced with permission.^[61] Copyright 2017, Wiley-VCH. Reproduced with permission.^[24] Copyright 2022, Wiley-VCH. Reproduced with permission.^[23] Copyright 2021, Royal Society of Chemistry.

self-reconfigurability^[152–155]) and supporting functionalities (self-healing,^[156] self-sensing,^[157] self-powering^[158,159]) (Section 3.7).

3.1. Kinematic Constraints

From a robotic perspective, liquids, like other soft bodies, have a much higher-dimensional state space than rigid bodies as their shape is determined by the motion of all the surface molecules. They are considered to have very high degrees of freedom ($\gg 1$). With a means of modulating the 1D surface

tension, a liquid can be viewed as *underactuated* since only a small number of configurations in the state space are reachable by surface tension modulation. This suggests that many useful modes of actuation, such as linear contraction with one degree of freedom, can only be achieved by imposing *kinematic constraints* on the liquid surface, where more constraints result in less degrees of freedom and simpler motions (Figure 4C). In principle, the selection of degrees of freedom is a trade-off between motion complexity (e.g., 1D liquid bridge stretching, 2D droplet merging and separation) and controllability (i.e., number of independent means of surface tension modulation).

It is useful to categorize kinematic constraints by their purposes and effects on the droplet behaviors. For instance, a space constraint can confine a droplet in a closed space (Figure 4A, bottom) as opposed to allowing it to move in an open space (Figure 4A, top). Likewise, a deterministic constraint (Figure 4A, right) can make the droplet behavior predictable and repeatable (e.g., by encapsulating the droplet in a closed unbranched tube or channel). Another common type of constraint restricts the motion by anchoring the droplet (Figure 4B, bottom) as opposed to letting it move freely (Figure 4B, top). Depending on the desired motion, sometimes a constraint needs to guarantee symmetry (Figure 4B, left) or asymmetry (Figure 4B, right) in the droplet motion.

Constraints may exist implicitly in all liquid configurations. For instance, a bare droplet placed on a glass slide has several implicit constraints. First, the incompressible droplet must keep a constant volume. Second, the wettability of the glass slide influences the droplet contact angles.^[162] Lastly, the existence of a glass slide provides a space constraint for the otherwise falling droplet. All kinematic constraints, whether explicit or implicit, play a central role in modeling and numerical simulation of the liquid shape, which relies on energy minimization with equality and inequality constraints.

3.2. Electrodes and Electrolytes

Every electrochemical liquid metal actuator is an electrolytic cell in which redox reactions are triggered by electrical stimulation. This requires the basic elements of two electrodes (anode and cathode) immersed in an electrolyte (Table 2). Since surface tension modulation requires an alternating polarity, it should be noted that the roles of anode and cathode alternate as well. For clarity, we differentiate the working electrode (in contact with the liquid metal droplet) from the counter electrode (in contact with the electrolyte). When the liquid metal is being oxidized (relaxed), the working electrode is the anode while the counter electrode is the cathode. Their roles are reversed when the reduction (contraction) takes place.

3.2.1. Electrodes

In many designs, the working electrode also functions as a kinematic constraint, with which the liquid metal droplet forms a liquid bridge between rigid metal plates. In these cases, the electrodes should have a strong metallic bonding with the liquid metal, which ideally guarantees a fixed wetted area that does not expand or recede during actuation.^[23] In a multi-droplet system, the number of electrodes proportionally increases with the number of droplets. It is important to avoid undesired merging of multiple droplets in this type of design by including gaps between electrodes. Electrically, any design should avoid short circuits between the working and counter electrodes.

3.2.2. Electrolytes

The electrolyte provides an ionic medium in which the redox reactions take place. For electrochemical oxidation of gallium,

aqueous solutions of alkaline hydroxide (e.g., NaOH, KOH) are typically selected^[23,24,47,167] for their ability to dissolve gallium into gallate ions ($\text{Ga}(\text{OH})_4^-$),^[136,168] which can later form gallium oxides (Ga_2O_3)^[24] at the interface. Besides alkaline electrolytes, it is also possible to use acids (e.g., HCl^[32,169]) and pH-neutral electrolytes (e.g., NaF^[47,170]). The electrolyte concentration has a direct influence on the rate of oxidation and actuation strain rate as a result (e.g., strain rate >1000 % with 2.5 M KOH^[24]). A high electrolyte concentration, however, also speeds up the production of hydrogen byproduct due to water electrolysis.^[59,171]

3.3. Electrical Activation



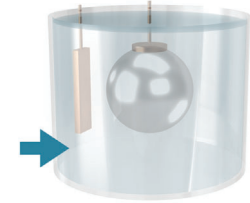
The electrical characteristics of liquid metal actuators are dependent on how surface tension is modulated. The electrical activation is summarized in Table 3. With the electrocapillary method, where surface tension γ is linked to interaction of the Coulomb forces, a quadratic relation to electric potential ($\gamma \propto \Delta U^2$) is expected. This is similar to electrostatic actuators (e.g., $p \propto \frac{\Delta U^2}{d^2}$ in DEA) for which mechanical response also comes from the Coulomb forces. By this method, typically a voltage $\approx 10^1$ V is necessary to generate a response similar to electrochemical methods, which only need $\approx 10^0$ V to initiate oxidation and reduction on the liquid metal surfaces. The voltage requirement in both methods is independent of the length scale. Current consumption, on the other hand, scales with surface area by current density, which is influenced by electrolyte concentration^[172] and distance between the liquid metal and counter electrode.^[173] For mm-scale liquid metal droplets, current draws $\approx 10^0 - 10^1$ mA have been reported.^[23,24,59]

The electrical activation for contraction (increasing surface tension) is fundamentally different from the activation for relaxation (decreasing surface tension) for several reasons. First, the mechanical response of the liquid metal actuator is governed by the increasing surface tension during contraction and more by the antagonistic forces (e.g., weights and additional load) during relaxation. Second, the contractile velocity is known to be significantly faster than its restoration (by ≈ 10 times^[24]), which should be taken into consideration for activation durations. Third, the liquid metal droplet is susceptible to overstretch and breaking during relaxation, which implies that it is risky to maintain a relaxing potential for too long. In general, the durations for contraction and relaxation are ≈ 0.1 s at a minimum, with relaxation typically kept at $\approx 0.1 - 1$ s.^[23,24] These characteristics are also the basis for activation at higher frequencies (typically up to 10 Hz^[24,59]).

3.4. Reversibility: Droplet Contraction and Relaxation

From an actuator standpoint, the reversibility of an actuator, or the ability to restore to the original state, can be analyzed by the degree to which the actuator response relies on its internal states. This characteristic, as summarized in Table 4, is central to the structural configuration of any actuator as it determines whether the actuator can operate by itself or should be paired with antagonists. We consider the following two types of responses:

Table 2. Summary of electrochemical setup of liquid metal actuators.

Component	Functions	Properties	Typical materials
<p>Working Electrode</p> <ul style="list-style-type: none"> As anode during LM oxidation/relaxation As cathode during LM reduction/contraction 	<p>Connection to LM droplet</p> <ul style="list-style-type: none"> Typically bond to LM metallurgically (perfect wetting^[23]). Electrical connection for LM droplets. Kinematic constraints for LM surfaces. Transmission of actuation output. 	<ul style="list-style-type: none"> Dimensions: Create kinematic constraints for LM surfaces. Motion: As an anchor for LM or as a moving part. Gap: Should avoid undesired merging in a multi-droplet system.^[24] 	<p>Metals with strong LM bonding capabilities</p> <ul style="list-style-type: none"> Copper^[163] Silver^[164] Gold^[165] Platinum^[166]
<p>Counter Electrode</p> <ul style="list-style-type: none"> As cathode during LM oxidation/relaxation As anode during LM reduction/contraction 	<p>Completing the electrical circuit. Act as the cathode when the working electrode is anode and vice versa.</p> <ul style="list-style-type: none"> Exposed in electrolyte. 	<ul style="list-style-type: none"> Dimensions: Depend on the droplet surface area to balance reaction rate and charges. Distance to droplets: Ideally minimized while avoiding short circuits. 	<p>Electrochemically inert (e.g., carbon-based) materials (e.g., graphite)^[59]</p>
<p>Electrolyte</p> 	<p>Ionic medium for LM redox reactions</p> <ul style="list-style-type: none"> Typically aqueous solution that allows free movement of LM^[47,48] 	<ul style="list-style-type: none"> Volume: Ideally minimized for better efficiency.^[24] Concentration: Affects solution conductivity and actuation speed. 	<p>Typically alkaline electrolyte with higher conductivities (e.g., KOH, NaOH) but other acidic and pH-neutral solutions are applicable.</p>

- **Continuous response** (without internal states): The actuator output is solely determined by its input variables. Typical examples include electric motors (torque is determined by current) and dielectric elastomers (stress is determined by voltage). These actuators can reverse by themselves.
- **One-way response** (with internal states): The actuator has internal states (e.g., liquid crystal phases, liquid metal surface tensions, natural muscle tensions) which are coupled with stimuli and respond in a manner that is more complex than the internal state-free actuators. These actuators are typically adept at switching from one state to another (e.g., transformation to austenite in SMA, reduction of gallium in LMA, depolarization in natural muscles) but often need help from an antagonist force to achieve reversible motion.

For liquid metal actuators to be reversible, the need for an antagonist can be explained by the typical force-length relationship (**Figure 5A**) in which the actuator at equilibrium is described by its force F , length ΔL , and surface tension γ . Contractions (isotonic and isometric) are only possible when surface tension (agonist) is paired with a competing force (antagonist). In other words, contraction only occurs when modulation of γ maps to the switch from $(F_1, \Delta L_1)$ to a different $(F_2, \Delta L_2)$. In this view, surface tension does not play an active role for *relaxation* but let the antagonist forces (e.g., load, gravity) take over as the surface tension becomes insignificant.

The most common antagonist for surface tension comes from the actuator load, which in most cases includes the weight of liquid metal itself (**Figure 5B**). With the load being the

Table 3. Summary of electrical activation of liquid metal actuators.

Electrical property	Typical values	Effects on actuation	Implication on design
Voltage	≈ 1 V independent of length scales ^[24,47,59,60]	<ul style="list-style-type: none"> • Voltage above the oxidative potential initiates LM oxidation, decreases surface tension and relaxes the droplet. • The reverse increases surface tension and contracts the droplet. 	Power source capable of ≈ 1 V is necessary for operating the liquid metal actuator.
Current	$\approx 10^0 - 10^1$ mA for mm-scale droplets ^[23,24] Depends on total surface area at a given length scale	<ul style="list-style-type: none"> • Current density may influence the efficiency of water electrolysis^[173] and overall performance. 	All electrodes and wires must be capable of carrying the current according to length scale.
Waveform	<p>Duration</p> <ul style="list-style-type: none"> • Reduction: Minimum ≈ 0.1 s, no upper limit. • Oxidation: Minimum ≈ 0.1 s, maximum $\approx 0.1-1$ s (to avoid overstretch^[23,24]) <p>Cycles</p> <ul style="list-style-type: none"> • Frequency: Typically up to 10 Hz^[24,59] for load-carrying actuation; resonate at ≈ 100 Hz for vibration.^[62] 	<ul style="list-style-type: none"> • Contraction/relaxation cycling behaviors are dependent on activation duration, with continuous oxidation posing the risk of overstretching the droplet (avoidable by a mechanical stop, Section 3.5). • Actuation frequency relies on the speed of contraction (factors: activation voltage, electrolyte concentration) and relaxation (factors: antagonist forces).^[24] 	Activation waveform should be programmed with a time limit on oxidation to avoid breaking the droplet (Section 3.5).

antagonist,^[23,60,143] the liquid metal actuator can be designed to produce linear contraction, rotation, and other complex motions. Depending on application, the actuators can be built in mm-scale to take advantage of the weights or in sub-mm-scale to operate in a regime dominated by surface tension.

Interesting interactions arise when the liquid metal droplet is designed to compete with elastic solids (Figure 5C) or fluid flow (Figure 5D). With elasticity (or *elastocapillary* coupling^[175,176]) being the antagonist,^[174] actuation can be viewed as transfer between elastic energy and surface energy. In another example^[62] where the droplet position (i.e., neutral vs shifted) is determined by the interaction between surface tension and fluid flow, actuation is characterized by creating an imbalance in surface energy.

Liquid metals can also function as antagonists to themselves (Figure 5E). Taking advantage of the high speeds ($>1000\% \text{ s}^{-1}$) in liquid metal contraction, two droplets can be configured with a prestretch that one droplet always relaxes when the other is contracting.^[24] In this way, higher operation frequencies (up to 5 Hz) can be achieved. This rapid switching by the inter-droplet configuration eliminates the need for an explicit load on the droplet to produce contraction.

3.5. Structural Integrity: Droplet Coalescence and Separation

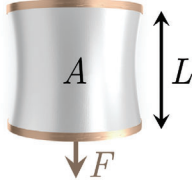
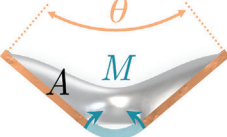
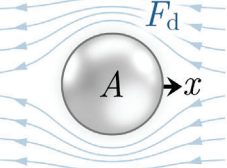
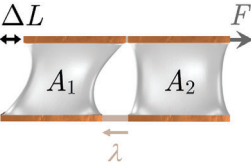
The high deformability of soft actuators hints at their vulnerability: they are subject to rupture when overstretched. Like solid materials, liquids typically contract transversally at the *neck* as strain increases (Figure 6A,B) before the system becomes unstable such that the only possibility to minimize the total potential energy is

by shrinking the neck toward zero, thereby *breaking* the liquid into smaller droplets.^[177] There exists a maximum strain below which the system is stable, where the droplet remains coalesced for actuation. An ideal design of liquid metal actuator should limit the stretch below this maximum to guarantee stable operation. Unlike solid materials, however, breaking in liquids is usually reversible by merging droplets,^[61,178,179] which suggests that liquid metal actuator has fundamentally higher reparability than typical self-healing in solid actuators. As represented by the examples in Figure 6A (stretching a liquid bridge between two solid spheres^[177]) and Figure 6B (shearing a liquid bridge between two rectangular plates^[24]), the analysis of the liquid metal behavior for a given volume typically identifies a coalesced regime where the actuator is operational, a separated regime where the actuator is damaged, and a transitional instability in between. Understanding where the boundary is located (i.e., maximum strain of coalescence) is important for determining relevant parameters in the liquid metal actuator design.

One simple approach to limit the droplet strain is by incorporating a mechanical hard stop into the design (Figure 6C). For a liquid bridge actuator with electrodes on both ends, such hard stops ideally restrict the gap between the electrodes.^[24,59] In practice, however, the liquid shape may be influenced by factors unstopable by gap constraints. For instance, it is observed that at a length scale where gravity is non-negligible, liquid metals in oxidized state tend to droop^[24] and spread^[95] regardless of the mechanical constraint.

Another strain-limiting strategy, particularly for restricting the oxidative behaviors, such as drooping and spreading, that may ultimately lead to breaking, is through a time constraint on the

Table 4. Types of antagonistic forces for liquid metal actuators.

Antagonist	Definition	Governing equations	Characteristics
Load	<p>Surface tension competes with a load (droplet weight or external forces acting on the droplet)</p> 	$L = \operatorname{argmin}_L \Pi(L)$ where $\Pi(L) = \gamma A - FL$	<ul style="list-style-type: none"> Total force = Weights of droplet and electrodes + Other force output Droplets at mm-scales (greater than LM characteristic length) are loaded with non-negligible self-weight \approx mN. At sub-mm scales, self-weights of droplets should become insignificant relative to surface tension and cannot act as an antagonistic force by themselves. Isotonic contraction (changing L while fixing F) or isometric contraction (changing F while fixing L). Can perform normal contraction,^[23,60] shear contraction,^[24] rotation and other complex motions. Applicable to most actuation tasks.
Elasticity	<p>Surface tension competes with an elastic restoring force, also known as <i>elastocapillary coupling</i> (e.g., surface tension competing with a flexural bending moment on an elastic hinge).</p> 	$\theta = \operatorname{argmin}_\theta \Pi(\theta)$ where $\Pi(\theta) = \gamma A - M\theta/2$ (Flexural)	<ul style="list-style-type: none"> Total bending moment = Moment due to weights of droplet and electrodes + Other torque output Bending by weight becomes insignificant at sub-mm scales. Work produced by surface tension is stored as elastic energy in the hinge, which is restored once the surface tension is reversed.^[174–176] Also applicable to any non-bending motion.
Fluid Flow	<p>Surface tension competes with a viscous fluid flow</p> 	$x = \operatorname{argmin}_x \Pi(x)$ where $\Pi(x) = \gamma A - F_d \Delta L$	<ul style="list-style-type: none"> Likely driven by local pressure differences (e.g., Marangoni effect) in a free space. When relaxed, the droplet assumes a neutral position ($x = 0$) and, when activated, moves against the flow by continuous Laplace pressure.^[62] Limited application in fluid flow where fluid drag on the droplet is near the surface tension.
Surface Tension	<p>Surface tension of two droplets competes against each other.</p> 	$\Delta L = \operatorname{argmin}_{\Delta L} \Pi_1(\Delta L) + \Pi_2(\Delta L - \lambda)$ where $\Pi(\Delta L) = \gamma A - F \Delta L$	<ul style="list-style-type: none"> Eliminate the requirement of an explicit load on the droplet to produce contraction.^[24] Functional in both weight-dominated and surface tension-dominated scales. Exact behavior can be programmed by setting prestretch λ. Frequency is purely determined by the LM strain rate ($> 1,000\% \text{ s}^{-1}$ with 2.5 M KOH electrolyte) and hence higher frequencies are possible.

* All $\min(\cdot)$ are subject to a constant volume V and additional kinematic constraints.

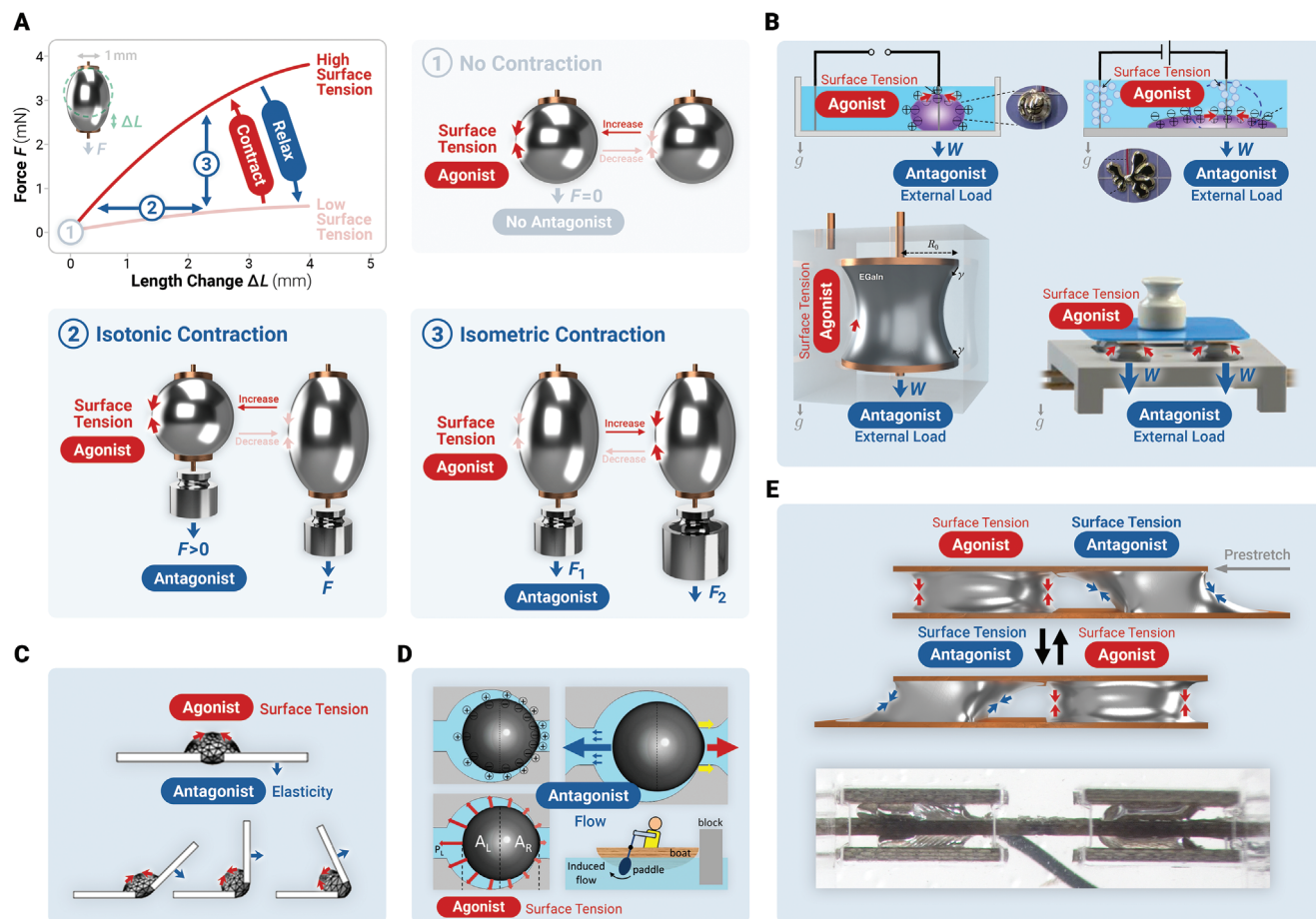


Figure 5. Agonist versus Antagonist: Reversibility in liquid metal actuators. A) Reversible contraction of liquid metal relies on pairing the agonist (i.e., surface tension of liquid metal) with an antagonist force to produce a pair of reversible motions (e.g., contraction vs relaxation, push vs pull). Otherwise no contraction will occur (1). Depending on the antagonistic configuration, the contraction can occur isotonicly (2) or isometrically (3). B) Typical antagonistic pairs with an external load (e.g., droplet self-weight or external payload to the actuator.) Adapted with permission.^[143] Copyright 2014, Springer Nature. Adapted with permission.^[23] Copyright 2021, Royal Society of Chemistry. Adapted with permission.^[60] Copyright 2021, Wiley-VCH. C) Elastically coupled surface tension, or *elastocapillarity*, where the elasticity acts as the antagonist to surface tension. Adapted with permission.^[174] Copyright 2007, American Chemical Society. D) Fluid flow as an antagonist to the surface tension. Adapted with permission.^[62] Copyright 2014, National Academy of Sciences. E) Two sets of liquid metal droplets alternately acting as agonist and antagonist, which enables operations at higher frequencies (5 Hz). Adapted with permission.^[24] Copyright 2022, Wiley-VCH.

oxidation duration. By discontinuing the oxidation before overstretched (typical $t_{\max} < 1$ s^[23]), the actuator is able to remain in the coalescence regime by a constrained length $h(t_{\max}) \leq h_{\max}$.

It is possible to completely reverse the damage to liquid metal actuators after the droplet separates. In theory, the split droplets can be merged mechanically or electrochemically through an imbalanced surface tension gradient. While demonstrated for electrical connection in a liquid metal transistor,^[61] electrically triggered self-merging of droplets also shows promise in active damage repair for liquid metal actuators.

The observation that state transitions between coalescence and separation involve changes in shape and tension suggests an alternative way to create a bistable liquid metal actuator, where the merging motion acts as contraction. Similarly, it is theoretically possible to achieve lengthening of an actuator by breaking a droplet, provided that the separated half-droplets are mechanically constrained. This configuration may potentially achieve a muscle-like “catch-state” or “lock-state”^[180] because the droplet

will stably maintain (i.e., be “locked” in) a merged or a separated state without applying current. This bistability also resembles the “step-and-hold” mechanism in stepper motors and is achievable with proper designs.

3.6. Structural Scalability: Toward Contact Splitting for Higher Performance

It is a common strategy in nature and engineered systems to generate greater forces with repeating units of smaller force producing elements that are arranged in parallel. For instance, natural muscles are capable of producing more forces when they comprise more contractile units (e.g., bicep: $\approx 10^5$ fibers,^[181] force $\approx 10^2$ N^[182]) and less forces with fewer units (e.g., stapedius: $\approx 10^3$ fibers,^[183] force $\approx 10^{-2}$ N^[184]). Similar strategies have been found in dielectric elastomers (e.g., single layer at mm-scale: force ≈ 0.2 N,^[4] compared to stacked DEA with 400 layers: force

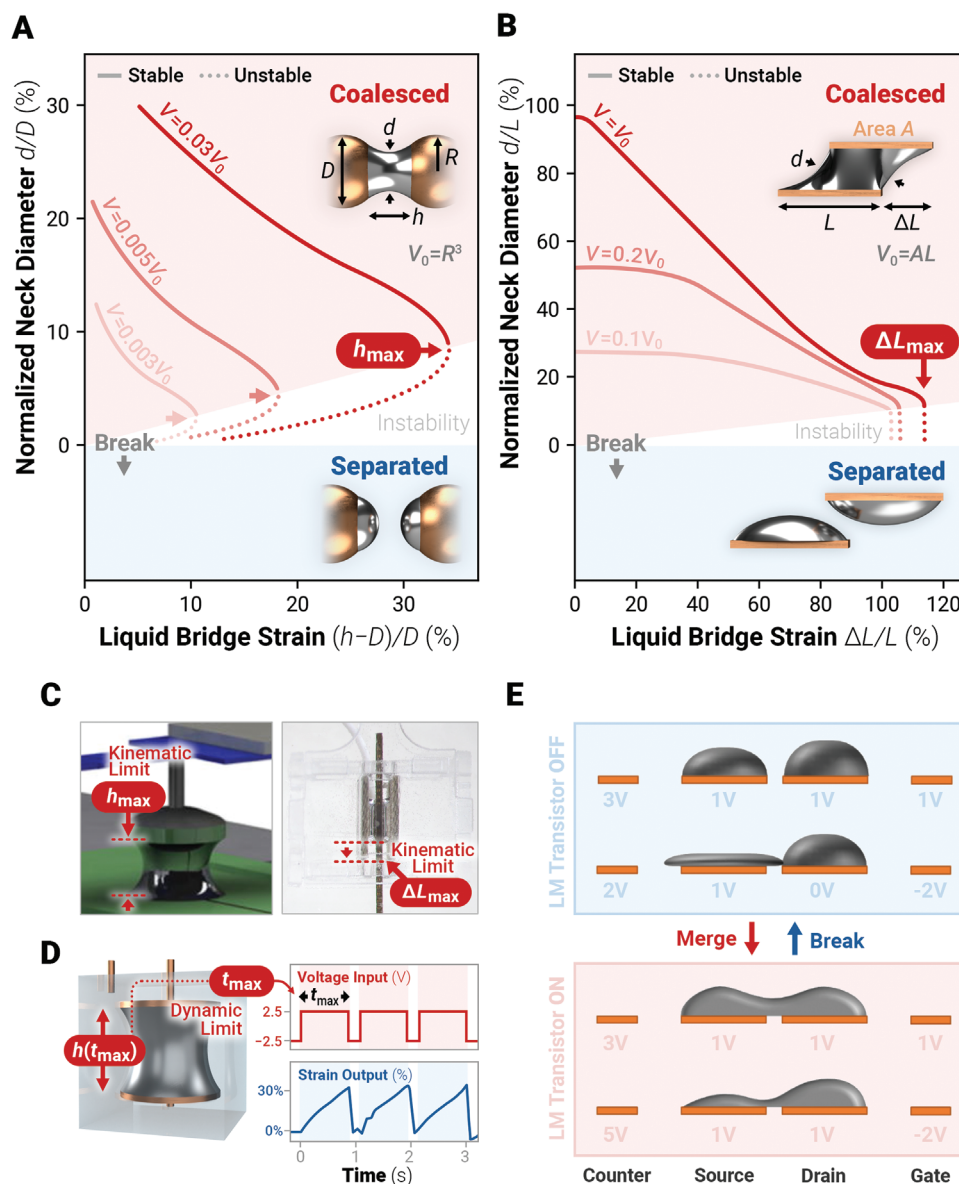


Figure 6. Structural integrity of liquid metal actuators. A) Upon stretching normally, a liquid bridge (distance h) between two spheres (radius R , diameter D) shrinks transversally at the neck, whose diameter d becomes unstable after a maximum strain is reached. The liquid bridge in the instability regime will likely break ($d \rightarrow 0$) and no longer be coalesced. Liquid bridges with larger volumes V have higher strain limits. Dimensionless theoretical curves from Ref. [177]. B) A sheared liquid bridge (simulation data from Ref. [24]) displays similar behavior of separation at instability, where the bridge neck diameter $d \rightarrow 0$. C) Kinematic limit on the length of liquid bridge (Left: Height limit h_{max} .^[59] Right: Length limit ΔL_{max} .^[24]) Adapted with permission.^[59] and Ref. [24] Copyright 2017, AIP Publishing. Copyright 2022, John Wiley & Sons, Inc. D) Dynamic limit on stretching (oxidation) duration, which prevents overstretch by a predefined time limit t_{max} . Adapted with permission.^[23] Copyright 2021, Royal Society of Chemistry. E) Separated droplets can be electrochemically merged by altering the potential gradients, which makes the separated droplets shear toward each other and causes merging. Adapted with permission.^[61] Copyright 2017, John Wiley & Sons, Inc.

$\approx 25.6 \text{ N}^{[185]}$). With these simple scaling strategies, however, the actuator volume is also multiplied, which may have implications in the applications (e.g., microbots typically have stricter volume constraints). It is therefore necessary to consider the *structural scalability* of an actuator, by which the output of an ideal actuator is *denser* at smaller length scales. With this strategy, the actuator can have higher overall performance by splitting the same volume to smaller units and summing up the output from every unit.

Surface tension, due to its scaling laws, is one of the very few types of forces that would benefit greatly from splitting the contact area. As previously discussed, work is primarily produced in a liquid by the intermolecular interactions between the liquid molecules in contact with the interface. By contrast, all other interior molecules have little contribution to actuation while taking up space. This motivates the splitting of liquid volume into smaller actuation units, whose total surface areas can be considered as a whole that have more contact with the interface. **Figure 7**

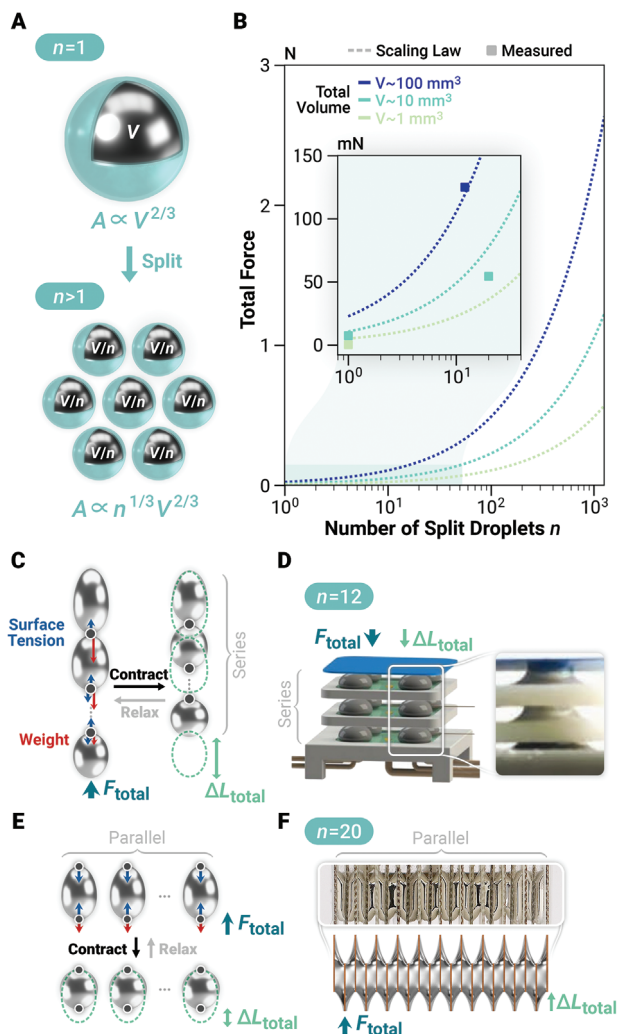


Figure 7. Surface splitting and structural scalability of liquid metal actuators. A) Scaling law of surface area by splitting a liquid volume V into n smaller droplets, where the surface area A is proportional to $n^{1/3}V^{2/3}$. B) Estimated total force with increasing number of droplets split from liquid volume V on the order of 1, 10, and 100 mm^3 . Squares: Actual force measurements from Refs. [23, 24, 59, 60]. C–F) Structural scaling strategies for organizing split droplets. (C) Droplets in series are capable of summing up deformation while the force output is susceptible to the cancellation of self-weights. (D) The experiment from Ref. [60] shows a series configuration (12 droplets stacked in 3 layers) scales poorly with each droplet having non-negligible weights. Adapted with permission.^[60] Copyright 2021, John Wiley & Sons, Inc. (E) Droplets in parallel in theory are capable of summing up force output at the same deformation. The effect of self-weights does not aggregate with the number of droplets in the parallel configuration. (F) The experiment from Ref. [24] shows a successful multi-droplet actuator (20 droplets) with greater total force output. Adapted with permission.^[24] Copyright 2022, John Wiley & Sons, Inc.

summarizes this strategy for liquid metals (i.e., splitting a liquid metal with volume V into n units of equal size) where each unit surface area $A/n = 9/(4\pi)(V/n)^{2/3}$ and therefore the total surface area A scales with $n^{1/3}V^{2/3}$ (Figure 7A). The theoretical total forces summed up from all the individual units can be estimated by $\frac{d}{dx}[\gamma A]$ ^[20] along the actuation direction x . Figure 7B predicts (with validation from experimental measurements for up to 20

droplets^[23,24,59,60]) that a total force ≈ 1 N from $V \approx 10^0 - 10^2$ mm^3 when the liquid metal volume is split into $N \approx 10^2 - 10^3$ smaller droplets.

3.6.1. Serial Configuration

A system of multiple droplets can be organized into many possible topologies, each having its own characteristics. At the lowest level, every connection between two or more droplets can be categorized into either serial or parallel. Note that it is implied that supporting mechanisms, whose effects are insignificant compared to surface tension, are incorporated into the design for coupling the droplet force and displacement. When organized in series, the hypothetical massless string of droplets will have equal tensile force anywhere (Figure 7C and Table 8). However, regardless of how small the droplets are, their weights quickly add up to an extent that interferes the overall behavior. As discovered with a compressive stacked setup,^[60] the mm-scale liquid metal actuator collapses when there are more than 3 layers (4 droplets per layer, Figure 7E). From the perspective of the i -th droplet along the series, with $i = 1$ being the bottommost droplet, this can be explained by the cancellation of surface tension by the weights of droplets, that is, $F_i = F_{\text{surface}} - (n - i)mg$ with the second term increases linearly with n . As a result, it now takes an even smaller mass m for the surface tension to resist a higher n .

By this analysis, stacking a larger number of liquid metal droplets into a contractile string may offer a possibility of higher displacement $\Delta L_{\text{total}} = \sum_{i=1}^n \Delta L_i$ but would need a sufficiently small length scale. For example, consider an ideal string of n spherical EGaIn droplets (radius R , density $\rho = 6250$ kg m^{-3} , surface tension $\gamma = 624$ mN m^{-1} ^[30]) in series. Assume that the string is anchored vertically at the top. The topmost droplet sees a downward net force $F_{\text{top}} \approx 2\pi R\gamma - \rho g(4/3)\pi R^3 \cdot (n - 1)$. For surface tension (first term) to be able to resist its self-weight (second term), it is necessary that the radius R is sufficiently smaller than a critical length R_{crit} , that is, $R < R_{\text{crit}} = \sqrt{\frac{3\gamma}{2\rho g(n-1)}}$. This implies that a string with $n = 10$ droplets needs to have a radius $R < 1.30$ mm while a string with $n = 100$ droplets needs a further smaller radius $R < 393$ μm for the topmost droplet to withstand the entire weight. Performance-wise, it can be estimated that displacement $\Delta L \approx R_{\text{crit}} \approx n^{-1}$ and hence the overall displacement $\Delta L_{\text{total}} \approx nR_{\text{crit}} \approx n^0$, which suggests that overall displacement from a series of n droplet, provided that they are sufficiently small, can be seen as algebraically independent of n .

3.6.2. Parallel Configuration

In parallel configurations of liquid metal droplets (Figure 7E), the overall displacement equals that from the individual droplets ($\Delta L_{\text{total}} = \Delta L_i$) and the overall force output is ideally the sum of all forces produced ($F_{\text{total}} = \sum_{i=1}^n F_i$). We note that n droplets are subject to their total weight $n \cdot mg$ (linear in n) in a parallel configuration, compared to $\sum_{i=1}^{n-1} (n - i)mg$ (quadratic in n) in a serial configuration. This shows the higher structural scalability of parallel configuration, which is demonstrated by a multi-droplet liquid metal actuator of $n = 20$ droplets in parallel (Figure 7F). Unlike serial configurations, however, parallel droplets do not produce

Table 5. Summary of performance of the liquid metal actuators.

Type	Metric	Definition	Typical values	Scalability
Static	Stress	$\frac{\text{Force Output}}{\text{Neck Area}}$	$\approx 10^3$ Pa (mm-scale) ^[23,24]	Higher stresses are possible at smaller length scales. (Theoretical: $\approx 10^6$ Pa at μm scale)
	Strain	$\frac{\text{Length Change}}{\text{Resting Length}}$	40% ^[24]	Higher strains are possible with larger droplet volumes (which would lower work density)
	Work Density	$\frac{\text{Force} \times \text{Displacement}}{\text{Volume}}$	$\approx 10^2$ J m ⁻³ (mm-scale) ^[23,24]	Higher work densities are possible at smaller length scales. (Theoretical: $\approx 10^6$ J m ⁻³ at μm scale)
Dynamic	Strain Rate	$\frac{\text{Strain}}{\text{Time}}$	$> 1,000\% \text{ s}^{-1}$ (typical) (Electrolyte: 2.5M KOH) ^[24]	Higher strain rates are possible with higher activation voltage or more conductive electrolyte (e.g., at higher concentration).
	Frequencies	Range of operational frequencies without significant degradation in output	≈ 10 Hz ^[24,59]	Higher frequencies are possible with higher strain rates.
	Power Density (Specific Power, Power-to-Mass Ratio)	$\frac{\text{Work Output/Time}}{\text{Mass}}$	≈ 0.2 W kg ⁻¹ (Estimated from Ref. [24])	Unknown
	Efficiency	$\frac{\text{Power Output}}{\text{Power Input}}$	$< 0.1\%$ ^[24]	Unknown
	Cycle Life	Number of cycles before significant degradation in output	$> 10^3$ cycles ^[24]	Unknown

more displacement than any individual droplet and, as a result, can only generate very small displacements when scaled down.

3.7. Liquid Metal Actuator Functionalities





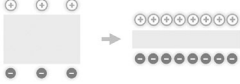
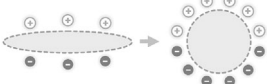
3.7.1. Actuation Functionalities

At a higher level, liquid metals are known for their versatile functionalities that produce or support actuation. This section examines the liquid metal actuators from a standpoint of

their complex roles in robots rather than simply as a work-producing device. In this view, an actuator can be seen as a means for the robot to deform (self-contractility), to transport (self-mobility), or to switch between states (self-reconfigurability). It is also useful to define actuation functionalities by what is changed (e.g., shape, location, configuration) as a result of actuation. We discuss these actuation functionalities as follows:

- **Self-Contractility:** Liquid metals are capable of muscle-like contraction (**Figure 8A**), typically in the form of

Table 6. Comparison of liquid metal actuators to other soft actuators.

Activation	Actuator	working principle	Key characteristics	Force Scaling Law	Work Density Scaling Law
–	Natural Muscle	Neural signaled sliding of protein filaments 	<ul style="list-style-type: none"> • Responds to electrochemical action potential ≈ 70 mV. • Consumes chemical energy, which can be stored as glucose within the muscle itself. • Very high cycle life ($\approx 10^9$ cycles) through metabolism. • High strain rate ($\approx 500\%$ s^{-1}). • Decent stress (10^3 Pa) and strain (20%). • Stiffness increases (5x) during contraction.^[2] • Contraction produces byproducts (heat, lactic acid) 	$F \propto L^3$	$\frac{W}{V} \propto L^0$
Electrochemical	LMA	Surface tension modulation of liquid metal droplets 	<ul style="list-style-type: none"> • Responds to redox reactions at ≈ 1 V • Very high strain rate ($> 1,000\%$ s^{-1}) • Muscle-relevant strain (20-80 %^[24]) • Stress and work density vary with length scale. • Contraction produces byproducts (hydrogen) • Very low efficiency in current designs ($< 0.1\%$^[24]) • Cycle life $> 10^3$ cycles^[24] (maximum unknown) 	$F \propto L$	$\frac{W}{V} \propto L^{-1}$
Electrothermal	SMA	Crystal structure transformation 	<ul style="list-style-type: none"> • Responds to temperature above austenite transition temperature. • Low efficiency ($< 10\%$) due to thermal dissipation. • Very high stress (200 MPa), work density (10 MJ m^{-3}), and power density ($> 1,000$ W kg^{-1}) compared to all other soft actuators. • Low strain rate ($\approx 10\%$ s^{-1}) and frequencies (≈ 1 Hz). • Cycle life: Strain dependent (300 cycles at $\approx 5\%$ strain, $> 10^7$ cycles at $\approx 0.5\%$ strain^[9]) 	$F \propto L^3$	$\frac{W}{V} \propto L^0$
	LCE	Liquid crystal phase transition 	<ul style="list-style-type: none"> • Responds to temperature above isotropic transition temperature. • Low stress (≈ 100 kPa) and high strain ($> 300\%$). • High cycle life ($> 10^6$ cycles^[243]) 	$F \propto L^3$	$\frac{W}{V} \propto L^0$
Electrostatic	DEA	Electrostatic attraction across an elastomer film 	<ul style="list-style-type: none"> • Responds to very high voltages (1-10 kV). Also vulnerable to dielectric breakdown at high voltages. • Very high strain ($> 300\%$^[4]) at high strain rate ($> 100\%$ s^{-1}^[244]). • Capable of very high frequencies (> 10 kHz^[244]). • Medium work density (150 kJ m^{-3}^[5,245]) • High power density (≈ 500-1000 W kg^{-1}^[246,247]). • High cycle life (10^6 at 50% strain, VHB^[9]) 	$F \propto L^2$	$\frac{W}{V} \propto L^0$
	HASEL	Electrostatic attraction across a liquid dielectric 	<ul style="list-style-type: none"> • Responds to very high voltages (1-10 kV). • Lower strain (79%), strain rate ($\approx 100\%$ s^{-1}) and frequencies (20 Hz) compared to traditional DEA.^[6,7] • High power density (≈ 100 W kg^{-1}^[6]) • Liquid medium enables self-healing for damage repair after dielectric breakdown. • High cycle life ($> 10^6$ cycles^[6]) 	$F \propto L^2$	$\frac{W}{V} \propto L^0$

- *Force scaling law:* Assume volume dependence (natural muscles, SMA, and LCE) and area dependence (DEA and HASEL).
- *Work density scaling law:* Assume all dimensions scale with L (i.e., gap and displacement scale with L) in electrostatic actuators. Therefore, work output $W \propto FL$ and work density $W/V \propto L^0$.

Table 7. Ideal designs and behaviors of liquid metal actuators.

Property	Ideal characteristics	Practical consideration
Droplet	<ul style="list-style-type: none"> LM surface area is maximized per unit volume. LM strongly adheres to the electrodes.^[23] Surface tension is the dominating force. 	<ul style="list-style-type: none"> The given LM volume is split into smaller droplets wherever possible. LM perfectly wets to electrodes by metallic bonding to metals is significantly higher than surface tension Influence of weight on actuator (e.g., orientation) should be considered for mm-scale droplets.
Electrode	<ul style="list-style-type: none"> Strong adhesion to LM droplets.^[23,249,250] Rigid-body kinematics relative to LM droplets. Electrochemically inert to the electrolyte.^[59] 	<ul style="list-style-type: none"> Surface oxide is removed to ensure bonding with LM. Ideally material with minimal thickness while being flexural rigid with respect to surface tension. Proper spacing to allow free movement of LM. Working electrode: Electrical and mechanical contact with LM only. Avoid corrosion to electrolyte. Common material: Copper.^[23,24] Counter electrode: Distance to LM is minimized to avoid power losses. Preferably electrochemical inert. Common material: Copper^[23,24] (subject to corrosion into cupric hydroxide), graphite.^[59]
Electrolyte	<ul style="list-style-type: none"> High electrical conductivity for higher actuation speed Electrolyte volume is minimized for encapsulation. 	<ul style="list-style-type: none"> Common electrolytes: KOH or NaOH at 1-3 M.^[23,24,47,59,60] Higher electrolyte concentration is preferred (Tradeoff: Higher rate of gas byproduct generation).^[24] Design should contain a minimal volume of electrolyte surrounding LM (Theory: A minimum electrolyte volume $\approx 1/10$ of LM surface molecules is sufficient^[24]).
Transmission	<ul style="list-style-type: none"> Reliable delivery of LM force and displacement output. 	<ul style="list-style-type: none"> Moving parts (e.g., shaft, cantilever) should maintain full range of motion according to the kinematic constraints. Typically coupled with the electrodes. Corrosion by electrolyte should be avoided.
Structure	<ul style="list-style-type: none"> LM droplets remain coalesced for actuation. 	<ul style="list-style-type: none"> Avoid droplet breaking through mechanical strain limits and electrical activation time limits. Optional: Droplet merging mechanism (self-healing)
Byproducts	<ul style="list-style-type: none"> Hydrogen gas from redox reaction should be minimized and efficiently handled. 	<ul style="list-style-type: none"> Design should avoid accumulation of hydrogen gas on LM surfaces For open-tank design, gas should be allowed for upward bubbling and evaporation. For encapsulation, excess pressure due to hydrogen growth should be considered.

liquid bridges that produce linear contraction and relaxation between plates.^[23,24,59,60] Similar to natural muscles, liquid metal contraction can be described as a one-way motion due to its requirement of an antagonist to restore.^[24] Both liquid metal actuators and natural muscles are electrochemically driven and generate byproducts (e.g., hydrogen gas with liquid metals, lactic acid with muscles) that are irrelevant to actuation and whose buildup often degrades the performance such as natural muscle fatigue.

- **Self-Mobility:** Liquid metals are capable of electric field-driven transportation from one location to another (Figure 8B), typically by a pressure gradient generated by continuous electrowetting,^[51,186–188] electrochemical oxidation,^[62,64,189] chemical-induced imbalance.^[137] It is possible for a liquid

metal droplet to carry cargo.^[190] As a mobile robot, the liquid metal droplets are suitable for moving through a confined space such as channel and tube due to their high deformability.^[47,53,191]

- **Self-Reconfigurability:** Liquid metals are capable of encoding information (e.g., logical on/off,^[56] fluidic open/closed,^[62] electrically conducting/insulating,^[61] optically passing/blocking^[192]) in bistable states, which are switchable through actuation (Figure 8C). Higher-order manipulation beyond bistability is possible and can be achieved in a magnetic field.^[161] Configurations of liquid metals typically express the electrical,^[61] mechanical,^[193] thermal,^[194] optical^[192] connection or disconnection between objects that are bridged by liquid metals.

Table 8. Theoretical limits of the liquid metal actuators.

Property	Governing equations	Theoretical limit
Strain	Rayleigh-Plateau Instability ^[255] Dispersion relation $\omega^2 \left(\frac{\rho R^3}{\gamma} \right) = kR(1 - k^2 R^2) \frac{l_0(kR)}{l_0(kR)}$ is unstable when $R < \frac{1}{k} \Rightarrow$ Droplet length $\lambda > 2\pi R$. Dimensionless Rupture Distance ^[177] (Empirical) Liquid bridge is ruptured when separation $2S > (1 + 0.5\theta) \left(\frac{V}{R} \right)^{1/3}$	Breaking strain: For a spherical droplet (radius R), <ul style="list-style-type: none"> Maximum strain $\epsilon_{\max} = \frac{\lambda}{2R} = \pi$ (Rayleigh-Plateau Instability) Maximum strain $\epsilon_{\max} = \frac{\lambda}{2R} \approx 0.81R^{-1/3}$ (Empirical^[177] with $\theta = 0$)
Frequency	Bandwidth Estimation from Strain Rate: (Assumed a cyclic 3 dB $\approx 70.7\%$ strain output) $f = \sqrt{2} \frac{\epsilon}{t}$	Bandwidth: <ul style="list-style-type: none"> $f \approx 14.14$ Hz for $\frac{\epsilon}{t} = 1000\% \text{ s}^{-1}$ Higher bandwidths are possible with higher electrolyte conductivity.^[24]
Volume	Actuator Total Volume: $V_{\text{Actuator}} = V_{\text{LM}} + V_{\text{Electrode}} + V_{\text{Electrolyte}}$	LM Volume: Preferably split into smaller volumes. Electrode Volume: Typically $\propto L^2$ assuming negligible thickness. Electrolyte Volume: Minimum $\approx 10\%$ of LM volume to enable redox reactions.
Repetition	Serial Configuration of n Droplets: <ul style="list-style-type: none"> Force: $F_{\text{total}} = F_i - \sum_{i=1}^{n-1} (n-i)mg$ Displacement: $\Delta L_{\text{total}} = \sum_{i=1}^n \Delta L_i$ Parallel Configuration of n Droplets: <ul style="list-style-type: none"> Force: $F_{\text{total}} = \sum_{i=1}^n F_i$ Displacement: $\Delta L_{\text{total}} = \Delta L_i$ 	Serial Configuration: Forces cancel quickly at mm-scale. ^[60] Parallel Configuration: No theoretical limit on force stacking. ^[24]

3.7.2. Supporting Functionalities

The unique versatility of liquid metals also gives them a wide range of functionalities in support of actuation. For instance, their fluidic properties provide the ability to repair after breaking (self-healing). Liquid metals are also known for their strain-dependent electrical properties that can be used for measurement (self-sensing). Lastly, liquid metals can function as electrodes in a voltaic cell, which show promises in providing or augmenting the power for actuation without the need for an external energy source (self-powering). We discuss these supporting functionalities as follows:

- **Self-Healing:** Liquid metals are capable of reconnection after a droplet breaks, which can take place actively (e.g., by actuating the liquid metals with an electric field^[61]) or passively (e.g., by flowing more liquid metals into the cracks^[195]). Unlike solid materials such as elastomers and hydrogels, whose healing typically needs a minimum of tens of seconds for polymeric crosslinking,^[198,199] healing of broken liquid droplets by merging arguably occurs instantaneously, where the two droplets merge as soon as their molecules begin to contact (Figure 8D).
- **Self-Sensing:** Liquid metals are capable of measuring their own states such as strains by the dependence of their electrical conductivity on the geometry. Strain is typically sensed by liquid metals encapsulated in an elastomeric channel^[200–203] (Figure 8E). Besides strain, stress^[204,205] and inertia^[206,207] are also possible with liquid metals.

- **Self-Powering:** Liquid metals are capable of spontaneous energy production in a voltaic cell (Figure 8F). Typically, the liquid metals function as the anode of the battery.^[197,208,209] Recharging of liquid metal-based batteries is possible through reversible plating of gallium on manganese dioxide.^[197] The liquid metal batteries in the literature typically produce a current of $\approx 0.5 - 1.5 \text{ mA cm}^{-2}$ at a voltage $\approx 1 - 2 \text{ V}$, which in theory can initiate the redox reactions for liquid metal actuators. It is unknown, however, whether practical actuation such as contraction or transportation of liquid droplets can be sufficiently powered by the energy that they generate. Beyond electrochemistry, it has been shown that liquid metal actuation can be completely driven by onboard chemical reactions similar to fuel consumption (e.g., aluminum-driven self-propulsion of liquid metals^[137]), which may also inform future iterations of self-powered liquid metal actuation.

4. Fabrication Methods: Integration of Liquid Metal Droplets for Actuation

For the purpose of actuation, the devices with modifiable surface tension of liquid metal droplets or bridges, which are the focus of this review, where liquid metals are the *active* components, are fundamentally different from other materials with liquid metal dispersion, which typically benefits from enhancing their electrical and thermal conductivity, where liquid metals are the *passive* components such as microdroplets embedded in elastomers^[68,210–212]. In terms of the principles from Section 3, the former tends to require a fabrication process that

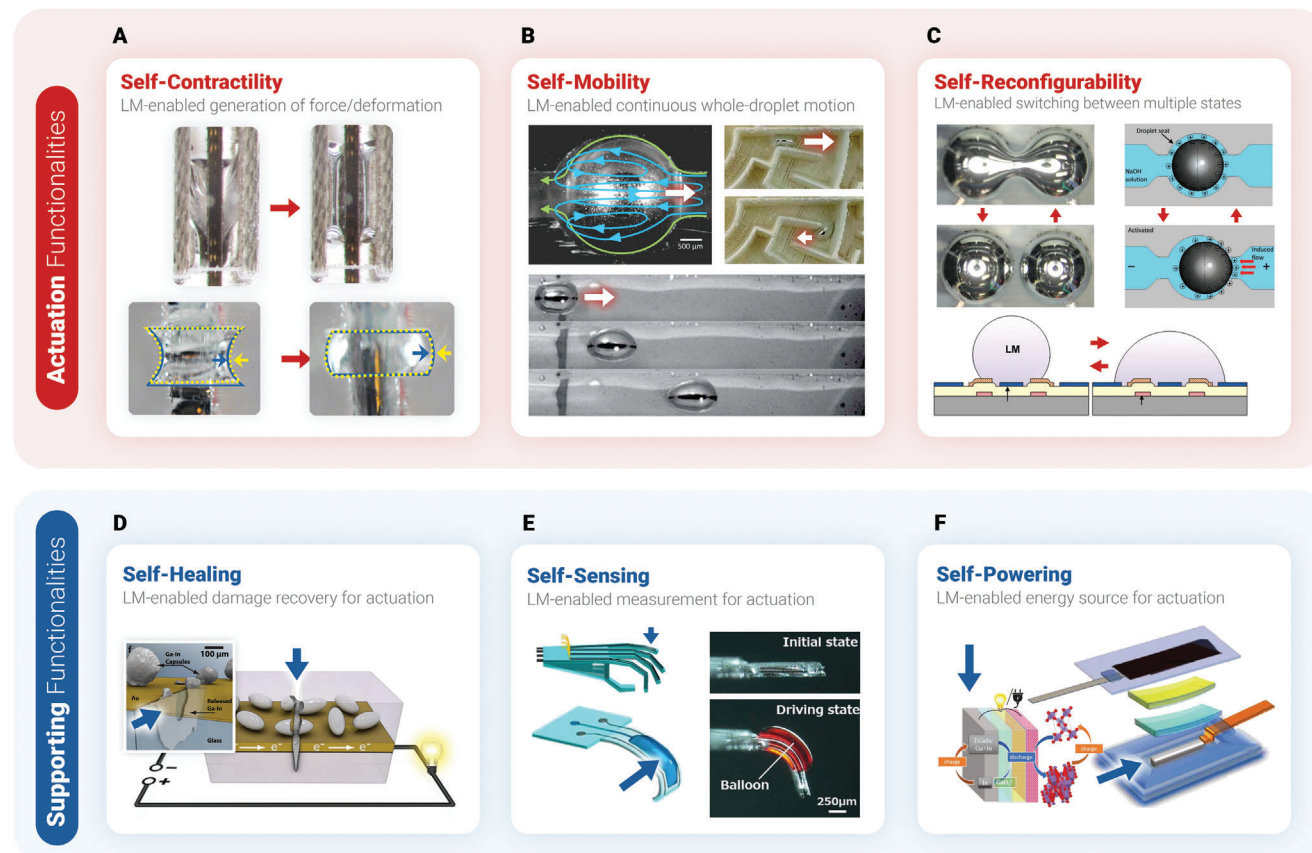


Figure 8. Versatile functionalities of the liquid metal actuators. The versatility of liquid metals enables functionalities that directly enable A–C) or support D–F) actuation. (A) Liquid metals are capable of contraction by surface tension modulation. (Top: Muscle-inspired contraction,^[24] Bottom: Parallel-plate contraction^[23]) Adapted with permission.^[24] Copyright 2022, John Wiley & Sons, Inc. Adapted with permission.^[23] Copyright 2021, Royal Society of Chemistry. (B) Liquid metals are able to travel from any position to a controlled destination by continuous electrowetting. (Top left: Liquid metal pump,^[62] Top right: Liquid metal traveling in a maze^[189], Bottom: Liquid metal traveling in a channel^[64]) Adapted with permission.^[62] Copyright 2014, National Academy of Sciences. Adapted with permission.^[64] Copyright 2013, Royal Society of Chemistry. Adapted with permission.^[189] Copyright 2020, Royal Society of Chemistry. (C) Liquid metals can switch between multiple stabilities by actuation. (Top left: Connected vs disconnected states in a liquid metal transistor,^[61] Top right: Stopped vs pumping in a liquid metal pump,^[62] Bottom: Power off vs on in a liquid metal switch^[56]) Adapted with permission.^[61] Copyright 2017, John Wiley & Sons, Inc. Adapted with permission.^[62] Copyright 2014, National Academy of Sciences. Adapted with permission.^[56] Copyright 2008, IEEE. (D) Liquid metal can recover electrically and mechanically from damages. Adapted with permission.^[195] Copyright 2012, John Wiley & Sons, Inc. (E) Liquid metal can sense its own shape change. Adapted with permission.^[196] Copyright 2018, IEEE. (F) Liquid metal can function as battery electrodes. Adapted with permission.^[197] Copyright 2019, John Wiley & Sons, Inc.

heavily relies on various structural considerations (i.e., architectures for structural reversibility, integrity, and scalability) for achieving prescribed actuation functions (e.g., contraction and mobility) are built. By contrast, fabrication of materials with liquid metal dispersion is generally more concerned with the aggregation of droplets across a polymeric medium, whose overall functions (e.g., as conductive ink,^[213] self-healing circuit,^[156] thermal conductor^[214]) are enabled by the interplay of their elemental properties and less by meso/microscale architectures and mechanisms.

From another perspective, this difference in fabrication steps is a result of the underlying operation principles, which can be categorized into interfacial and volumetric interactions in liquid metal droplets. Functionalities enabled by interactions across the interface, such as charging and oxidation, typically require more complex architectures than those across the entire liquid metal volume, such as providing pathways for current or heat. For the

scope of this review, this section focuses on the structural considerations (e.g., components, mechanisms, integration) for the assembly of liquid metal actuators with modifiable surface tension.

4.1. Components for Surface Tension Modulation in Liquid Metals

The minimal electrical setup for surface tension modulation in liquid metals (Figure 2A) consists of a liquid metal droplet (or a liquid metal bridge if wetted to other metallic surfaces), whose surface tension is modulated by activation potentials (provided by an external power source) between an electrode (typically connected to the liquid metal droplet both electrically and mechanically) and a counter-electrode. The requirement for an electrolyte as an electrical or electrochemical medium is

dependent on the modulation method. For instance, electrowetting-on-dielectric achieves charging through high voltages across a dielectric and does not need an electrolyte. The intended motion of the droplet (e.g., whole-droplet transport, self-contraction) also affects the degree to which the fabrication should leave the droplet wetted on the surface. In general, the challenges in fabrication of these components vary at different length scales, where mm-scale droplets are subject to influences by their weights and sub-mm-scale droplets have the same physical challenges as in all the microfabrication schemes.^[215] The general fabrication consideration is summarized as follows.

4.1.1. Droplet

Liquid metals, particularly gallium alloys with low melting points are favored. The most significant challenge in creating liquid metal droplets at a prescribed volume is the influence of the metal oxide layer, which often needs to be removed to avoid the non-Newtonian rheology.^[216] Since a liquid metal droplet in many configurations needs to be anchored to metal plates by metallic bonding, which can be difficult with the presence of metal oxides, the production of liquid metal droplets needs to minimize or eliminate the oxide skins before assembly. For gallium-based liquid metals, this is typically done by chemically dissolving the gallium oxide in alkaline hydroxides (e.g., NaOH and KOH^[47]) or acids (e.g., HCl^[217]).

Further challenges remain for creating microscale droplets with accurate size control, which can be categorized into monodisperse (uniform in size) and polydisperse systems (non-uniform in size). Sonication is a popular method for producing a larger number of small-scale droplets in a nonsolvent but usually produces droplets with a wide range of diameter distribution.^[213,218] For creating uniform liquid metal droplets for actuation, monodisperse methods such as microfluidic flow focusing^[218–220] are more suitable. In certain configurations, such as EWOD droplet arrays, the entire liquid volume can also be stored in a common reservoir from which smaller droplets are withdrawn by electric field.^[221–223] Lastly, with prescribed dimensions and gaps, dip coating can be used to create a system of liquid metals that are wetted to other metallic surfaces.^[217]

4.1.2. Electrode

Material selection of the electrodes depends on whether they are in contact with the liquid metal droplets or electrolyte. For electrodes that represent the interior potential of a liquid metal droplet, metals known to be highly wettable to the liquid metal are usually selected. Copper, for instance, is a common electrode material for wetting gallium. For liquid metal actuators at length scales $\approx 0.1 - 1$ mm, patterning of copper can be achieved by conventional PCB milling or etching techniques on copper-laminate sheets of glass-reinforced epoxy such as FR-4.^[23,24] For counter electrodes that represent the exterior potential, on the other hand, electrochemically inert materials such as graphite are favorable. Many implementations that use chemically reactive metals such as copper to be in contact with the electrolyte (e.g., NaOH or KOH) have also reported long-term corrosion.^[24,61]

For instance, cupric hydroxide, a blue insulating patina-like substance, is formed from the reaction between copper and alkaline hydroxide. In the case of EWOD, the electrodes are not in contact with the liquid metal but separated with an insulating coating, such as PDMS,^[224] gel,^[225] Teflon^[226,227] and polyimide^[228], with a thickness ranging from ≈ 10 nm to $\approx 10 \mu\text{m}$ depending on the dielectric properties.^[229]

4.1.3. Electrolyte

As an ionic medium, the electrolyte is typically an aqueous solution in which electrocapillarity or electrochemical redox reactions take place. Although the solution can be acidic (HCl,^[217,230] acidified siloxane^[231] and silicone^[58] oil), alkaline (NaOH,^[47,59,61,62,232,233] KOH^[23,24]), or pH-neutral (e.g., NaF^[47]), the electrolyte is typically selected in accordance with the particular modulation method. For instance, there is a chemical benefit for using alkaline hydroxide solutions with electrochemical redox reactions of gallium, where gallium oxide is soluble in these solutions at a electrically neutral potential.

For electrochemical modulation, the ionic concentration of the electrolyte solution (and hence the electrical conductivity) has a direct effect on the rate of redox reactions and actuation speed as a result. Higher conductivities are possible by electrolyte selection (e.g., at the same molar concentration 1 mol L^{-1} , KOH has higher electrical conductivity: 20.13 S m^{-1} ^[234] than NaOH: 17.6 S m^{-1} ^[235] both at 20°C) and concentration (e.g., KOH has higher electrical conductivity at 5 mol L^{-1} : 56.03 S m^{-1} than 0.5 mol L^{-1} : 9.37 mol L^{-1} ^[234] both at 20°C).

The use of aqueous electrolyte in liquid metal actuators limits their practical applications. For dry-air operation, the electrolyte solution would need to be encapsulated in a container, where design challenges remain. Alternatively, dry electrolytes based on ionically conductive hydrogel such as polyacrylamide^[236,237] have been used for interfacing with liquid metals and show promise for better encapsulation. However, encapsulation with gel electrolytes would likely also trap the hydrogen gas produced by the redox reactions, which itself presents another design challenge.

4.2. Assembly of Liquid Metal Actuators

The general assembly strategies for liquid metal actuators, in particular for electrochemically modulated contraction, are concerned with hierarchical bridging of liquid metal droplets between the electrodes. While a single-droplet system can be assembled by manual placement of the droplet,^[23] multi-droplet systems at higher dimensionalities (e.g., chain of liquid metal droplets in 1D^[24] or planar/multi-planar arrays in 2D and 3D^[60]) can benefit from self-assembly methods (e.g., dip coating^[238]) by which a uniform volume of liquid metal can be orderly coated and bridged between each pair of electrodes.^[24] With these methods, droplet assembly is self-driven toward an equilibrium where excess volumes break up from oversized liquid bridges until pairwise stability is reached.

Structural arrangement is another key factor in the assembly for kinematically constrained liquid metal actuators. For instance, in actuators where the droplets need to bridge two electrodes in parallel in order to achieve a particular motion (e.g.,

shear contraction^[24]), the overall design that houses the electrodes should encode such structural constraints (e.g., by patterning multiple electrodes on the same rigid sheet^[60,61]). Besides electrode dimensions, electrode gaps are another common structural factor, where the resting gap of the liquid bridge is programmed either by predetermined mechanisms (e.g., housing electrodes in an acrylic assembly^[24]) or by the geometry of the droplets themselves (e.g., droplets, upon assembled, are stabilized at an energetically favored gap^[24,60]).

5. Actuator Performance: Toward Higher Work Densities in Small-Scale Actuators

This section quantifies the actuation performance of the liquid metal actuators and analyzes their advantages over other types of soft actuators. As a work-producing device, every actuator can be characterized by the ability to generate force and displacement. In the context of scalability, particularly for applications at smaller scales for microrobotics, the performance is often normalized by volume such that meaningful comparisons can be made across different length scales. We will highlight the unique characteristic of liquid metal actuators where work densities are higher at smaller length scales, which shows promises in achieving higher performance with the same volume (Section 3.6). A higher-level comparison of the liquid metal actuators to other types of soft actuators will be provided to highlight the advantages and limitations of the liquid metal actuators.

5.1. Definition and Typical Values of Liquid Metal Actuator Performance

5.1.1. Static Performance

Force generation in liquid metal actuators (Table 5), when normalized by their cross-sectional areas, is typically $\approx 10^3$ Pa at mm-scales^[23,24,59,60] (compared to 10^5 Pa in natural muscles^[9]) and expected to increase at smaller length scales (e.g., 10^6 Pa predicted for μ m-scales). The actuation strain, on the other hand, is strongly influenced by the actuator design factors such as kinematic constraints, volume, and aspect ratio, although recent work has reported representative values near 40%^[23,24] (compared to typical 20% in natural muscles^[9]). Based on the force-length relationship, the work and its volumetric density can be calculated (measured: $\approx 10^2$ J m⁻³ at mm-scale, predicted: $\approx 10^6$ J m⁻³ at μ m-scale, Table 5). Scaling of work densities will be further discussed in Section 5.3. Overall, the liquid metal actuators can generate high stresses (at a sufficiently small length scale) at a decent strain (in a range relevant to natural muscles).

5.1.2. Dynamic Performance

Liquid metals, when electrochemically actuated, are capable of contraction at very high strain rates (>1000 % s⁻¹,^[24] compared to >50 % s⁻¹ in natural muscles^[9]). Cyclic actuation, which is known to have a cycle life of $>10^3$ cycles^[24] (compared to 10^9 in natural muscles^[9]), has a bandwidth that is theoretically

estimated^[23] and experimentally characterized^[24] at ≈ 10 Hz. On the downside, low efficiency ($< 0.1\%$ ^[24]) and low specific power (≈ 0.2 W kg⁻¹, estimated from Ref. [24]) are found by recent work, whose exact mechanism and possibility for improvement are unclear. In Section 6.3.3, we will discuss possible limiting factors on efficiency. Cycle life has been observed to be at least thousands of cycles without measurable degradation (at 1 Hz for 1 h,^[24] Table 5) but the maximum number of operational cycles remains an open question. Overall, the liquid metal actuators have remarkable dynamic performances brought about by their high contraction speeds.

5.1.3. Implication of Performance Definitions

As comparisons are often made between actuators for which performances do not have exactly the same definitions, caution is needed in interpreting the values across all the types and implementations of soft actuators. One notable example is actuation strain, whose definition varies by the displacement of interest (e.g., axial strain^[23,24,185] vs area strain^[4,239]) and the reference length (e.g., to normalize by the minimum^[60] or the maximum length^[24]). Ambiguities may also exist in the calculation of specific power and work density, where the actuator volume and mass may or may not include the entire supporting structure (e.g., all of the electrodes and electrolytes in the liquid metal actuators), in which case assumptions must be made (e.g., by assuming the electrodes and electrolytes can be negligible small compared to the liquid metals) to justify for a particular definition. The errors due to varying definitions, however, are relatively small that meaningful comparisons can generally be made within an order of magnitude.

5.2. Analytical Models and Numerical Simulation

The evaluation of the static performance of any actuator is based on their stress-strain relationship, or in the simplest case, the force-length relationship in a linear contractile actuator such as natural muscle. For a liquid metal actuator, this relationship can be modeled analytically by solutions to a closed-form differential equation or numerically by energy minimization of a geometric mesh. In both cases, the actuator length generally takes the form $\Delta L = \text{argmin } E(\Delta L; F)$ where E is the system potential energy associated with the droplet shape and load (simplified to ΔL and F in linear contraction). For a closed system where only shape and force are concerned, the potential energy has the form $E(\Delta L; F) = \gamma A - F\Delta L$, where A is the surface area.^[23,24] Several assumptions are typically made to simplify the model. For instance, influence by gravity on droplets at smaller length scales can be neglected. It is also common to restrict the model to a coalesced droplet and neglect the behaviors in the separation regime.^[23] In terms of differential geometry, the liquid metal surfaces can be assumed to have a constant mean curvature H ^[240,241] as a result of pressure balance in the Young–Laplace equation $P = -2\gamma H$, which can lead to exact solutions and further simplifications.^[23] These ideal mathematical models, however, only exist for a few special cases such as liquid bridges with normal stretches. Shapes under more complex motions, such as liquid bridges with shear stretches, on

the other hand, do not have a close-form expression and must resort to numerical simulation such as the Surface Evolver^[242] for energetically stationary results. In general, a model should provide the predictive power that captures the nonlinearities in the force-length relationships.

5.3. Work Density: Evaluations and Theoretical Predictions

For a liquid metal actuator with a particular kinematic configuration (e.g., linear contraction: force F , displacement x , volume V), the work density can be theoretically evaluated anywhere on the force-length curve $F(x)$ by $(F\Delta x)/V$ (assuming isotonic contraction). For meaningful comparison, however, the typical work density (i.e., the average $(F\Delta x)/V$ across all possible F and x) or the maximum work density (i.e., the largest possible $(F\Delta x)/V$ across all possible F and x) are calculated. The experimental measurement can be carried out in a similar manner, where the actuator load and displacement are recorded for the calculation. It should be noted that the work density is not a measure of the surface energy density ($E = \gamma A$ with A always being spherical when unconstrained) but rather of the ability to generate mechanical work per unit volume from a kinematically constrained droplet. In other words, measuring surface energy in one particular configuration (F , x) is not necessarily related to measuring work output between two states (F_1 , x_1) and (F_2 , x_2). This metric provides a way to quantitatively compare the actuation capability among different actuators of interest.

As surface tension is one of the few types of forces that scale linearly with length (i.e., $F \propto L$), the work density should approximately scale inversely with length (i.e., $W/V \propto L^{-1}$) (Table 6). This suggests that smaller lengths give higher densities of work, a scaling law that is confirmed by the simulation results with various designs.^[23,24] For instance, in circular-plate designs for normal contraction^[23,60] the dimensions should be described by independent radius R and gap h , whereas in rectangular-plate designs for shearing contraction^[24] more variables are necessary for describing the aspect ratio. In all cases, the liquid metal actuator is predicted to perform with higher work densities at smaller scales (e.g., reaching $\approx 10^5 \text{ J m}^{-3}$ at $L < 50 \text{ }\mu\text{m}$,^[24] which is comparable to a typical dielectric elastomer actuator). This theoretical trend, as captured in Figure 1F with mm-scale actuators, will need further validation at smaller length scales.

5.4. Comparison of Liquid Metal Actuators to Other Soft Actuators

To put the liquid metal actuators in the context of electrically responsive actuators in order to compare their advantages and drawbacks, we summarize the key characteristics of electrochemical, electrothermal, and electrostatic actuators and compared them to natural muscles (Table 6). Categories here are meant to be high-level descriptions of how work is produced by electrical activation. For instance, with electrochemical actuators, electrical activation triggers chemical reactions that eventually produce mechanical work (e.g., natural muscles contract with the energy provided by ATP hydrolysis, which is initiated by an electric potential). By this analysis, we highlight the working principles of

electrochemical (by chemical reaction), electrothermal (by phase transition^[248]), and electrostatic actuators (by Coulomb forces of attraction). The liquid metal actuators, although operating with principles that are unrelated to natural muscles, are also electrochemical actuators (i.e., contraction is generated from the energy released by electrically triggered redox reaction). Some key differences among these actuators are the activation voltage (electrochemical < electrothermal < electrostatic), stress output (electrochemical < electrostatic < electrothermal), and strain rate (electrothermal < electrostatic < electrochemical). In general, electrochemical actuators stand out for their meaningful performance while requiring only a low voltage input.

5.5. Comparison of Static Performance

LMA architectures have a length-dependent stress ($\approx 1 \text{ kPa}$ at mm-scale and $\approx 1 \text{ MPa}$ at μm -scale, compared to muscles: 0.1 MPa), whereas SMA is capable of very high stress output regardless of the length scale (200 MPa). In general, LMAs produce modest strains (theoretical 20-80%, measured 20-40%, compared to muscles: 20%), whereas large strains are a hallmark of electrostatic actuators (DEA: $>300\%$ area strain, HASEL: 79% axial strain). LMAs have a work density $\approx 10^2 \text{ J m}^{-3}$ at mm-scale and are predicted to have higher work densities at smaller scales, in contrast to shape memory alloys, which has a significantly higher work density (10 MJ m^{-3}). Overall, in terms of static performance, LMAs perform similarly to natural muscles and opposite to SMA (by stress) and DEA (by strain).

5.6. Comparison of Dynamic Performance

LMA architectures are capable of very high strain rates ($>1000 \text{ }\% \text{ s}^{-1}$, relevant to muscles: $500 \text{ }\% \text{ s}^{-1}$), compared to very low strain rates in SMA ($\approx 10 \text{ }\% \text{ s}^{-1}$). LMAs also have a good bandwidth ($\approx 10 \text{ Hz}$, comparable to natural muscle: 20 Hz), compared to the very high bandwidth in DEA ($>10 \text{ kHz}$) and the very low bandwidth in SMA ($\approx 1 \text{ Hz}$). However, LMAs have a relatively low power density ($\approx 0.2 \text{ W kg}^{-1}$) similar to DEA ($\approx 0.1 \text{ W kg}^{-1}$), compared to very high power densities in SMA ($>1000 \text{ W kg}^{-1}$). Natural muscles, for comparison, have much higher power densities ($50\text{--}284 \text{ W kg}^{-1}$) than LMAs. Overall, in terms of dynamic performance, the LMA (high strain rate, decent frequencies, low power density) performs similarly to natural muscles (high strain rate, decent frequencies) and opposite to SMA (low strain rate, low frequencies, high power density).

5.7. Scaling Laws of Force and Work Density

As the length scale (L) decreases, LMAs exhibit a unique scaling law by which force (F) and work density (W/V) increase faster than other actuators of interest. By this analysis (Table 6), there is no benefit in terms of work density if an electrostatic ($W/V \propto L^0$) or an electrothermal actuator ($W/V \propto L^1$) is to be downscaled. By contrast, since surface tension scales with length ($F \propto L$), liquid metal actuators have the advantage of exhibiting higher work densities at smaller scales ($W/V \propto L^{-2}$).

6. Toward Higher-Performance Actuation: Theoretical Limits and Open Challenges

There are many theoretical pathways toward higher performances in liquid metal actuators. For instance, work density increases when length scale decreases. Actuation speed increases when electrolyte concentration increases. Furthermore, force and displacement can increase by repetition of droplets. Many performance capabilities, however, are limited by their theoretical upper bounds, where actuation strain is limited by droplet-breaking instabilities. It is therefore necessary to understand the capabilities of liquid metal actuators, as well as many other actuators, from these two aspects: How do we enhance LMA performance to approach its ideal characteristics? How far can we go before they hit the theoretical limits? These two opposing factors are central to many soft actuators. For instance, stress can be theoretically output from an dielectric elastomer by decreasing the film thickness z (i.e., $p \propto z^{-2}$) at a cost of an increasing likelihood of dielectric breakdown ($E = V/z$), which poses an upper bound on improvement. In this view, the development of liquid metal actuators, besides their fundamental principles, involves discoveries of practical pathways toward performance enhancement, which is the focus of this section.

6.1. Ideal Characteristics of Liquid Metal Actuators

Table 7 summarizes the characteristics of an ideal liquid metal actuator from the standpoint of each property. At a higher level, the ideal liquid metal actuators are a result of the following optimizations:

- **Maximized Actuator Output** (Minimized Operational Cost): An ideal LMA uses a minimized volume to produce a maximized mechanical work (i.e., ideal static performance: high work densities) over a minimized period of time (i.e., ideal dynamic performance: high speed).
- **Maximized Efficiency** (Minimized Waste and Redundancy): An ideal LMA is space-efficient (i.e., redundant LM and electrolyte volumes are minimized), energy-efficient (i.e., electrical energy input to the LMA is mostly converted to mechanical work) and chemically efficient (i.e., reactions produce minimum undesired byproducts).
- **Maximized Durability** (Minimized Damage and Degradation): An ideal LMA is free from liquid breaking due to overstretching and maintains its operation for long life cycles.

For optimization, it is important to note the opposing effects between many factors here. Higher actuation speed, for instance, can be typically achieved at higher voltages and higher electrolyte concentrations, which will generate chemical byproducts at a higher rate. Another observation is made on the complication due to downscaling of all components, which ideally increase the density of work output. To see this, consider the assumption of flexural rigidity in an electrode, which will no longer be valid when the thickness is downscaled proportionally, at which point the actuator may not be operational. In general, optimizing a liquid metal actuator for higher performances often entails a primary design goal for which other secondary goals may need to be compromised.

6.2. Theoretical Limits and Practical Consideration

Table 8 summarizes the theoretical limits of selected properties in liquid metal actuators. One of the key limitations on actuation of any liquid is their tendency to break when overstretched.^[251–253] Unlike other soft materials, whose ability to stay unbroken is inherently tied to their tensile strength, the behavior of liquids are governed by the surface free energy, which is unstable when the liquid may favor separation for minimizing the potential energy. When does a liquid droplet break upon stretch? Representative models, such as the Rayleigh-Plateau instability for a continuous stream,^[254] are often used to bound the strain by a length λ exceeding the diameter $2R$ (maximum strain $\lambda/(2R) \approx \pi$, Table 8). In terms of actual geometry, however, liquid metal actuators are more similar to the theoretical liquid bridge between two solid spheres,^[177] by which an upper bound on the maximum strain (empirical: $\lambda/(2R) \approx 0.81R^{-1/3}$, Table 8) can be empirically calculated. Calculation of such theoretical limits on strain, as discussed in structural integrity in Section 3.5, is typically encoded into the actuator design to prevent breaking.^[24]

Dynamic bandwidth of the liquid metal actuators is directly related to the strain rate of contraction and relaxation of a droplet. Since liquids metals are known for their intrinsically high contractile strain rate compared to their antagonist-dependent relaxing strain rate (Section 3.4), the behavior of cyclic motions is design-dependent. Here, we simplify the consideration by assuming the same strain rate (ϵ/t) during relaxation and contraction. We note that the analysis here assumes negligible mass of liquid metal droplet and hence damping is ignored. The theoretically estimated bandwidth is then $f = \sqrt{2}(\epsilon/t)$, which is a maximum frequency at which the strain drops to half (-3 dB) of the DC amplitude (Table 8). A representative value is $f \approx 14.14$ Hz with a strain rate of 1000 \% s^{-1} , which can be further increased by higher voltages and higher electrolytic concentration.

Actuator volume, which is a combination of liquid metal droplets (no known lower bound on the volume), electrolyte (lower bound: $\approx 1/10$ of surface LM molecules^[24]), and electrodes (lower bound linked to the flexural rigidity assumption as discussed in Section 6.2), appears to be a factor that has been far from exploited in the literature, where the liquid metal droplets have been operated within a giant electrolyte bath (length scale: $\approx 10^{-1}$ m compared to liquid metal droplets: $\approx 10^{-3}$ m) whose volume is mostly redundant. How small can an electrolyte be to support structurally and electrochemically the actuation of liquid metals? Further studies are necessary for pathways toward a denser liquid metal actuator.

Liquid metal actuators are structurally scalable by reducing the size of the droplets and arranging them in parallel and serial arrays for greater total force and displacement output (Section 3.6). How many droplets, by this principle, can be theoretically packed into the system before it can no longer produce the desired work? In particular for serial configurations such as a serial chain of liquid droplets, the forces from individual droplets will quickly cancel each other out when influenced by gravity.^[60] In other words, repetition can be limited by the buildup of weights along the direction of tension. A parallel configuration, on the other hand, can be a more ideal strategy for repetition as the weights do not add up across the droplet.

6.3. Open Challenges in Higher-Performance Actuation

On the path toward an ideally high-performance liquid metal actuator that operates within the bounds of theory, there are still a number of engineering challenges that often extend beyond the electrochemical architectures discussed so far. Fully addressing these challenges relies on advances in the materials and micro-fabrication for electrochemical systems, which may ideally continue to scale down for higher performances as predicted by this review. The rest of this section discusses some of the major challenges toward this ideal.

6.3.1. Miniaturization

The theoretical prediction that very high work densities can be achieved in liquid metal actuators simply by downscaling without the requirements of higher voltages suggests that sub-mm miniaturization is an inevitable trend for future development. The work density is expected to continue to increase as the length scale further decreases if permitted by the fabrication at μm or nm scales. At these sub-mm length scales, fabrication precision can become a crucial factor. For instance, in the shear contraction design,^[24] a sophisticated sliding mechanism is required for restraining movement of the electrodes such that they are kept aligned and parallel to each other while allowing lubrication with other structures. The dependence of actuation on precision mechanisms like this presents a fabrication challenge at smaller scales.

Effects of downscaling every component by the same factor can potentially become an issue that interferes with the operation. From a material perspective, certain behaviors of the liquids, solids, and interaction between them, vary at smaller scales. One instance is, as previously discussed, that the electrodes may begin to be bent by surface tension if their thickness is also proportionally downscaled. To see this, consider a hypothetical flexural film (elastic modulus E) with a fixed aspect ratio (length L with thickness and depth scaling proportional to L). The film is wetted on one side by a liquid metal droplet (surface tension γ , radius R). We assume that $R \approx L$ and adopt the scaling law for bending angle $\alpha \approx (R/\ell_B)^2$ from Ref. [256], where ℓ_B is the capillary bending length defined by $\ell_B = \sqrt{EI/(p\gamma)}$ (p : contact perimeter). It follows that the bending angle scales by $\alpha \approx L^{-1}$, which suggests that the film bends further as L decreases. Furthermore, the common assumption of perfect wettability between the electrodes and liquid metals, which is central to liquid bridge-based actuation, is not yet examined in a μm -scale regime.

A miniaturized multi-droplet system, for all its theoretical benefits, is also subject to the inter-droplet interactions such as coalescence and separation. In an EWOD system, for instance, a droplet array is sometimes viewed as having a high dimensional state space in which all droplets are supplied by a common reservoir and allowed to move, break, and combine freely.^[257–259] In a liquid bridge system, on the other hand, whose overall work output relies on the collective droplet behaviors, cautions may be needed to handle the unwanted merging and breaking of some bridges. Further studies are also needed to examine whether a larger number of droplets may operate with higher redundancy, where local malfunctions can be corrected and repaired.^[50]

6.3.2. Chemical Byproduct

Electrochemical modulation of surface tension inevitably produces hydrogen gas at the cathode during both oxidation (hydrogen formed at the counter-electrode) and reduction (hydrogen formed on the liquid metal). Insoluble in water, the hydrogen gas typically forms bubbles within the aqueous electrolyte and rises quickly until evaporation or becoming trapped by some structure. In the latter case, the gas can build up over time and, depending on implementation, may degrade the actuation performance (if the bubbles build up on the liquid metal surface^[23]) or has no effect on the performance (if the bubbles build up elsewhere^[24]). Challenges presented by the hydrogen buildup may become even more significant at very small scales, where the feature size of electrodes may be even smaller than a typical bubble diameter. In this scenario, a bubble may block the ionic connection and stop the operation. How can the hydrogen formation be minimized (e.g., by alternative redox reactions that do not need to take place in water^[260]), properly handled (e.g., absorbed and stored by some materials^[261,262]), or even utilized (e.g., as an energy source as in fuel cells^[263,264])? Further studies are required to address these challenges.

6.3.3. Energy Efficiency

The redox reactions for modulating liquid metal surface tension, at least in current bulk setups, are highly redundant. For instance, the electrical energy input to the system is mostly lost during ion transport and water electrolysis, of which only a small portion is necessary for the redox reactions. This explains the very low energy efficiency that is currently measured ($<0.1\%$ ^[24]). The improvement of efficiency may be possible by reducing the redundancy in the current systems (e.g., minimizing the electrolyte distance and electrode areas) or by using alternative reactions to initiate the surface oxidation. As an energy conversion device from electrical energy to mechanical work, further studies in liquid metal-enabled energy generation^[197] and energy harvesting^[214] will be beneficial for creating liquid metal actuators capable of higher energy efficiency.

7. Practical Uses of Liquid Metal Actuators: A Robotic and Computational Perspective

The versatility of liquid metal actuators makes them suitable for a wide range of tasks where the generation of mechanical work plays a central role. Beside the performance advantages of liquid metal actuators, which makes them an excellent general-purpose actuator, many unique properties that are specific to liquid metals (e.g., wettability, electrical conductivity, liquid density) also enable a number of specialized functionalities that otherwise would require integration of extrinsic components. At a higher level, liquid metal actuators are intrinsically multimodal actuators that, through the modulation of surface tension, are capable of locomotion (i.e., producing motion for themselves to move with a medium), manipulation (i.e., handling and assembly of external objects), and logic (i.e., representing digital states for carrying computation). This section examines these modalities (**Figure 9**

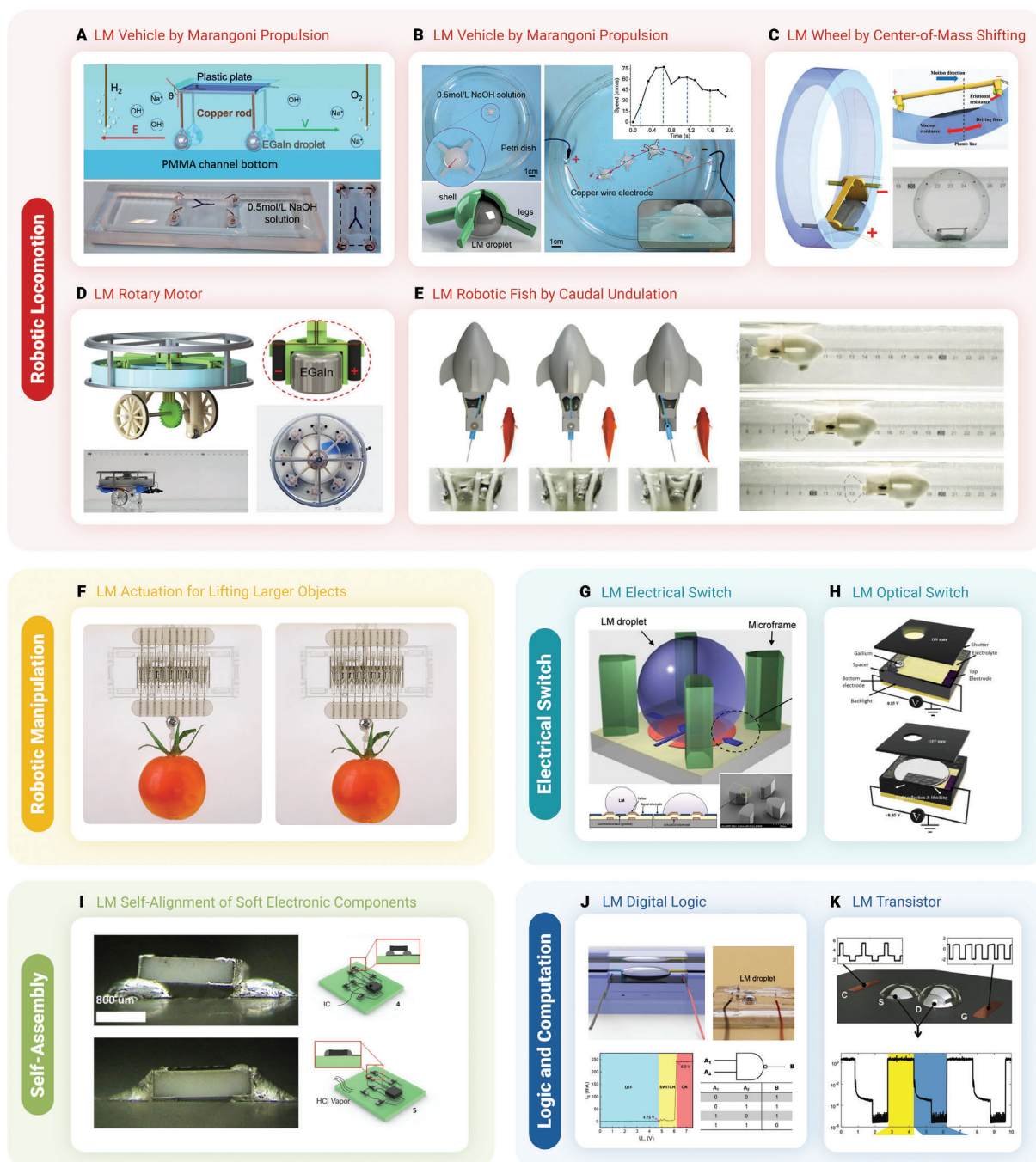
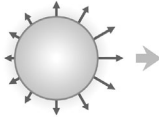

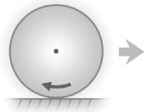
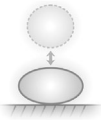

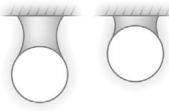
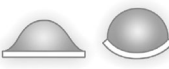

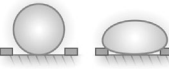



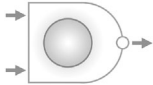
Figure 9. Robotic and computational tasks enabled by liquid metal actuators. A,B) Electrochemically-driven Marangoni propulsion allows multi-droplet (A) and single-droplet (B) liquid metal to travel in open space while carrying additional structures (e.g., shell, plate, rod). Reproduced with permission.^[190] Copyright 2016, Royal Society of Chemistry. C) A wheel robot with a large drop of liquid metal is able to rotate and move by shifting the center of mass with small steps of the liquid metal drop. Reproduced with permission.^[160] Copyright 2018, John Wiley & Sons, Inc. D) Rotary motion can be achieved by a circular configuration of liquid metal stepper units. Reproduced with permission.^[50] Copyright 2021, Elsevier. E) A fish robot with a caudal fin actuated by a pair of liquid metal droplets, which alternately contract and relax to generate undulation for propelling the robot. Reproduced with permission.^[60] Copyright 2021, John Wiley & Sons, Inc. F) A multi-droplet actuator is capable of generating a greater force that is sufficient for lifting a cherry tomato. Reproduced with permission.^[24] Copyright 2022, John Wiley & Sons, Inc. G) A liquid metal droplet functions as a fast-switching electrical switch. Reproduced with permission.^[56] Copyright 2008, IEEE. H) A liquid metal droplet functions as a light switch by electrocapillary spreading. Reproduced with permission.^[192] Copyright 2009, AIP Publishing. I) Chemical modulation of liquid metal surface tension by HCl vapor allows self-alignment of surface-mount components for soft electronics assembly. Reproduced with permission.^[217] Copyright 2018, John Wiley & Sons, Inc. J) Multistability in liquid metal droplet enables digital logic and more complex logic gate computation. Reproduced^[191] Copyright 2021, John Wiley & Sons, Inc. K) Transistor behavior enabled by breaking and merging of liquid metal droplets shows capabilities of liquid metal-based logic and computation. Reproduced with permission.^[61] Copyright 2017, John Wiley & Sons, Inc.

Table 9. Liquid metal actuator modalities for practical uses in robotic and computational tasks.

Type	Task	Figure	Definition	Role of liquid metals
Locomotion	Propulsion		<ul style="list-style-type: none"> Self-propelling of robots by generating thrusts in liquid environments. Often achieved by an imbalanced pressure gradient (e.g., Marangoni effect). 	<ul style="list-style-type: none"> Continuous electrowetting of the LM surface creates locally imbalanced Laplace pressure, which propels the LM in free space^[190] (Figure 9B). Alternatively, the imbalance can be created by chemically disrupting (e.g., by feeding aluminum to) the LM electrical double layer^[137] (Figure 9A).
	Undulation		<ul style="list-style-type: none"> Swimming of robots by whole-body lateral oscillation in liquid environments (e.g., by a flapping appendage). 	<ul style="list-style-type: none"> Oscillation of LM can be produced by alternately contracting and relaxing a pair of LM bridges, which move a fin back and forth^[60] (Figure 9E).
	Rolling		<ul style="list-style-type: none"> Locomotion of land vehicles which involves rotating a wheel without sliding. 	<ul style="list-style-type: none"> Rotation can be achieved by continuously shifting a large LM droplet in a wheel, which alters the center of mass^[160] (Figure 9C). Alternatively, rotation can be produced with a circular array of LM droplets driven by continuous electrowetting^[50] (Figure 9D).
	Jumping		<ul style="list-style-type: none"> Self-propelling of robots (projectiles) entirely off the ground followed by landing. 	<ul style="list-style-type: none"> Vertical bouncing of a LM droplet can be achieved by vertical electrowetting at a higher voltage (10 V)^[66].
Manipulation	Gripping		<ul style="list-style-type: none"> Picking and releasing objects by force closure. 	<ul style="list-style-type: none"> A water droplet (non-LM) with EWOD is able to attract and adhere to a micro-object by a liquid bridge. Releasing the object is achieved by intentionally breaking the liquid bridge.^[265]
	Lifting		<ul style="list-style-type: none"> Raising objects upward against gravity. 	<ul style="list-style-type: none"> Lifting a large object relative to the size and weight of LM can be achieved by a multi-droplet LM actuator, where the split smaller droplets simultaneously contract for a greater lifting force^[24] (Figure 9F).
	Folding		<ul style="list-style-type: none"> Bending thin films by surface tension. 	<ul style="list-style-type: none"> A water droplet (non-LM) with EWOD is capable of folding and unfolding a thin elastic membrane.^[266]
	Alignment		<ul style="list-style-type: none"> Automatic lateral alignment of soldered components. 	<ul style="list-style-type: none"> Self-alignment of surface-mount electronic components with LM solder can be initiated by chemically removing the gallium oxide and hence increasing the surface tension, where LM actuates the component to an energetically favored position^[217] (Figure 9I).
Logic	Switch		<ul style="list-style-type: none"> Devices with binary (on/off) states that can connect or disconnect electrical current, light, etc. 	<ul style="list-style-type: none"> LM can function as an electrical switch in an electrical circuit where LM separates the circuit when beading up and completes the circuit when fattened^[56] (Figures 9G-H).

(Continued)

Table 9. (Continued).

Type	Task	Figure	Definition	Role of liquid metals
	Transistor		<ul style="list-style-type: none"> Three-terminal device in which the gate can open or close the signal pathway between the source and drain. 	<ul style="list-style-type: none"> LM can function as a transistor by electrochemically merging two LM droplets to connect source and drain and break them to disconnect^[61] (Figure 9K).
	Logic Unit		<ul style="list-style-type: none"> Devices for boolean operations (e.g., NOT, AND, OR), typically implemented with transistors. 	<ul style="list-style-type: none"> LM logic gates can be created from combinations of binary LM switches^[191] (Figure 9J).

and Table 9) by analyzing the role of liquid metals for each particular task. We will discuss the practicality and advantages of these use cases from a robotics and computation perspective.

For a meaningful analysis, it is often useful to define what exactly is a robotic task and a computational task. For robotic tasks, we adopt the definition of a robot as an intelligent agent^[267] with the intrinsic ability to actively interact with the external world (e.g., moving in a medium or handling an object). Here we emphasize the physical interaction with the environment, where an observable change in the system (e.g., droplet position in a channel, object displacement by a droplet) takes place as a result of work generated by the actuator. In other words, a robotic task is not synonymous with any force production but, using the definitions for living systems,^[268] has to result in some meaningful change in energy, matter, and information.

Computation, on the other hand, is any action that transforms a logic input to an output, which is often built on representations of logic. For instance, logic can be represented with synapses between neurons in a brain and, in modern computers, transistors in a CPU. While modern computers are largely based on electrical transistors, studies into mechanical computing based on mechanologic^[269–272] has become a recent trend where logic states and mapping are enabled more by forces in a material than electricity through a semiconductor. Despite being in an early and primitive stage, the liquid metals have shown promise in similar logic functions, which will be examined below as a distinct modality enabled by actuation.

7.1. Robot Locomotion

This section examines locomotion of mobile robots enabled by liquid metal actuators. We note that, in the literature, the boundaries are often blurred between liquid metals as a component^[50,60,160,190] and as an entire robot^[137,189,273] to the extent where any *moving droplet* can be arbitrarily referred to as a *robot*. For the analysis here, we will adopt this broader definition and focus on the role of liquid metals in the generation of locomotion across a medium.

Due to their fundamental differences, it is useful to discuss locomotion in an aqueous medium (e.g., swimming in water or electrolyte bath) and locomotion on land separately.^[274] For swimming in an aqueous environment, liquid metals are typi-

cally used to provide a net positive force, or a thrust, to move the robot. The thrust can be generated from an imbalanced pressure gradient and is typically done by continuous electrowetting (similar to the Marangoni effect,^[186,275] Figure 9A) around the droplet surface^[190] (Figure 9B) or asymmetric disruption of the interface.^[137,276] Alternatively, liquid metals can be used to drive a flapping appendage for undulation^[60] (Figure 9E). In another form of propulsion, where the liquid metal droplet jumps and bounces against its weight inside an electrolyte bath,^[66] the locomotion can be viewed as a special case where the thrust overcomes the gravity and is able to lift the droplet. In general, liquid metal locomotion in aqueous environments, such as electrolytic solutions, often takes advantage of the control of liquid metal through an electric field. In this sense, the field-driven liquid metal droplets can be viewed as enabling untethered robots.

Locomotion gaits on dry surfaces, on the other hand, are commonly friction-enabled motion achieved in animals and robots with wheels (for rolling), legs (for walking^[277]), or limbless bodies (for crawling^[278]). Liquid metals have been used in wheeled robots in which motion of the droplets is translated into overall rotation^[50,160] (Figure 9C,D). These rolling robots encapsulate the liquid metal droplets and electrolytes within their structure and can be operated in dry air. For this reason, even though they are essentially a circular version of the same droplet-transport mechanism, these early instances show promise in achieving land locomotion with liquid metal actuators.

One common feature in all these instances of locomotion is the net motion of liquid metal droplets due to a pressure gradient driven by an electric field. In most cases, the robots use the liquid metal droplets not for their high deformability but for their electrocapillary tendency to be attracted in an ionically charged electric field. This can be attributed to the lack of better encapsulation, which for the time being limits the source of locomotion to droplet motion within electrolytes. Further studies, when enabled by encapsulation, are necessary to exploit the deformability of liquid metals as a source of locomotion on land.

7.2. Robot Manipulation

Manipulation is commonly defined by the control of an object through selective contact^[279], which typically involves picking up an object, moving it to a different location and releasing it.

Traditionally, a contact between an end effector and the object is done by imposing kinematic constraints and force closure through actuation^[280]. Liquids, however, with their controllable surface tension and wettability, can enable the same object manipulation tasks. This process typically involves modulation of wettability for picking and releasing the object^[265] (comparable to gecko-adhesion in gripping^[281]) and modulation of surface tension for generating displacement^[24] (Figure 9F). In all cases, liquid metals are used for their high deformability for interaction with external objects.

Beyond these traditional manipulation tasks, we will also highlight the self-assembly ability^[282] of liquid metals to control a structure from a disordered organization into an ordered one. We note that the definition for self-assembly typically focuses on the spontaneous organization of the objects without intervention of external forces,^[283] which is traditionally the opposite of robotic manipulation, where the robot arms handle the objects into a desired state as a means of external intervention. For the analysis here, we argue that liquid-enabled organization of objects^[87,284,285] is at the intersection of these two concepts. Most notably, traditional soldering can be viewed as a surface tension-driven self-assembly process, where the components are aligned by increasing the solder surface tension. The same concept is demonstrated in soft electronics with liquid metal-connected components^[217] (Figure 9I), where the surface tension is modulated by HCl treatment to move the misaligned component to an aligned (energetically favored) position. Liquid-driven origami is another emerging topic, where self-folding and unfolding can be generated with liquid droplets.^[266,286]

At a higher-level, all robotic manipulation tasks involve some shifting of a system from one stability to another. In the case of gripping and lifting, for instance, the work produced by the actuator is used to move the object from one stationary position to another. Likewise, self-assembly can be driven by the tendency of liquids to minimize their total potential energy. The role of liquid metals in these tasks tends to take more advantage of their higher deformability than the previously mentioned locomotion tasks.

7.3. Logic and Computation

Multistability, by which a system has two or more energetically stationary states, exists in many liquid metal configurations. One simple example is a liquid metal droplet inside a channel within an electric field, where the droplet can be attracted to one end or another depending on the polarity, where the “on” and “off” states are represented by the droplet position. Another instance is the transitioning between the regimes of coalescence, which represents the “on” state, and separation, which represents the “off” state, of a droplet. Higher-order state representations are also possible with systems with more droplets^[161] or more complex kinematic constraints.

We emphasize the switchability between stable states through liquid metal actuation, where a control signal alters the stability by changing the forces and shapes of the liquid metal actuators. This process is similar to traditional field-effect transistors, in which an electrical control signal at the gate alters the conductivity between the source and drain. Similar to transistors, which are the fundamental building block for logic cir-

cuits, computer memory, and microprocessors, the bistability in liquid metals make them a promising candidate for logic and computation, which is shown as a pure electrical switch^[56] (Figure 9G), a transistor-like device^[61] (Figure 9K), and higher-level logic gates^[191] (Figure 9J).

Unlike other recent work on pure mechanical memory and computation in metamaterials,^[269,271,287–289] all of which rely on propagation of mechanical signals and are significantly slower than semiconductor-based transistors, liquid metal computation is still built upon switchable electrical connections and can potentially be faster than pure mechanical computation. Overall, logic and computation based on liquid metal actuators not only take advantage of their high deformability but also their reconfigurable multistability. Their ability to form and remove electrical connections through mechanical actuation offers an intriguing alternative to modern semiconductor devices. One potential advantage of liquid metals is their high thermal conductivity and hence excellent heat dissipation, unlike the temperature-sensitive MOSFETs. Furthermore, many semiconductor devices are vulnerable to irreversible electrical breakdown at very low voltages, while the inherent high deformability and shape-reversibility of liquid metals may prevent damages beyond healing. The logic units based on liquid metals are neither completely electrical, as in the case of semiconductor-based transistors, nor purely mechanical, as with recent advances in metamaterials. Instead, they are enabled by electrically responsive mechanical response in liquid metal droplets, which, by the analysis in this review, are energy-dense at smaller scales (i.e., mechanically altering the logic state may take less energy when miniaturized). These niche advantages may provide a new paradigm of logic and computation that lies in between purely electrical and purely mechanical devices.

8. Energy Coupling: Implication and Opportunities for Small-Scale Robots

The integration of liquid metal actuators into robotic systems is strongly influenced by their coupling with an energy source. In a bulky electrochemical setup, where the energy input often comes from a wired power source, operation of the *tethered* liquid metal actuators relies on the wired connection and is thus not suitable for most mobile robots. To eliminate the wires, energy coupling is essential, which may have further implications to the overall design. For robots at sub-mm scales, it is often difficult to carry an onboard energy source that can deliver the electrical energy needed for liquid metal actuation. In these cases, more advanced strategies such as powering by fuel, remote power source, and energy harvesting can help achieve untethered robots. This section examines these energy-coupling strategies for the liquid metal actuators and provides a guideline for their incorporation into a robotic system.

It is important to differentiate liquid metal actuators driven by electrical potential differences across the interface (i.e., between the interior and exterior of a liquid metal droplet^[47]) from those driven by gradients (i.e., the liquid metal droplet is placed in an electric field across a medium^[90]). The former, which is usually used to drive electrochemical modulation of surface tension or electrocapillary modulation at a higher voltage, requires separate

electrical connections across the liquid metal interface (i.e., typically through electrodes vs counter-electrodes). The latter typically actuates the liquid metal droplet by an electric field-induced pressure gradient across the electric double layer on the droplet. The overall result is the attraction of the liquid metal droplet toward the anode in the electrolyte medium. In this case, the electrodes on both ends are in contact with the electrolyte rather than the liquid metal itself. In terms of actuation capabilities that have implications in energy coupling, interface-driven actuators are more capable of in-body deformation while the gradient-driven actuators induce whole-body motion of the droplet.

Remote power delivery to a robot is most notably achieved by magnetic fields^[290–294] for their excellent ability to penetrate most media.^[40,295] In contrast, liquid metal actuators in this review are not known to be capable of being remotely powered in a similar fashion for at least two reasons: First, the modulation of surface tension relies on the current to flow through wires into and out of the liquid metal droplets (i.e., interface-driven actuation). Second, even with gradient driven actuation, the electric field must be applied near the liquid metal droplets and thus still requires wiring. Despite not being intrinsically capable of deformation by remote powering, whole-body motion and control is reported in liquid metal composites with magnetic particles.^[161,296–298] We emphasize that these composites do not use liquid metals to generate force and are not within the scope of this review. These principles, however, may inform the development of truly remotely powered liquid metal actuators.

In a typical tethered electrochemical configuration, the energy supplied from a distant power supply through the wires (**Figure 10A**^[24]). The distinction between a tethered and an untethered robot, however, may be ambiguous sometimes and is often linked to what is defined as the robot. For instance, the droplet that moves across a wired rail (**Figure 10B**^[299]) can be viewed as untethered to some extent (i.e., the droplet is not anchored) but is better described as tethered because it requires the delivery of energy from a distance source through wires.

Untethered actuators, on the other hand, can be achieved by incorporating an onboard battery into the mobile robot. Usually a minimum or no circuitry, such as voltage converters, is required as most portable batteries provide voltages on the order of several volts, which is near the activation voltage of electrochemical oxidation. We note the ambiguity in these robots between being tethered and untethered since energy is still delivered through a wire. This strategy is demonstrated in a wheel robot that rolls by shifting a large blob of liquid metal (cm-scale) powered by an onboard lithium battery^[160] (**Figure 10C**). We note that this design has to operate at a weight-dominating scale and may not be scalable to mm-scales and sub-mm-scales, where the droplet weight may become relatively insignificant.

Toward self-powered liquid metal actuators: How much battery materials are necessary to power the liquid metal actuators? A typical current consumption up to $\approx 10^1$ mA for mm-scale liquid metal actuators (**Table 3**) suggests that they need a battery with a characteristic cross section of at least $\approx 10^0$ cm² using a lithium polymer battery (current density: $\approx 10^1$ mA cm⁻²^[302]). We note that this estimation only considers the instantaneous current drawn from the battery to the actuator. Regardless of current densities, however, any additional materials to a mobile robot will inevitably increase the cost of transport. Is it possible to power

the liquid metal actuators by directly using them as batteries? Liu et al. reported a soft battery architecture with a liquid metal anode,^[197] which supplies a current density ≈ 1 mA cm⁻². If this design were to be used to power a mm-scale liquid metal actuator, a characteristic cross section of at least $\approx 10^1$ cm² would be sufficient for a self-powering liquid metal anode. However, the mismatch between the characteristic length (≈ 3.2 cm for a cross section $\approx 10^1$ cm²) of the liquid metal as a battery anode (cm-scale) and as an actuator (mm-scale) suggests that a self-powering liquid metal actuator may be practical at sub-mm-scales, where the self-weight of liquid metal ($\propto L^3$) becomes less significant while the current requirement scales with liquid metal surface area ($\propto L^2$).

We note that while the above focuses on current supply, the electrical power may not need to be consumed constantly but only need to be used to initiate and, when necessary, maintain the oxidation or reduction state. For example, one possible low-power design is to partly reduce the oxide skin by a zero potential (i.e., zero power is drawn from the energy source) by spontaneously dissolving the gallium oxide within the electrolyte solution. While this in theory compromises the performance, it can potentially be used to optimize a self-powered design.

Toward fuel-powered liquid metal actuators: Powering an actuator with the energy released from chemical reactions of a consumable material such as fuel is widely seen in natural muscles (e.g., contraction can use the energy from glycogen stored in muscles) and engineered systems (e.g., carbon nanotubes function as actuators and hydrogen fuel cell electrodes^[303]). Likewise, fuel-driven actuation is a promising strategy for untethering. This is demonstrated in self-propelling of liquid metal droplets by imbalanced interfacial disruption due to corrosion by aluminum, which functions as the fuel^[137,276] (**Figure 10D**). The motion of the liquid metal droplet continues as long as there is a continual supply of aluminum. Despite not being electrically powered, this intriguing concept can be used to decouple liquid metal actuators from an immediate electric power source by consuming energy out of a fuel.

The complete elimination of an immediate power source, as previously discussed, is not possible with electrical actuation of liquid metal droplets. However, alternative actuation principles exist for liquid metal composites that are magnetically responsive (Ref. [300], **Figure 10E**). Furthermore, energy harvesting from the environment by liquid metal droplets (e.g., acoustic energy,^[301] **Figure 10F**) is another instance where liquid metal functions simultaneously as an actuator and as an energy harvester. In summary, the choice of energy source for liquid metal actuators is coupled with their actuation principle, where additional strategies are possible (e.g., for chemical and magnetic actuation) beyond typical electrical actuation.

9. Conclusion and Future Directions

The liquid metal actuators summarized in this review are capable of a unique combination of low operational voltages, high contractile strain rates, and higher work densities at smaller length scales. Enabled by electrocapillary or electrochemical modulation of surface tension, LMAs generate mechanical work by taking advantage of the high surface tension, high deformability, and high electrical responsivity in liquid metals. The construction of liquid

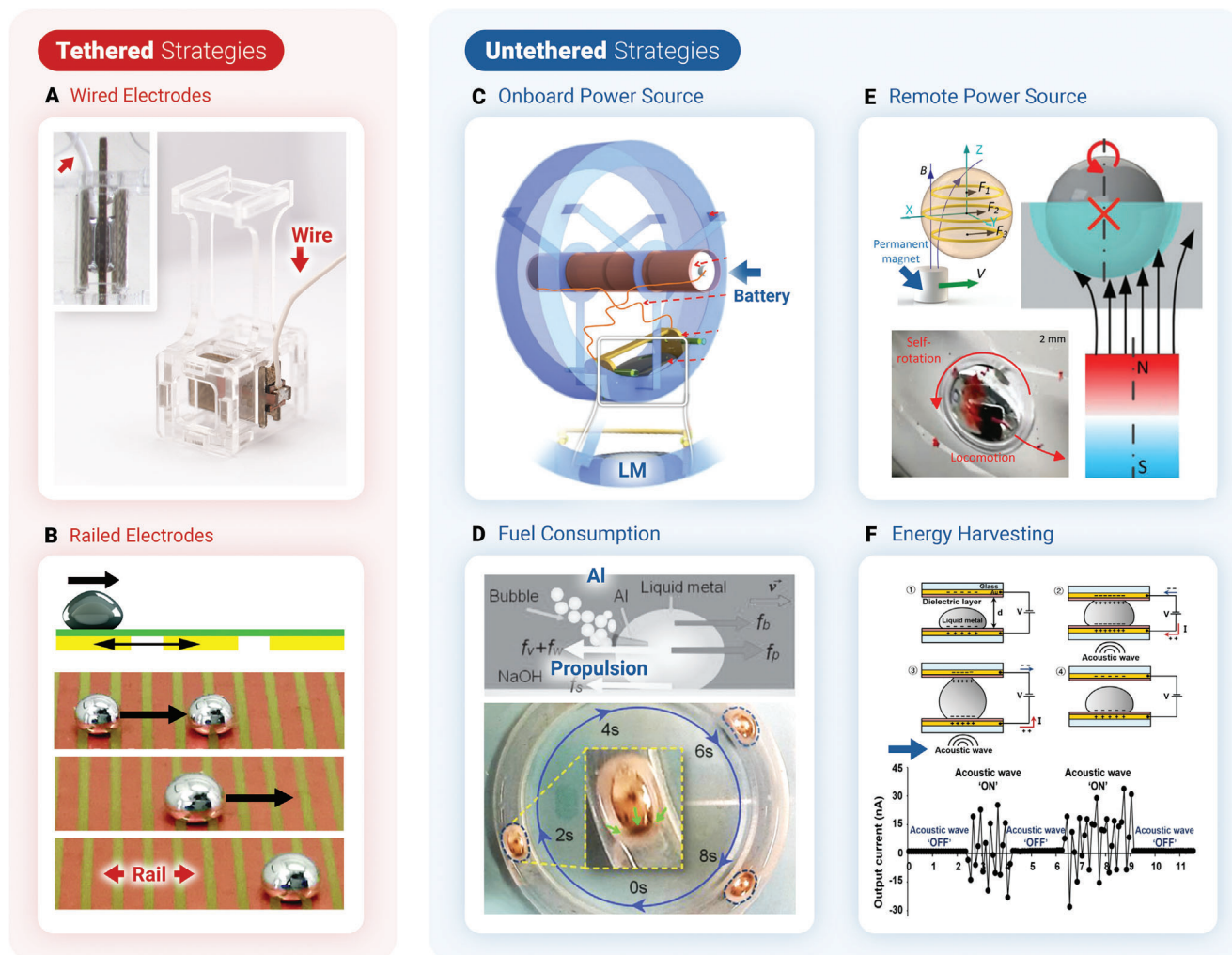


Figure 10. Energy strategies for liquid metal actuators. The energy source of liquid metal actuators in mobile robot designs is dependent on whether the robot needs to be tethered (A,B) or untethered (C–F). (A) All electrodes are connected to an external power source through wires. Adapted with permission.^[24] with permission. Copyright 2022, John Wiley & Sons, Inc. (B) The liquid metal droplet is not fixed to a wire but only draws power from a rail when in contact. Adapted with permission.^[299] Copyright 2019, Mary Ann Liebert, Inc. (C) The robot carries an onboard battery to supply the energy for the liquid metal actuator. Adapted with permission.^[160] Copyright 2018, John Wiley & Sons, Inc. (D) Consumable fuel (or food) is used by the liquid metal to propel itself. Adapted with permission.^[137] Copyright 2015, John Wiley & Sons, Inc. (E) The liquid metal takes remote energy from an external magnetic field. Adapted with permission.^[300] Copyright 2018, Royal Society of Chemistry. (F) The liquid metal interacts with the environment (e.g., acoustic waves) to generate power. Adapted with permission.^[301] Copyright 2018, EDP Sciences.

metal actuators requires an understanding of the design principles of droplet kinematics, reversibility, structural integrity and scalability, with which higher-performance actuation is achievable at smaller length scales. Overall, liquid metal actuators are characterized by a low activation voltage (≈ 1 V), a muscle-relevant strain (40%), a length-scalable stress ($\approx 10^3$ Pa at mm-scale, even higher at sub-mm-scales) and work density ($\approx 10^2$ J m^{-3} at mm-scale, even higher at sub-mm-scales), very high strain rate (> 1000 % s^{-1}), and biologically-relevant bandwidth (≈ 10 Hz). However, LMAs also typically exhibit a low power density (≈ 0.2 W kg^{-1}) and low energy conversion efficiency ($< 0.1\%$). Nonetheless, they possess a combination of useful properties that makes them stand out from other types of soft actuators.

Liquid metal actuators are highly versatile and can be utilized for a wide range of robotic and computational tasks. This in-

cludes locomotion in a fluidic medium, manipulation of objects, and representation of logic—capabilities that are all enabled by surface tension modulation of liquid metals. For activation by an electric potential difference across the interface, the liquid metal actuator is typically integrated into a tethered robot. However, untethered functionality can be enabled through more advanced strategies for supplying energy. There is also significant room for improvement in the performance of LMAs, which are still in their infancy and have a long way to go before reaching their theoretical limits. Understanding the underlying principles that govern actuator performance (e.g., bandwidth, efficiency) will require new models and perspectives on the physics of LMAs. Beyond their actuation capabilities, there are also open questions about cytotoxicity and the biocompatibility of liquid metal alloys with human tissue and organs for potential applications in medicine.

Overall, several engineering challenges will still need to be overcome before liquid metal actuators can fulfill their theoretical potentials and find use in more mainstream or commercial applications.

What are the next challenges in liquid metal actuators? As analyzed in this review, current implementations of liquid metal actuators are far from fulfilling their ultimate capabilities and further improvements are required. One area for potential improvement is concerned with the use of electrolytic solution, which can interfere with operation in dry environments. In terms of functionalities, liquid metals also have the potential for more intelligent behaviors in support of actuation. Moreover, liquid metals can be combined with other materials for new collective behaviors. Lastly, for applications in microrobotics, further study can explore the advantages of liquid metals at small length scales where their surface tension can dominate force and motion. From the vantage point of this review, we offer the following roadmap of future research directions of liquid metal actuators:

- **Enhancing actuation performances toward theoretical limits:** Increase the work output from a given volume by surface area splitting. Achieve structural scaling of forces from a large number of droplets. Increase strain rate and frequency by speeding up the redox reactions at higher voltages or electrolyte concentrations. Improve energy efficiency.
- **Encapsulating electrochemical components for dry operation:** Replace bulky electrolyte baths with smaller volumes of fluid. Design transmission systems for force output that are outside of the electrolyte. Explore the possibilities of gel electrolytes. Together, these could enable the use of LMAs for robotic tasks in dry conditions.
- **Exploiting liquid metal properties for intelligent functionalities:** Achieve active self-healing in separated liquid metal actuators. Explore the possibilities of self-powering and self-growth of liquid metal actuators.
- **Exploring novel composite behaviors with different materials:** Study composites of liquid metals with a different material (e.g., magnetic particles, elastomers, hydrogels, liquid crystals) for new functionalities that are otherwise difficult to achieve with an individual material.
- **Downscaling for untethered mobile microrobots:** Create functional microrobots from miniaturized liquid metal actuators. Study the suitable energy source for untethering the robot. Explore the practical applications of an untethered liquid metal microrobot.

These research directions offer great opportunities in the creation of a high-performance and multifunctional actuator that is entirely built on the theoretical foundations of surface tension modulation. The remarkable characteristics of liquid metal actuators make them stand out from other types of soft actuators. The emerging field of liquid metal actuators, as discussed in this review, is still at an early stage of development where the lower-level (elemental) aspects are still the primary focus compared to the higher-level (structural and functional) aspects. Ultimately, we envision a shift toward higher-level structures and functionalities. However, further work is required to completely establish a foundational understanding of liquid metal actuators so that they can reach their promised potential.

Acknowledgements

Open access funding enabled and organized by Projekt DEAL.

Conflict of Interest

The authors declare no conflict of interest.

Keywords

liquid metals, microrobotics, soft actuators, surface tension

Received: January 18, 2023

Revised: June 9, 2023

Published online:

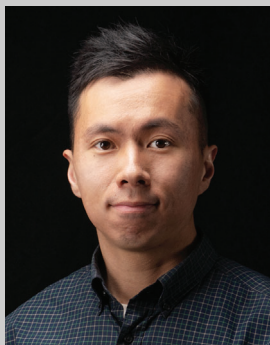
- [1] L. Hines, K. Petersen, G. Z. Lum, M. Sitti, *Adv. Mater.* **2017**, *29*, 1603483.
- [2] J. D. Madden, *Science* **2007**, *318*, 1094.
- [3] M. Li, A. Pal, A. Aghakhani, A. Pena-Francesch, M. Sitti, *Nat. Rev. Mater.* **2022**, *7*, 235.
- [4] R. Pelrine, R. Kornbluh, Q. Pei, J. Joseph, *Science* **2000**, *287*, 836.
- [5] F. Carpi, I. Anderson, S. Bauer, G. Frediani, G. Gallone, M. Gei, C. Graaf, C. Jean-Mistral, W. Kaal, G. Kofod, M. Kolloosche, R. Kornbluh, B. Lassen, M. Matyssek, S. Michel, S. Nowak, B. O'Brien, Q. Pei, R. Pelrine, B. Rechenbach, S. Rosset, H. Shea, *Smart Mater. Struct.* **2015**, *24*, 105025.
- [6] E. Acome, S. K. Mitchell, T. Morrissey, M. Emmett, C. Benjamin, M. King, M. Radakovitz, C. Keplinger, *Science* **2018**, *359*, 61.
- [7] N. Kellaris, V. Gopaluni Venkata, G. M. Smith, S. K. Mitchell, C. Keplinger, *Sci. Rob.* **2018**, *3*, eaar3276.
- [8] F. Carpi, S. Bauer, D. De Rossi, *Science* **2010**, *330*, 1759.
- [9] J. D. Madden, N. A. Vandesteeg, P. A. Anquetil, P. G. Madden, A. Takshi, R. Z. Pytel, S. R. Lafontaine, P. A. Wieringa, I. W. Hunter, *IEEE J. Oceanic Eng.* **2004**, *29*, 706.
- [10] S. M. Mirvakili, I. W. Hunter, *Adv. Mater.* **2018**, *30*, 1704407.
- [11] I. W. Hunter, J. M. Hollerbach, J. Ballantyne, *Robot. Rev.* **1991**, *2*, 299.
- [12] Y. Chen, H. Zhao, J. Mao, P. Chirarrattananon, E. F. Helbling, N.-s. P. Hyun, D. R. Clarke, R. J. Wood, *Nature* **2019**, *575*, 324.
- [13] X. Ji, X. Liu, V. Cacucciolo, Y. Civet, A. El Haitami, S. Cantin, Y. Perriard, H. Shea, *Adv. Funct. Mater.* **2021**, *31*, 2006639.
- [14] M. Warner, E. M. Terentjev, in *Liquid Crystal Elastomers*, Vol. 120, Oxford University Press, Oxford **2007**.
- [15] J. M. Jani, M. Leary, A. Subic, M. A. Gibson, *Mater. Des.* **2014**, *56*, 1078.
- [16] J. Mohd Jani, M. Leary, A. Subic, *J. Intell. Mater. Syst. Struct.* **2017**, *28*, 1699.
- [17] S. Wagner, S. Bauer, *MRS Bull.* **2012**, *37*, 207.
- [18] M. Doi, in *Soft Matter Physics*, Oxford University Press, Oxford **2013**.
- [19] G. Navascues, *Rep. Prog. Phys.* **1979**, *42*, 1131.
- [20] H. Kusumaatmaja, R. Lipowsky, *Langmuir* **2010**, *26*, 18734.
- [21] S. Asare-Asher, J. N. Connor, R. Sedev, *J. Colloid Interface Sci.* **2015**, *449*, 341.
- [22] Y. Chen, Z. Liu, D. Zhu, S. Handschuh-Wang, S. Liang, J. Yang, T. Kong, X. Zhou, Y. Liu, X. Zhou, *Mater. Horiz.* **2017**, *4*, 591.
- [23] J. Liao, C. Majidi, *Soft Matter* **2021**, *17*, 1921.
- [24] J. Liao, C. Majidi, *Adv. Sci.* **2022**, *9*, 2201963.
- [25] K. Kalantar-Zadeh, J. Tang, T. Daeneke, A. P. O'Mullane, L. A. Stewart, J. Liu, C. Majidi, R. S. Ruoff, P. S. Weiss, M. D. Dickey, *ACS Nano* **2019**, *13*, 7388.
- [26] W. M. Haynes, D. R. Lide, T. J. Bruno, in *CRC Handbook of Chemistry and Physics*, CRC Press, Boca Raton, FL, USA **2016**.

- [27] C. Kemball, *Trans. Faraday Soc.* **1946**, 42, 526.
- [28] P. Won, S. Jeong, C. Majidi, S. H. Ko, *Iscience* **2021**, 24, 102698.
- [29] T. Liu, P. Sen, C.-J. Kim, *J. Microelectromech. Syst.* **2011**, 21, 443.
- [30] M. D. Dickey, R. C. Chiechi, R. J. Larsen, E. A. Weiss, D. A. Weitz, G. M. Whitesides, *Adv. Funct. Mater.* **2008**, 18, 1097.
- [31] M. D. Dickey, *ACS Appl. Mater. Interfaces* **2014**, 6, 18369.
- [32] T. Cole, S.-Y. Tang, *Mater. Adv.* **2022**, 3, 173.
- [33] K. Y. Kwon, V. K. Truong, F. Krisnadi, S. Im, J. Ma, N. Mehrabian, T.-i. Kim, M. D. Dickey, *Adv. Intell. Syst.* **2021**, 3, 2000159.
- [34] M. L. Teodoro, G. N. Phillips, L. E. Kavraki, in *Proc. 2001 ICRA. IEEE Int. Conf. on Robot. and Autom. (Cat. No. 01CH37164)*, Vol. 1, IEEE, Piscataway, NJ, USA, **2001**, pp. 960–965.
- [35] C.-P. Chou, B. Hannaford, *IEEE Trans. Robot. Autom.* **1996**, 12, 90.
- [36] A. Miriyev, K. Stack, H. Lipson, *Nat. Commun.* **2017**, 8, 1.
- [37] D. E. Packham, *Int. J. Adhes. Adhes.* **2003**, 23, 437.
- [38] B. Spletzer, Scaling laws for mesoscale and microscale systems, Technical report, Sandia National Lab.(SNL-NM), Albuquerque, NM, USA; Sandia National Lab (SNL-CA), Livermore, CA, USA, **1999**.
- [39] M. Sitti, in *Mobile Microrobotics*, MIT Press, Cambridge, MA, USA **2017**.
- [40] M. Sitti, D. S. Wiersma, *Adv. Mater.* **2020**, 32, 1906766.
- [41] F. N. Piñan Basualdo, A. Boloipon, M. Gauthier, P. Lambert, *Sci. Rob.* **2021**, 6, eabd3557.
- [42] S. Martel, *Biomed. Microdevices* **2012**, 14, 1033.
- [43] D. C. Grahame, *Chem. Rev.* **1947**, 41, 441.
- [44] F. Mugele, J.-C. Baret, *J. Phys.: Condens. Matter* **2005**, 17, R705.
- [45] H. Moon, S. K. Cho, R. L. Garrell, C.-J. C. Kim, *J. Appl. Phys.* **2002**, 92, 4080.
- [46] W. C. Nelson, C.-J. C. Kim, *J. Adhes. Sci. Technol.* **2012**, 26, 1747.
- [47] M. R. Khan, C. B. Eaker, E. F. Bowden, M. D. Dickey, *Proc. Natl. Acad. Sci.* **2014**, 111, 14047.
- [48] C. B. Eaker, M. D. Dickey, *Appl. Phys. Rev.* **2016**, 3, 031103.
- [49] E. Rios, G. Brum, *Nature* **1987**, 325, 717.
- [50] E. Wang, J. Shu, H. Jin, Z. Tao, J. Xie, S.-Y. Tang, X. Li, W. Li, M. D. Dickey, S. Zhang, *Iscience* **2021**, 24, 101911.
- [51] J. Lee, C.-J. Kim, *J. Microelectromech. Syst.* **2000**, 9, 171.
- [52] H. Zeng, Z. Wan, A. D. Feinerman, *J. Microelectromech. Syst.* **2006**, 15, 1568.
- [53] K. Sarabia, S. Yamada, R. Gough, M. Moorefield, A. Combs, W. Shiroma, A. Ohta, *Electron. Lett.* **2017**, 53, 1635.
- [54] Z. Wan, H. Zeng, A. Feinerman, *Appl. Phys. Lett.* **2006**, 89, 201107.
- [55] H. Zeng, A. D. Feinerman, Z. Wan, P. R. Patel, *J. Microelectromech. Syst.* **2005**, 14, 285.
- [56] P. Sen, C.-J. Kim, *J. Microelectromech. Syst.* **2008**, 18, 174.
- [57] Z. Wan, H. Zeng, A. Feinerman, *J. Fluids Eng.* **2007**, 129, 388.
- [58] A. Diebold, A. Watson, S. Holcomb, C. Tabor, D. Mast, M. Dickey, J. Heikenfeld, *J. Micromech. Microeng.* **2017**, 27, 025010.
- [59] L. Russell, J. Wissman, C. Majidi, *Appl. Phys. Lett.* **2017**, 111, 254101.
- [60] J. Shu, D.-A. Ge, E. Wang, H. Ren, T. Cole, S.-Y. Tang, X. Li, X. Zhou, R. Li, H. Jin, W. Li, M. D. Dickey, S. Zhang, *Adv. Mater.* **2021**, 33, 2103062.
- [61] J. Wissman, M. D. Dickey, C. Majidi, *Adv. Sci.* **2017**, 4, 1700169.
- [62] S.-Y. Tang, K. Khoshmanesh, V. Sivan, P. Petersen, A. P. O'Mullane, D. Abbott, A. Mitchell, K. Kalantar-Zadeh, *Proc. Natl. Acad. Sci.* **2014**, 111, 3304.
- [63] R. C. Gough, J. H. Dang, M. R. Moorefield, G. B. Zhang, L. H. Hihara, W. A. Shiroma, A. T. Ohta, *ACS Appl. Mater. Interfaces* **2016**, 8, 6.
- [64] S.-Y. Tang, V. Sivan, K. Khoshmanesh, A. P. O'Mullane, X. Tang, B. Gol, N. Eshtiaghi, F. Lieder, P. Petersen, A. Mitchell, K. Kalantar-zadeh, *Nanoscale* **2013**, 5, 5949.
- [65] S. Handschuh-Wang, Y. Chen, L. Zhu, T. Gan, X. Zhou, *Langmuir* **2018**, 35, 372.
- [66] S. Bansal, Y. Tokuda, J. Peasley, S. Subramanian, *Langmuir* **2022**, 38, 6996.
- [67] B. Siciliano, O. Khatib, T. Kröger, in *Springer Handbook of Robotics*, Vol. 200, Springer, Berlin **2008**.
- [68] M. J. Ford, C. P. Ambulo, T. A. Kent, E. J. Markvicka, C. Pan, J. Malen, T. H. Ware, C. Majidi, *Proc. Natl. Acad. Sci.* **2019**, 116, 21438.
- [69] T. A. Kent, M. J. Ford, E. J. Markvicka, C. Majidi, *Multifunct. Mater.* **2020**, 3, 025003.
- [70] B. Ma, C. Xu, L. Cui, C. Zhao, H. Liu, *ACS Appl. Mater. Interfaces* **2021**, 13, 5574.
- [71] M. Yunusa, A. Adaka, A. Aghakhani, H. Shahsavan, Y. Guo, Y. Alapan, A. Jákl, M. Sitti, *Adv. Mater.* **2021**, 33, 2104807.
- [72] Y. Liu, M. Gao, S. Mei, Y. Han, J. Liu, *Appl. Phys. Lett.* **2013**, 103, 064101.
- [73] J. Wissman, L. Finkenauer, L. Deseri, C. Majidi, *J. Appl. Phys.* **2014**, 116, 144905.
- [74] Y.-L. Park, R. J. Wood, in *Sensors*, IEEE, Baltimore, MD, USA **2013**, pp. 1–4.
- [75] Z. Ren, M. Zarepoor, X. Huang, A. P. Sabelhaus, C. Majidi, *Front. Robot. AI* **2021**, 8, 599650.
- [76] D. Hartl, J. Mingear, B. Bielefeldt, J. Rohmer, J. Zamarrripa, A. Elwany, *Shape Mem. Superelasticity* **2017**, 3, 457.
- [77] X. Huang, Z. Ren, C. Majidi, in *2020 3rd IEEE Int. Conf. on Soft Robot. (RoboSoft)*, IEEE, New Haven, CT, USA **2020**, pp. 367–372.
- [78] A. Iakovlev, D. Bedrov, M. Müller, *J. Phys. Chem. Lett.* **2016**, 7, 1546.
- [79] K. Nogi, K. Ogino, A. McLean, W. Miller, *Metall. Trans. B* **1986**, 17, 163.
- [80] S. Handschuh-Wang, Y. Chen, L. Zhu, X. Zhou, *ChemPhysChem* **2018**, 19, 1584.
- [81] B. Keene, *Int. Mater. Rev.* **1993**, 38, 157.
- [82] Z. Suo, *Acta Mech. Solida Sin.* **2010**, 23, 549.
- [83] B. Lautrup, in *Physics of Continuous Matter: Exotic and Everyday Phenomena in the Macroscopic World*, CRC Press, Boca Raton, FL, USA **2011**.
- [84] T. J. Roberts, *J. Exp. Biol.* **2016**, 219, 266.
- [85] A. V. Hill, *Proc. R. Soc. London, Ser. B* **1953**, 141, 104.
- [86] C. Majidi, *Soft Rob.* **2014**, 1, 5.
- [87] M. Mastrangeli, *Adv. Mater.* **2015**, 27, 4254.
- [88] G. Lian, J. Seville, *Adv. Colloid Interface Sci.* **2016**, 227, 53.
- [89] C. D. Willett, M. J. Adams, S. A. Johnson, J. P. Seville, *Langmuir* **2000**, 16, 9396.
- [90] G. Beni, S. Hackwood, J. Jackel, *Appl. Phys. Lett.* **1982**, 40, 912.
- [91] X. Huang, M. Ford, Z. J. Patterson, M. Zarepoor, C. Pan, C. Majidi, *J. Mater. Chem. B* **2020**, 8, 4539.
- [92] M. G. Scott, in *Analysis of Human Motion: A Textbook in Kinesiology*, Ardent Media, London **1942**.
- [93] Y. Morimoto, H. Onoe, S. Takeuchi, *Sci. Rob.* **2018**, 3, eaat4440.
- [94] N. Vargaftik, B. Volkov, L. Voljak, *J. Phys. Chem. Ref. Data* **1983**, 12, 817.
- [95] C. B. Eaker, D. C. Hight, J. D. O'Regan, M. D. Dickey, K. E. Daniels, *Phys. Rev. Lett.* **2017**, 119, 174502.
- [96] Y. Lin, J. Genzer, M. D. Dickey, *Adv. Sci.* **2020**, 7, 2000192.
- [97] Z. J. Farrell, C. Tabor, *Langmuir* **2018**, 34, 234.
- [98] A. Holleman, E. Wiberg, N. Wiberg, in *Inorganic Chemistry*, Academic Press, Cambridge, MA, USA **2001**.
- [99] J. Tang, X. Zhao, J. Li, R. Guo, Y. Zhou, J. Liu, *ACS Appl. Mater. Interfaces* **2017**, 9, 35977.
- [100] S. Cheng, Z. Wu, *Lab Chip* **2012**, 12, 2782.
- [101] T. S. Light, S. Licht, A. C. Bevilacqua, K. R. Morash, *Electrochem. Solid-State Lett.* **2004**, 8, E16.
- [102] R. A. Cox, F. Culkun, J. Riley, in *Deep Sea Research and Oceanographic Abstracts*, Vol. 14, Elsevier, Amsterdam, **1967**, pp. 203–220.
- [103] A. J. Surowiec, S. S. Stuchly, J. R. Barr, A. Swarup, *IEEE Trans. Biomed. Eng.* **1988**, 35, 257.

- [104] J. H. Lee, Y. C. Yoon, H. S. Kim, J. Lee, E. Kim, C. Findekle, U. Katscher, *Sci. Rep.* **2022**, *12*, 73.
- [105] E. J. Chen, J. Novakofski, W. K. Jenkins, W. D. O'Brien, *IEEE Trans. Sonics Ultrason.* **1996**, *43*, 191.
- [106] A. Kalra, A. Lowe, A. Al-Jumaily, *J. Mater. Sci. Eng* **2016**, *5*, 1000254.
- [107] C. Gabriel, A. Peyman, E. H. Grant, *Phys. Med. Biol.* **2009**, *54*, 4863.
- [108] K. Comley, N. A. Fleck, *Int. J. Solids Struct.* **2010**, *47*, 2982.
- [109] J. Peters, G. Stinstra, M. M. Hendriks, *Electromagnetics* **2001**, *21*, 545.
- [110] J. Kerns, H. Pionov, C. Helder, F. Amirouche, G. Solitro, M. Gonzalez, *Anat. Rec.* **2019**, *302*, 2030.
- [111] D. Armani, C. Liu, N. Aluru, in *Technical Digest. IEEE Int. MEMS 99 Conf. 12th IEEE Int. Conf. on Micro Electro Mechanical Syst. (Cat. No. 99CH36291)*, IEEE, Orlando, FL, USA **1999**, pp. 222–227.
- [112] J. E. Mark, in *Polymer Data Handbook*, Vol. 27, Oxford University Press, New York **2009**.
- [113] A. Boonbumrung, P. Sae-Oui, C. Sirisinha, *J. Nanomater.* **2016**, *2016*, 6391572.
- [114] P. M. Visakh, S. Thomas, A. K. Chandra, A. P. Mathew, in *Advances in Elastomers I*, Springer Berlin, Heidelberg **2013**.
- [115] M. Czermer, L. S. Fellay, M. P. Suárez, P. M. Frontini, L. A. Fasce, *Procedia Mater. Sci.* **2015**, *8*, 287.
- [116] M. A. Kandadai, J. L. Raymond, G. J. Shaw, *Mater. Sci. Eng., C* **2012**, *32*, 2664.
- [117] D. Ji, J. M. Park, M. S. Oh, T. L. Nguyen, H. Shin, J. S. Kim, D. Kim, H. S. Park, J. Kim, *Nat. Commun.* **2022**, *13*, 1.
- [118] A. Ben Bouali, A. Montebault, L. David, Y. Von Boxberg, M. Viallon, B. Hamdi, F. Nothias, R. Fodil, S. Féréol, *Prog. Biomater.* **2020**, *9*, 187.
- [119] Z. Zhu, G. Yang, R. Li, T. Pan, *Microsyst. Nanoeng.* **2017**, *3*, 1.
- [120] T. Boudou, J. Ohayon, C. Picart, R. I. Pettigrew, P. Tracqui, *Biorheology* **2009**, *46*, 191.
- [121] L. Lu, Y. Shen, X. Chen, L. Qian, K. Lu, *Science* **2004**, *304*, 422.
- [122] H. Ledbetter, E. Naimon, *J. Phys. Chem. Ref. Data* **1974**, *3*, 897.
- [123] F. C. Walsh, *Trans. IMF* **1991**, *69*, 107.
- [124] M. D. Dickey, *Adv. Mater.* **2017**, *29*, 1606425.
- [125] J. K. Paik, E. Hawkes, R. J. Wood, *Smart Mater. Struct.* **2010**, *19*, 125014.
- [126] C. R. Knick, D. J. Sharar, A. A. Wilson, G. L. Smith, C. J. Morris, H. A. Bruck, *J. Micromech. Microeng.* **2019**, *29*, 075005.
- [127] H. v. Helmholtz, *Ann. Phys.* **1853**, *165*, 353.
- [128] G. Lippmann, *Ann. Chim. Phys* **1875**, *5*, 494.
- [129] D. L. Chapman, *London, Edinburgh Dublin Philos. Mag. J. Sci.* **1913**, *25*, 475.
- [130] C. Quilliet, B. Berge, *Curr. Opin. Colloid Interface Sci.* **2001**, *6*, 34.
- [131] W. Dreyer, C. Guhlke, M. Landstorfer, R. Müller, *Eur. J. Appl. Math.* **2018**, *29*, 708.
- [132] K. D. Hillaire, M. D. Dickey, K. E. Daniels, (Preprint) arXiv:2011.10016, submitted: November **2020**.
- [133] M. Song, K. E. Daniels, A. Kiani, S. Rashid-Nadimi, M. D. Dickey, *Adv. Intell. Syst.* **2021**, *3*, 2100024.
- [134] J. Rossmeisl, Z.-W. Qu, H. Zhu, G.-J. Kroes, J. K. Nørskov, *J. Electroanal. Chem.* **2007**, *607*, 83.
- [135] M. A. Creighton, M. C. Yuen, M. A. Susner, Z. Farrell, B. Maruyama, C. E. Tabor, *Langmuir* **2020**, *36*, 12933.
- [136] S. Handschuh-Wang, M. Rauf, T. Gan, W. Shang, X. Zhou, *ChemistrySelect* **2021**, *6*, 10625.
- [137] J. Zhang, Y. Yao, L. Sheng, J. Liu, *Adv. Mater.* **2015**, *27*, 2648.
- [138] L. Hu, J. Li, J. Tang, J. Liu, *Sci. Bull.* **2017**, *62*, 700.
- [139] L. Hu, B. Yuan, J. Liu, *Sci. Rep.* **2017**, *7*, 1.
- [140] J. Xie, F. Li, S. Kuang, H. Yang, X. Li, S. Tang, W. Li, S. Zhang, *IEEE/ASME Trans. Mechatron.* **2020**, *25*, 942.
- [141] Z. Yu, Y. Chen, F. F. Yun, D. Cortie, L. Jiang, X. Wang, *Phys. Rev. Lett.* **2018**, *121*, 024302.
- [142] A. F. Chrimes, K. J. Berean, A. Mitchell, G. Rosengarten, K. Kalantar-zadeh, *ACS Appl. Mater. Interfaces* **2016**, *8*, 3833.
- [143] J. Zhang, L. Sheng, J. Liu, *Sci. Rep.* **2014**, *4*, 1.
- [144] L. Y. Yeo, H.-C. Chang, *Mod. Phys. Lett. B* **2005**, *19*, 549.
- [145] L. Chen, E. Bonaccorso, *Adv. Colloid Interface Sci.* **2014**, *210*, 2.
- [146] Y. Zhang, K. Lu, G. Rao, Y. Tian, S. Zhang, J. Liang, *Appl. Phys. Lett.* **2002**, *80*, 888.
- [147] D. Vokoun, M. Beleggia, L. Heller, P. Šittner, *J. Magn. Magn. Mater.* **2009**, *321*, 3758.
- [148] D. Gatti, H. Haus, M. Matysek, B. Frohnapfel, C. Tropea, H. F. Schlaak, *Appl. Phys. Lett.* **2014**, *104*, 052905.
- [149] C. Fu, K. Wang, W. Tang, A. Nilghaz, C. Hurren, X. Wang, W. Xu, B. Su, Z. Xia, *Chem. Eng. J.* **2022**, *446*, 137241.
- [150] Z. Lin, T. Jiang, J. Shang, *Bio-Des. Manuf.* **2022**, *5*, 107.
- [151] M. D. Kutzer, M. S. Moses, C. Y. Brown, M. Armand, D. H. Scheidt, G. S. Chirikjian, in *2010 IEEE Int. Conf. on Robot. and Autom.*, IEEE, Piscataway, NJ, USA **2010**, pp. 2758–2764.
- [152] J. Wang, S. Li, D. Gao, J. Xiong, P. S. Lee, *NPG Asia Mater.* **2019**, *11*, 71.
- [153] S. Murata, H. Kurokawa, *IEEE Robot Autom. Mag.* **2007**, *14*, 71.
- [154] X. Fan, X. Dong, A. C. Karacakol, H. Xie, M. Sitti, *Proc. Natl. Acad. Sci.* **2020**, *117*, 27916.
- [155] X. Fan, Y. Jiang, M. Li, Y. Zhang, C. Tian, L. Mao, H. Xie, L. Sun, Z. Yang, M. Sitti, *Sci. Adv.* **2022**, *8*, eabq1677.
- [156] E. J. Markvicka, M. D. Bartlett, X. Huang, C. Majidi, *Nat. Mater.* **2018**, *17*, 618.
- [157] A. Kotikian, J. M. Morales, A. Lu, J. Mueller, Z. S. Davidson, J. W. Boley, J. A. Lewis, *Adv. Mater.* **2021**, *33*, 2101814.
- [158] Y. Wang, Y. Jiang, H. Wu, Y. Yang, *Nano Energy* **2019**, *63*, 103810.
- [159] S. Chen, Y. Pang, H. Yuan, X. Tan, C. Cao, *Adv. Mater. Technol.* **2020**, *5*, 1901075.
- [160] J. Wu, S.-Y. Tang, T. Fang, W. Li, X. Li, S. Zhang, *Adv. Mater.* **2018**, *30*, 1805039.
- [161] X. Li, S. Li, Y. Lu, M. Liu, F. Li, H. Yang, S.-Y. Tang, S. Zhang, W. Li, L. Sun, *ACS Appl. Mater. Interfaces* **2020**, *12*, 37670.
- [162] J. S. Sharp, D. J. Farmer, J. Kelly, *Langmuir* **2011**, *27*, 9367.
- [163] N. Ilyas, A. Cook, C. E. Tabor, *Adv. Mater. Interfaces* **2017**, *4*, 1700141.
- [164] E. B. Secor, A. B. Cook, C. E. Tabor, M. C. Hersam, *Adv. Electron. Mater.* **2018**, *4*, 1700483.
- [165] S. Park, H. J. Yoon, *Nano Lett.* **2018**, *18*, 7715.
- [166] Z. He, S. Jiao, Z. Wang, Y. Wang, M. Yang, Y. Zhang, Y. Liu, Y. Wu, J. Shang, Q. Chen, R.-W. Li, *ACS Appl. Mater. Interfaces* **2022**, *14*, 14630.
- [167] J. Yan, Y. Lu, G. Chen, M. Yang, Z. Gu, *Chem. Soc. Rev.* **2018**, *47*, 2518.
- [168] H. Fogg, *Trans. Electrochem. Soc.* **1934**, *66*, 107.
- [169] R. Guo, X. Sun, B. Yuan, H. Wang, J. Liu, *Adv. Sci.* **2019**, *6*, 1901478.
- [170] S.-Y. Tang, Y. Lin, I. D. Josphipura, K. Khoshmanesh, M. D. Dickey, *Lab Chip* **2015**, *15*, 3905.
- [171] D. Zhang, K. Zeng, *Ind. Eng. Chem. Res.* **2012**, *51*, 13825.
- [172] R. E. White, in *Electrochemical Cell Design*, Springer, Berlin **2012**.
- [173] S. Mazloomi, N. Sulaiman, *Renewable Sustainable Energy Rev.* **2012**, *16*, 4257.
- [174] T. G. Leong, P. A. Lester, T. L. Koh, E. K. Call, D. H. Gracias, *Langmuir* **2007**, *23*, 8747.
- [175] B. Roman, J. Bico, *J. Phys.: Condens. Matter* **2010**, *22*, 493101.
- [176] R. W. Style, A. Jagota, C.-Y. Hui, E. R. Dufresne, *Annu. Rev. Condens. Matter Phys.* **2017**, *8*, 99.
- [177] G. Lian, C. Thornton, M. J. Adams, *J. Colloid Interface Sci.* **1993**, *161*, 138.
- [178] N. Ashgriz, J. Poo, *J. Fluid Mech.* **1990**, *221*, 183.
- [179] S. K. Cho, H. Moon, C.-J. Kim, *J. Microelectromech. Syst.* **2003**, *12*, 70.

- [180] S. M. Mirvakili, I. W. Hunter, in *Electroactive Polymer Actuators and Devices (EAPAD) 2016*, Vol. 9798, SPIE, France **2016**, pp. 282–288.
- [181] C. S. Klein, G. D. Marsh, R. J. Petrella, C. L. Rice, *Muscle Nerve* **2003**, 28, 62.
- [182] C. Kuthe, R. Uddanwadiker, P. Padole, A. Ramteke, *MCB Mol. Cell. Biomech.* **2015**, 12, 1.
- [183] C. E. Blevins, *Anat. Rec.* **1964**, 149, 157.
- [184] S. Counter, E. Borg, J. Lännergren, *Acta Physiol. Scand.* **1981**, 111, 105.
- [185] G. Kovacs, L. Düring, S. Michel, G. Terrasi, *Sens. Actuators, A* **2009**, 155, 299.
- [186] J. Lee, C.-J. Kim, in *Proc. MEMS 98. IEEE. 11th Ann. Int. Workshop on Micro Electro Mech. Syst. An Investigation of Micro Structures, Sensors, Actuators, Machines and Systems (Cat. No. 98CH36176)*, IEEE, Piscataway, NJ, USA **1998**, pp. 538–543.
- [187] I. Frozanpoor, M. D. Cooke, V. Ambukan, A. J. Gallant, C. Balocco, *Langmuir* **2021**, 37, 6414.
- [188] S.-K. Fan, H. Yang, T.-T. Wang, W. Hsu, *Lab Chip* **2007**, 7, 1330.
- [189] A. Adamatzky, A. Chiolerio, K. Szaciłowski, *Soft Matter* **2020**, 16, 1455.
- [190] Y. you Yao, J. Liu, *RSC Adv.* **2016**, 6, 56482.
- [191] D.-D. Li, T.-Y. Liu, J. Ye, L. Sheng, J. Liu, *Adv. Intell. Syst.* **2021**, 3, 2000246.
- [192] J. T. Tsai, C.-M. Ho, F.-C. Wang, C.-T. Liang, *Appl. Phys. Lett.* **2009**, 95, 251110.
- [193] P. Sen, C.-J. C. Kim, *IEEE Trans. Ind. Electron.* **2008**, 56, 1314.
- [194] A. H. Hirs, J. Olles, C. Tilger, NASA 2013, Technical report No. NF1676L-17050.
- [195] B. J. Blaiszik, S. L. Kramer, M. E. Grady, D. A. McIlroy, J. S. Moore, N. R. Sottos, S. R. White, *Adv. Mater.* **2012**, 24, 398.
- [196] S. Otake, S. Konishi, in *2018 IEEE Micro Electro Mechanical Systems (MEMS)*, IEEE, Piscataway, NJ, USA **2018**, pp. 571–574.
- [197] D. Liu, L. Su, J. Liao, B. Reeja-Jayan, C. Majidi, *Adv. Energy Mater.* **2019**, 9, 1902798.
- [198] C. Wang, N. Liu, R. Allen, J. B.-H. Tok, Y. Wu, F. Zhang, Y. Chen, Z. Bao, *Adv. Mater.* **2013**, 25, 5785.
- [199] I. Jeon, J. Cui, W. R. Illeperuma, J. Aizenberg, J. J. Vlassak, *Adv. Mater.* **2016**, 28, 4678.
- [200] J.-B. Chossat, Y.-L. Park, R. J. Wood, V. Duchaine, *IEEE Sens. J.* **2013**, 13, 3405.
- [201] Y.-L. Park, C. Majidi, R. Kramer, P. Bérard, R. J. Wood, *J. Micromech. Microeng.* **2010**, 20, 125029.
- [202] Y.-L. Park, B.-r. Chen, R. J. Wood, in *Sensors IEEE*, IEEE, Piscataway, NJ, USA **2011**, pp. 81–84.
- [203] Y. Park, J. Jung, Y. Lee, D. Lee, J. J. Vlassak, Y.-L. Park, *npj Flexible Electron.* **2022**, 6, 1.
- [204] T. Jung, S. Yang, *Sensors* **2015**, 15, 11823.
- [205] H.-S. Shin, J. Ryu, C. Majidi, Y.-L. Park, *J. Micromech. Microeng.* **2016**, 26, 025011.
- [206] M. Varga, C. Ladd, S. Ma, J. Holbery, G. Tröster, *Lab Chip* **2017**, 17, 3272.
- [207] B. Zhang, L. Zhang, W. Deng, L. Jin, F. Chun, H. Pan, B. Gu, H. Zhang, Z. Lv, W. Yang, Z. L. Wang, *ACS Nano* **2017**, 11, 7440.
- [208] G. Liu, J. Y. Kim, M. Wang, J.-Y. Woo, L. Wang, D. Zou, J. K. Lee, *Adv. Energy Mater.* **2018**, 8, 1703652.
- [209] G. Costa, P. A. Lopes, A. L. Sanati, A. F. Silva, M. C. Freitas, A. T. de Almeida, M. Tavakoli, *Adv. Funct. Mater.* **2022**, 32, 2113232.
- [210] M. D. Bartlett, N. Kazem, M. J. Powell-Palm, X. Huang, W. Sun, J. A. Malen, C. Majidi, *Proc. Natl. Acad. Sci.* **2017**, 114, 2143.
- [211] C. Majidi, K. Alizadeh, Y. Ohm, A. Silva, M. Tavakoli, *Flexible Printed Electron.* **2022**, 7, 013002.
- [212] M. H. Malakooti, M. R. Bockstaller, K. Matyjaszewski, C. Majidi, *Nanoscale Adv.* **2020**, 2, 2668.
- [213] W. Lee, H. Kim, I. Kang, H. Park, J. Jung, H. Lee, H. Park, J. S. Park, J. M. Yuk, S. Ryu, J.-W. Jeong, J. Kang, *Science* **2022**, 378, 637.
- [214] M. Zadan, D. K. Patel, A. P. Sabelhaus, J. Liao, A. Wertz, L. Yao, C. Majidi, *Adv. Mater.* **2022**, 34, 2200857.
- [215] J. Wang, *TrAC, Trends Anal. Chem.* **2002**, 21, 226.
- [216] T. V. Neumann, M. D. Dickey, *Adv. Mater. Technol.* **2020**, 5, 2000070.
- [217] K. B. Ozutemiz, J. Wissman, O. B. Ozdoganlar, C. Majidi, *Adv. Mater. Interfaces* **2018**, 5, 1701596.
- [218] S.-Y. Tang, I. D. Joshipura, Y. Lin, K. Kalantar-Zadeh, A. Mitchell, K. Khoshmanesh, M. D. Dickey, *Adv. Mater.* **2016**, 28, 604.
- [219] S.-Y. Tang, B. Ayan, N. Nama, Y. Bian, J. P. Lata, X. Guo, T. J. Huang, *Small* **2016**, 12, 3861.
- [220] J. Thelen, M. D. Dickey, T. Ward, *Lab Chip* **2012**, 12, 3961.
- [221] J. Gong, C.-J. Kim, *J. Microelectromech. Syst.* **2008**, 17, 257.
- [222] Y. Fouillet, D. Jary, C. Chabrol, P. Clautre, C. Peponnet, *Microfluid. Nanofluid.* **2008**, 4, 159.
- [223] B. Hadwen, G. Broder, D. Morganti, A. Jacobs, C. Brown, J. Hector, Y. Kubota, H. Morgan, *Lab Chip* **2012**, 12, 3305.
- [224] C. Karuwan, K. Sukthang, A. Wisitsoraat, D. Phokharatkul, V. Patthanasettakul, W. Wechsato, A. Tuantranont, *Talanta* **2011**, 84, 1384.
- [225] V. Narasimhan, S.-Y. Park, *Langmuir* **2015**, 31, 8512.
- [226] J.-H. Kim, J.-H. Lee, J.-Y. Kim, A. Mirzaei, P. Wu, H. W. Kim, S. S. Kim, *J. Mater. Chem. C* **2018**, 6, 6808.
- [227] J. B. Chae, J. O. Kwon, J. S. Yang, D. Kim, K. Rhee, S. K. Chung, *Sens. Actuators, A* **2014**, 215, 8.
- [228] W. J. Welters, L. G. Fokkink, *Langmuir* **1998**, 14, 1535.
- [229] H. Liu, S. Dharmatilleke, D. K. Maurya, A. A. Tay, *Microsyst. Technol.* **2010**, 16, 449.
- [230] D. Kim, P. Thissen, G. Viner, D.-W. Lee, W. Choi, Y. J. Chabal, J.-B. Lee, *ACS Appl. Mater. Interfaces* **2013**, 5, 179.
- [231] S. Holcomb, M. Brothers, A. Diebold, W. Thatcher, D. Mast, C. Tabor, J. Heikenfeld, *Langmuir* **2016**, 32, 12656.
- [232] G. Li, J. Du, A. Zhang, D.-w. Lee, *Adv. Eng. Mater.* **2019**, 21, 1900381.
- [233] M. Wang, C. Trlica, M. Khan, M. Dickey, J. Adams, *J. Appl. Phys.* **2015**, 117, 194901.
- [234] R. Gilliam, J. Graydon, D. Kirk, S. Thorpe, *Int. J. Hydrogen Energy* **2007**, 32, 359.
- [235] K. S. Elassy, M. A. Rahman, N. S. Yama, W. A. Shiroma, A. T. Ohta, *IEEE Access* **2019**, 7, 150150.
- [236] V. Vallem, E. Roosa, T. Ledin, W. Jung, T.-i. Kim, S. Rashid-Nadimi, A. Kiani, M. D. Dickey, *Adv. Mater.* **2021**, 33, 2103142.
- [237] T. Shay, O. D. Velev, M. D. Dickey, *Soft Matter* **2018**, 14, 3296.
- [238] K. B. Ozutemiz, C. Majidi, O. B. Ozdoganlar, *Adv. Mater. Technol.* **2020**, 7, 2200295.
- [239] A. Poulin, S. Rosset, H. R. Shea, *Appl. Phys. Lett.* **2015**, 107, 244104.
- [240] N. P. Krut, O. Millet, *J. Fluid Mech.* **2017**, 812, 129.
- [241] T. I. Vogel, *Pacific J. Math* **2006**, 224, 367.
- [242] K. A. Brakke, *Exp. Math.* **1992**, 1, 141.
- [243] Q. He, Z. Wang, Y. Wang, Z. Wang, C. Li, R. Annapooranan, J. Zeng, R. Chen, S. Cai, *Sci. Rob.* **2021**, 6, eabi9704.
- [244] C. Keplinger, J.-Y. Sun, C. C. Foo, P. Rothmund, G. M. Whitesides, Z. Suo, *Science* **2013**, 341, 984.
- [245] L. J. Romasanta, M. A. López-Manchado, R. Verdejo, *Prog. Polym. Sci.* **2015**, 51, 188.
- [246] J. Madden, in *Dielectric Elastomers as Electromechanical Transducers: Fundamentals, Materials, Devices, Models and Applications of an Emerging Electroactive Polymer Technology*, (Eds: F. Carpi, D. De Rossi, R. Kornbluh, R. Pelrine, P. Sommer-Larsen), Elsevier, Amsterdam **2009**.
- [247] S. Chiba, in *Soft Actuators: Materials, Modeling, Applications, and Future Perspectives*, Springer, Berlin **2019**, pp. 259–273.
- [248] Z. Ye, G. Z. Lum, S. Song, S. Rich, M. Sitti, *Adv. Mater.* **2016**, 28, 5088.

- [249] M. Yunusa, G. J. Amador, D.-M. Drotlef, M. Sitti, *Nano Lett.* **2018**, 18, 2498.
- [250] M. Yunusa, A. Lahlou, M. Sitti, *Adv. Mater.* **2020**, 32, 1907453.
- [251] N. Maeda, J. N. Israelachvili, M. M. Kohonen, *Proc. Natl. Acad. Sci.* **2003**, 100, 803.
- [252] L. Yang, Y. Tu, H. Fang, *Soft Matter* **2010**, 6, 6178.
- [253] O. Pitois, P. Moucheront, X. Chateau, *Eur. Phys. J. B* **2001**, 23, 79.
- [254] J. A. F. Plateau, *Statique Expérimentale et Théorique des Liquides Soumis Aux Seules Forces Moléculaires*, Vol. 2, Gauthier-Villars, Toulouse, France **1873**.
- [255] L. Rayleigh, *Proc. Lond. Math. Soc.* **1878**, 1, 4.
- [256] J. Bico, É. Reyssat, B. Roman, *Annu. Rev. Fluid Mech.* **2018**, 50, 629.
- [257] J. Song, R. Evans, Y.-Y. Lin, B.-N. Hsu, R. B. Fair, *Microfluid. Nanofluid.* **2009**, 7, 75.
- [258] M. Torabinia, P. Asgari, U. S. Dakarapu, J. Jeon, H. Moon, *Lab Chip* **2019**, 19, 3054.
- [259] J. Lee, H. Moon, J. Fowler, T. Schoellhammer, C.-J. Kim, *Sens. Actuators, A* **2002**, 95, 259.
- [260] J.-H. Kim, Y.-J. Park, S. Kim, J.-H. So, H.-J. Koo, *Materials* **2022**, 15, 706.
- [261] M. Bououdina, D. Grant, G. Walker, *Int. J. Hydrogen Energy* **2006**, 31, 177.
- [262] S. Bouaricha, J. Dodelet, D. Guay, J. Huot, R. Schulz, *J. Alloys Compd.* **2001**, 325, 245.
- [263] Y. Takahashi, S. Matsuo, K. Kawakami, in *2008 Int. Conf. on Control, Autom. and Syst.*, IEEE, Piscataway, NJ, USA **2008**, pp. 1636–1640.
- [264] A. Wilhelm, B. Surgenor, J. Pharoah, in *IEEE Int. Conf. Mechatron. and Autom.*, 2005, Vol. 1, IEEE, Piscataway, NJ, USA **2005**, pp. 32–36.
- [265] A. Vasudev, J. Zhe, in *51st Midwest Sympos. on Circuits and Syst.*, IEEE, Piscataway, NJ, USA **2008**, pp. 49–52.
- [266] M. Pineirua, J. Bico, B. Roman, *Soft Matter* **2010**, 6, 4491.
- [267] M. Sitti, *Extreme Mech. Lett.* **2021**, 46, 101340.
- [268] J. G. Miller, J. L. Miller, *Behav. Sci.* **1990**, 35, 157.
- [269] T. Chen, M. Pauly, P. M. Reis, *Nature* **2021**, 589, 386.
- [270] B. Trembl, A. Gillman, P. Buskohl, R. Vaia, *Proc. Natl. Acad. Sci.* **2018**, 115, 6916.
- [271] C. El Helou, P. R. Buskohl, C. E. Tabor, R. L. Harne, *Nat. Commun.* **2021**, 12, 1.
- [272] H. Yasuda, P. R. Buskohl, A. Gillman, T. D. Murphey, S. Stepney, R. A. Vaia, J. R. Raney, *Nature* **2021**, 598, 39.
- [273] F. Li, J. Shu, L. Zhang, N. Yang, J. Xie, X. Li, L. Cheng, S. Kuang, S.-Y. Tang, S. Zhang, et al., *Appl. Mater. Today* **2020**, 19, 100597.
- [274] M. Calisti, G. Picardi, C. Laschi, *J. R. Soc., Interface* **2017**, 14, 20170101.
- [275] W. Liu, Y. Tao, Z. Ge, J. Zhou, R. Xu, Y. Ren, *Electrophoresis* **2021**, 42, 950.
- [276] J. Zhang, R. Guo, J. Liu, *J. Mater. Chem. B* **2016**, 4, 5349.
- [277] M. H. Raibert, *Commun. ACM* **1986**, 29, 499.
- [278] S. Chen, Y. Cao, M. Sarparast, H. Yuan, L. Dong, X. Tan, C. Cao, *Adv. Mater. Technol.* **2020**, 5, 1900837.
- [279] M. T. Mason, in *Mechanics of Robotic Manipulation*, MIT Press, Cambridge, MA, USA **2001**.
- [280] A. Bicchi, V. Kumar, in *Proc. 2000 ICRA. Millennium Conf. IEEE Int. Conf. on Robot. and Autom. Sympos. Proc. (Cat. No. 00CH37065)*, Vol. 1, IEEE, Piscataway, NJ, USA **2000**, pp. 348–353.
- [281] S. Song, C. Majidi, M. Sitti, in *2014 IEEE/RSJ Int. Conf. on Intell. Robot. and Syst.*, IEEE, Piscataway, NJ, USA **2014**, pp. 4624–4629.
- [282] G. M. Whitesides, B. Grzybowski, *Science* **2002**, 295, 2418.
- [283] R. F. Ismagilov, A. Schwartz, N. Bowden, G. M. Whitesides, *Angew. Chem., Int. Ed.* **2002**, 41, 652.
- [284] M. Mastrangeli, W. Ruythooren, J.-P. Celis, C. Van Hoof, *IEEE Trans. Compon., Packag., Manuf. Technol.* **2010**, 1, 133.
- [285] K. S. Kwok, Q. Huang, M. Mastrangeli, D. H. Gracias, *Adv. Mater. Interfaces* **2020**, 7, 1901677.
- [286] N. Lazarus, G. L. Smith, M. D. Dickey, *Adv. Intell. Syst.* **2019**, 1, 1900059.
- [287] T. Mei, Z. Meng, K. Zhao, C. Q. Chen, *Nat. Commun.* **2021**, 12, 1.
- [288] C. El Helou, B. Grossmann, C. E. Tabor, P. R. Buskohl, R. L. Harne, *Nature* **2022**, 608, 699.
- [289] Z. Meng, W. Chen, T. Mei, Y. Lai, Y. Li, C. Chen, *Extreme Mech. Lett.* **2021**, 43, 101180.
- [290] C. Pawashe, S. Floyd, M. Sitti, *Appl. Phys. Lett.* **2009**, 94, 164108.
- [291] S. Yim, M. Sitti, *IEEE Trans. Robot.* **2011**, 28, 183.
- [292] S. Yim, M. Sitti, *IEEE Trans. Robot.* **2012**, 28, 1198.
- [293] W. Hu, G. Z. Lum, M. Mastrangeli, M. Sitti, *Nature* **2018**, 554, 81.
- [294] B. Yigit, Y. Alapan, M. Sitti, *Soft Matter* **2020**, 16, 1996.
- [295] S. Wu, W. Hu, Q. Ze, M. Sitti, R. Zhao, *Multifunct. Mater.* **2020**, 3, 042003.
- [296] D. Kim, J.-B. Lee, *J. Korean Phys. Soc.* **2015**, 66, 282.
- [297] J. Zhang, R. H. Soon, Z. Wei, W. Hu, M. Sitti, *Adv. Sci.* **2022**, 9, 2203730.
- [298] R. Zhao, H. Dai, H. Yao, *IEEE Robot. Autom. Lett.* **2022**, 7, 4535.
- [299] T. Bu, H. Yang, W. Liu, Y. Pang, C. Zhang, Z. L. Wang, *Soft Rob.* **2019**, 6, 664.
- [300] J. Shu, S.-Y. Tang, Z. Feng, W. Li, X. Li, S. Zhang, *Soft Matter* **2018**, 14, 7113.
- [301] J. Jeon, S. K. Chung, J.-B. Lee, S. J. Doo, D. Kim, *Eur. Phys. J.: Appl. Phys.* **2018**, 81, 20902.
- [302] H. Wang, D. Lin, Y. Liu, Y. Li, Y. Cui, *Sci. Adv.* **2017**, 3, e1701301.
- [303] V. H. Ebron, Z. Yang, D. J. Seyer, M. E. Kozlov, J. Oh, H. Xie, J. Razal, L. J. Hall, J. P. Ferraris, A. G. MacDiarmid, R. H. Baughman, *Science* **2006**, 311, 1580.



Jiahe Liao is a postdoctoral researcher advised by Prof. Metin Sitti in the Physical Intelligence Department at the Max Planck Institute for Intelligent Systems, Stuttgart, Germany. He received his Ph.D. and M.S. in Robotics from Carnegie Mellon University, Pittsburgh, PA, USA under the guidance of Prof. Carmel Majidi. His current research interests include liquid metal actuators and physical intelligence in small-scale soft actuators.



Carmel Majidi is the Clarence H. Adamson Professor of Mechanical Engineering at Carnegie Mellon University, where he leads the Soft Machines Lab. His research is focused on the development of new classes of soft multifunctional materials for stretchable electronics, sensing, and muscle-like actuation. The purpose of these novel materials is to enable wearable computing and bio-inspired robotics that intrinsically match the mechanical properties of natural biological tissue. Prof. Majidi has been a co-author on over 200 peer reviewed scientific publications and is an inventor on over 30 issued patents.



Metin Sitti is the director of Physical Intelligence Department at Max Planck Institute for Intelligent Systems in Stuttgart, Germany. He is also a professor at ETH Zurich and Koç University. He was a professor at Carnegie Mellon University (2002–2014) and research scientist at UC Berkeley (1999–2002) in USA. He received B.Sc and M.Sc degrees (1994) from Boğaziçi University and Ph.D. degree from University of Tokyo (1999). His research interests include physical intelligence, small-scale mobile robotics, bio-inspiration, and wireless medical devices. He received the Breakthrough of the Year Award in Falling Walls World Science Summit 2020, ERC Advanced Grant in 2019, Rahmi Koç Science Medal in 2018, SPIE Nanoengineering Pioneer Award in 2011, and NSF CAREER Award in 2005.